

DISSERTATION

MACROPHAGE IMMUNOMETABOLISM DURING FLAVIVIRUS INFECTION

Submitted by

Jasmine Donkoh

Department of Microbiology, Immunology, and Pathology

In partial fulfillment of the requirements

For the Degree of Doctor of Philosophy

Colorado State University

Fort Collins, Colorado

Fall 2022

Doctoral Committee:

Advisor: Joel Rovnak

Sandra Quackenbush

Rushika Perera

Brian Foy

Chaoping Chen

Copyright by Jasmine Donkoh 2022

All Rights Reserved

## ABSTRACT

### MACROPHAGE IMMUNOMETABOLISM DURING FLAVIVIRUS INFECTION

Dengue virus (DENV) and Zika virus (ZIKV) are mosquito borne flaviviruses that are transmitted by the *Aedes* spp. mosquito and have caused outbreaks in Africa, Asia, the south Pacific, and the Americas. Infection with DENV can cause severe illness, such as dengue hemorrhagic fever and dengue shock syndrome, while infection with ZIKV can result in congenital abnormalities, such as microcephaly, and spontaneous abortions. Although disease outcome for these viruses is markedly different, both DENV and ZIKV both target monocytes and macrophage for pathogenesis. Macrophage are among the first cells to be infected by DENV and ZIKV and are disseminated throughout the body. While macrophage are an important cell in flavivirus pathogenesis, the mechanisms by which viruses modulate macrophage function are not fully understood. In this dissertation, I present data that attempts to explain the interaction between macrophage and flaviviruses, as well as investigate the mechanisms in which DENV and ZIKV control macrophage gene expression and metabolism.

The most widely used macrophage cell line, THP-1 cells, are cultured as immature monocytes. To become naïve macrophage, these cells are treated with phorbol 12-myristate- 13 acetate (PMA). Once THP-1 monocytes are differentiated into naïve macrophage, they can be polarized into different macrophage subsets. Even though THP-1 macrophage are widely used, the protocols in which to differentiate and polarize cells are not consistent. In chapter 2, we optimize methods to differentiate and polarize THP-1 cells. We measure gene expression and cellular metabolism during differentiation and polarization to characterize macrophage

phenotype. These data, coupled with published literature, show that this model is a reliable system to study macrophage biology and flavivirus-macrophage interactions. We use the methods developed in this aim throughout the dissertation.

Macrophage metabolism and phenotype determine immune function. Inflammatory (M1) macrophage are inflammatory and mount a strong anti-viral response, while anti-inflammatory (M2) macrophage dampen anti-viral responses. Viruses can alter macrophage phenotype for efficient replication and immune evasion. In chapter 3 we elucidated the role of macrophage polarization on DENV replication, showing that M1 macrophage have suppressed DENV replication while M2 macrophage support replication. In addition, we characterized the impact of DENV infection on M1 and M2 gene expression and metabolism. DENV infection resulted in an upregulation of inflammatory and anti-inflammatory genes in both M1 and M2 macrophage. Infection resulted in similar metabolic profiles in M1 and M2 cells, suggesting that DENV infection reprograms cellular metabolism in a way that is favorable for replication, regardless of macrophage phenotype. The key difference between M1 and M2 cells was the upregulation of interferon genes, where M1 mounted a strong interferon response, M2 mounted a subdued response. The difference in the interferon response could explain the difference in DENV replication observed in the two phenotypes. These data add to the ongoing literature on immunometabolism and its impact on viral pathogenesis.

Cyclin dependent kinase 8 (CDK8) and CDK19 are transcriptional cofactors that regulate expression of inflammatory and anti-inflammatory genes. In addition, inhibition of CDK8/19 during DENV infection leads to decreased replication, as well as metabolic shifts in Huh7 cells, a liver cell line. In chapter 4, we investigate the role of CDK8/19 on viral replication and inflammatory/ anti- inflammatory gene expression. We found that inhibition of CDK8/19 kinase

activity increased DENV replication and anti-inflammatory gene interleukin 10 (*IL-10*) expression. In contrast, inhibition of kinase activity decreased expression of inflammatory genes C-X-C motif chemokine ligand 10 (*CXCL10*). Furthermore, I found distinct mechanisms for each kinase through analysis of DENV-infected CDK8 and CDK19 knockdown cells. Knockdown of CDK8 mimics chemical inhibition of CDK8/19, while knockdown of CDK19 did not change expression in *CXCL10* or *IL-10*. These data indicate that CDK8 and CDK19 regulate the transcription of different genes during DENV infection in macrophage. These data contribute the basic understanding of CDK8/19 regulation during viral infection.

Macrophage phenotype plays a large role in ZIKV pathogenesis, where macrophage found near the placenta are an anti-inflammatory phenotype and are susceptible to infection. In chapter 5, we investigated the role of cyclin dependent kinase 8 and phenotype in Zika virus pathogenesis. We found *CDK8* gene expression increase throughout infection, while CDK8 kinase inhibition decreased viral replication. Furthermore, inhibiting CDK8/19 kinase activity led to a decrease in *CXCL10* and an increase in *IL-10*, as seen in a DENV model of infection. We also found that M2 macrophage were more susceptible to infection than M0 or M1. These data suggest that CDK8/19 kinase activity could be a pan-flavivirus mechanism to regulate host gene expression during infection.

## ACKNOWLEDGEMENTS

I know most people end their acknowledgments with their family, but I had to start mine with them because they are the only reason I am here. My parents immigrated from Ghana when they were around my age, and I am now starting to understand the sacrifices they must have made to provide for me and my siblings. My mom worked three jobs at one point in my undergraduate career so she could help pay for my rent and tuition, so I wouldn't have to worry about bills and 'focus on my studies'. My dad has always been my biggest cheerleader, letting me know from an early age that I'm only as capable as I think I am, and he let me know every day of my life that I'm more than capable. These two have shown me that hard work, love, and support can get you through any situation. I don't know how I could ever thank them for everything they gave me but having a Dr. in the family will have to suffice for now.

My siblings are my best friends. Nick and Tasha have been there for me through every hard day and have told me they would still love me if I quit. Nick will always have a great joke about basketball or the weather, while Tasha will always remind me of brighter days ahead. Our sibling zoom sessions have been the highlight of my PhD career and I hope we continue them forever. I am so very lucky to have these two in my life and I thank God every day I get to call them family.

Chase Calvi has been my rock and he really deserves a whole page dedicated to him. Throughout every breakdown, he has been there to make sure I'm okay and to let me know I got this. Over the past 5 years he has been the person I call whenever an experiment failed at 11pm at night or when I finally got that stubborn western blot to work. And throughout it all he's been patient, understanding and knows exactly what to say to make me feel like a capable person. I'm

so happy I took that physics class all those years ago and I look forward to a lifetime of awful puns and dad jokes with you.

The friends I have made in these five years are really going to be my ride or dies. Molly Butler is the reason I joined the Quackenbush/Ronak lab. Under her sweet veneer is one of the most snarky and funny people I have had the pleasure of knowing. She has always been there for me with a bottle of wine and a bag of gummies and is the best office buddy I could have asked for. Thank you to the bottom of my heart to Eve Mozur and Annalise Maughan, who have not only been there with me every single Tuesday/ Friday night of graduate school, but also sent groceries when I was too busy to make food for myself. Hannah Berry and Jemma Fadum were there to remind me that grad students can have hobbies, and I've enjoyed every pot thrown, rock climbed, wine sipped, and cheese plate eaten along the way. Alex Moskaluk has helped me through my last years of grad school when I was the only student in my lab. She's been there for me when I didn't understand formatting and grad school deadlines and when I needed to go off on a feminist rant. Speaking of feminist rants, Chilingh Nguyen has been one of the best roommates I could have asked for. Her calm logical presence has helped tame my anxiety spirals and remind me that if I don't calm down, I'll only suffer twice. Thank you so much for allowing me and Iris to crash at your house for the past 5 years. Thanks to the chemists and the physicists for letting this random biology grad student infiltrate your parties and (future) ski vacations.

My committee has been the worst and best part of grad school. They have pushed me to tears almost every meeting, but I have become a better scientist because of it. Dr Chaoping Chen has been great to brainstorm with and has always given me great ideas for future experiments. Dr. Rushika Perera has become somewhat of a role model for me. I am so lucky I have a fellow woman of color as assertive and kind as her to help me along my PhD career. I am so lucky to

have Drs. Rovnak and Quackenbush as my advisors. As a black woman in science, I am always nervous that people lower their expectations for me. I can honestly say that that was NOT the experience I had with Q and Joel. Every lab meeting pushed my boundaries of experimental design, data analysis and data interpretation. And every time I wanted to give up I was sternly, but kindly, reminded that I can do this and this is how science works. They have also been great company in our lab of three. Sharing a lab space with Joel meant that there was always radio paradise or NPR on and a handful of snarky comments made (by the both of us). Q made sure I never felt too lonely as has asked about my day/ Chase/ my family every time she sees me. It has been great working for people who care for me not just as a student but as a person. Last of all, I want to thank the person who first accepted me into his lab 8 years ago. I'm not sure what you saw in me Brian, but thank you for creating a lab space so welcoming and interesting that I decided to pursue a career in science. You have been one of the best mentors I could have asked for.

Lastly, I want to thank every single student I have taught/ mentored in the five years I've been here. You all have taught me so much about what it means to be a graduate student and mentor and I don't think I would be heading where I am without you all.

## TABLE OF CONTENTS

ABSTRACT.....	ii
ACKNOWLEDGEMENTS.....	v
LIST OF TABLES.....	xiii
LIST OF FIGURES.....	xiv
CHAPTER 1: OVERVIEW OF THE LITERATURE.....	1
1.1 Dengue virus.....	1
1.1a DENV genome and proteins.....	2
1.1b DENV life cycle.....	6
1.1c Cellular metabolism.....	9
1.1d DENV induced metabolism shifts.....	10
1.2 Host response to infection.....	11
1.2a Macrophage role during infection.....	14
1.2b Antibody dependent enhancement and vascular leakage.....	16
1.2c Interferon response to infection.....	16
1.2d Macrophage immunometabolism.....	18
1.3 CDK8 and CDK19.....	20
1.3a CDK8 during virus infection.....	22
1.3b CDK8 regulates immune function.....	23
CHAPTER 2: OPTIMIZING MACROPHAGE DIFFERENTIATION AND POLARIZATION IN A THP-1 MONOCYTE CELL LINE.....	25
2.1 Summary.....	25

2.2 Introduction .....	25
2.3 Methods and Materials .....	28
2.3a: Cell culture and PMA stimulation .....	28
2.3b: Polarization of PMA treated THP-1 cells.....	28
2.3c: DENV infection.....	29
2.3d: RNA extraction and qPCR .....	29
2.3e Mitochondrial and Glycolytic Stress Tests.....	29
2.3f Statistics .....	31
2.4 Results .....	31
2.4a PMA concentration and timing.....	31
2.4b Polarization of THP-1 cells to M1 phenotype with IFN $\gamma$ treatment .....	33
2.4c IFN $\gamma$ increases oxidative phosphorylation and glycolysis early in treatment .....	35
2.4d: IL-4 stimulates anti-inflammatory genes later in polarization .....	38
2.4e Longer M2 polarization results in increased mitochondrial respiration .....	39
2.5 Discussion .....	40
 CHAPTER 3: DENGUE VIRUS REPROGRAMS MACROPHAGE GENE	
EXPRESSION AND METABOLISM .....	46
3.1 Summary .....	46
3.2 Introduction .....	46
3.3 Materials and Methods .....	50
3.3a Cells and infection .....	50
3.3b Macrophage polarization and infection .....	50
3.3c RNA extraction and qPCR.....	50

3.3d Plaque assays .....	51
3.3e Metabolic Stress Tests .....	52
3.3f Subcellular Extracts and Protein Analysis .....	53
3.3g Statistics.....	54
3.4 Results .....	54
3.4a Inflammatory and immunosuppressive genes are upregulated during DENV2 infection.....	54
3.3b DENV2 infection upregulates cellular metabolism in macrophage .....	57
3.3c M2 macrophage support DENV2 infection.....	60
3.3d DENV2 infection of M2 cells increases immunosuppressive markers but decreases inflammatory cytokines compared to infected M0 cells. ....	62
3.3e No difference in inflammatory gene expression levels in infected M1 and infected M0 cells .....	65
3.4f Expression of glycolytic genes are upregulated in M1 cells upon DENV2 infection, while DENV2 increases expression of both glycolytic and fatty acid oxidation genes in M2 cells.....	66
3.3g DENV2 infection increases mitochondrial respiration.....	69
3.4h DENV2 does not increase glycolysis in M1 or M2 cells .....	72
3.4i Increases in expression of type I interferon genes during infection correlate with decreases in DENV2 replication in M1 cells .....	74
3.5 Discussion .....	76
<b>CHAPTER 4: INVESTIGATING THE ROLE OF CDK8 AND CDK19 IN DENV2 INFECTION OF MACROPHAGES .....</b>	<b>82</b>

4.1 Summary .....	82
4.2 Introduction .....	83
4.3 Methods and Materials .....	86
4.3a: Cell culture and PMA stimulation .....	86
4.3b: Polarization of PMA treated THP-1 cells.....	86
4.3c: DENV2 infection .....	86
4.3d: RNA extraction and qPCR .....	86
4.3e Plaque assays .....	87
4.3f Senexin treatment.....	88
4.3g CDK8/19 knockdown.....	88
4.3h Protein analysis.....	89
4.3i Statistics.....	89
4.4 Results .....	90
4.4a CDK19 is upregulated during DENV2 infection and CDK8/19 kinase inhibition increases DENV2 replication .....	90
4.4b CDK8/19 kinase regulates CXCL10 and IL-10 expression during infection.....	92
4.4c Knockdown of CDK8 increased DENV2 replication.....	94
4.4d CDK8 controls IL-10 and CXCL 10 gene expression.....	96
4.4e Regulation by CDK8/19 is not phenotype specific .....	98
4.5 Discussion .....	100
 CHAPTER 5: INVESTIGATING THE ROLE OF CYCLIN DEPENDENT KINASE 8 AND MACROPHAGE PHENOTYPE IN ZIKA VIRUS PATHOGENESIS .....	
5.1 Summary .....	105

5.2 Introduction .....	105
5.3 Methods and Materials .....	108
5.3a: Cell culture and PMA stimulation .....	108
5.3b: Polarization of PMA treated THP-1 cells.....	109
5.3c: ZIKV infection .....	109
5.3d: RNA extraction and qPCR .....	109
5.3e Plaque assay .....	110
5.3f Senexin treatment.....	110
5.3g Statistics.....	111
5.4 Results .....	111
5.4a: ZIKV infection upregulates IL-10 and CXCL10 gene expression.....	111
5.4b: Inhibition of CDK8/19 kinase activity decreases ZIKV replication .....	112
5.4c: ZIKV infection upregulates both inflammatory and anti-inflammatory markers in M0, M1 and M2 cells .....	113
5.5 Discussion .....	115
CONCLUSION.....	119
REFERENCES .....	124

## LIST OF TABLES

2.1	PCR Primers .....	31
3.1	PCR Primers .....	52
4.1	PCR Primers .....	88
4.2	shRNA sequences .....	89
5.1	PCR Primers .....	122

## LIST OF FIGURES

1.1	DENV replication cycle.....	8
1.2	An overview of cellular metabolism.....	12
1.3	Macrophage phenotypes .....	21
2.1	PMA concentration and duration of incubation impact macrophage maturation.....	34
2.2	Markers for M1 macrophage peak early in polarization.....	36
2.3	M1 metabolism is upregulated early in polarization .....	38
2.4	Markers for M2 macrophage peak later in polarization .....	40
2.5	M2 metabolism is upregulated later during polarization.....	42
3.1	DENV2 upregulates expression of inflammatory and immunosuppressive genes.....	57
3.2	DENV2 drives mitochondrial respiration in M0 cells.....	60
3.3	M2 macrophage provide a conducive environment for DENV2 replication.....	62
3.4	DENV2 infection of M2 cells increases immunosuppressive markers but decreases inflammatory cytokines compared to infected M0 cells.....	65
3.5	No difference in inflammatory gene expression levels in infected M1 and infected M0 cells.....	67
3.6	Glycolytic gene expression is upregulated in M1 cells upon DENV2 infection, while DENV2 increases glycolytic and fatty acid oxidation gene expression in M2 cells .....	70
3.7	DENV2 drives oxidative phosphorylation in M1 and M2 cells .....	72
3.8	DENV2 does not increase rates of glycolysis in in M1 and M2 cells .....	75
3.9	Increase in IFN-stimulated genes leads to a decrease in DENV2 replication .....	77

4.1	CDK19 expression is increased during DENV2 infection and CDK8/19 kinase inhibition increases DENV22 replication .....	92
4.2	CDK8/19 regulates CXCL10 and IL-10 expression.....	94
4.3	Knockdown of CDK8 increased DENV2 replication.....	96
4.4	CDK8 controls IL-10 and CXCL10 gene expression.....	98
4.5	CDK19, not CDK8, is upregulated during infection .....	102
5.1	ZIKV upregulates both IL-10 and CXCL10 during infection .....	113
5.2	CDK8 kinase activity increases ZIKV replication and regulates IL-10 and CXCL10 expression .....	115
5.3	ZIKV upregulates inflammatory and immunosuppressive genes.....	117

## CHAPTER 1: OVERVIEW OF THE LITERATURE

In this chapter, I summarize concepts that are important background for my research. I summarize the dengue virus (DENV) genome, proteins, and lifecycle. Next, I give an overview about cellular metabolism and how it relates to DENV infection and replication. I give an overview of the host response to infection, focusing on the role of macrophage during the initiation and resolution of inflammation. I go into depth about macrophage phenotypes and their distinct metabolism. Lastly, I review the literature on cyclin dependent kinase 8 and cyclin dependent kinase 19 and their role in viral infection.

### **1.1 Dengue virus**

Dengue virus (DENV) is the leading cause of arthropod borne viral disease in the world (Diamond & Pierson, 2015). DENV outbreaks have been reported throughout the world, with cases primarily occurring in the Americas, Africa, south Asia, and the Pacific islands (S. Bhatt et al., 2013). The global burden of DENV has been increasing over the past 30 years, with estimates at 50-100 million infections worldwide in 1988, to 400 million infection in 2013 (S. Bhatt et al., 2013). There are four DENV serotypes (DENV1-4) circulating in the tropic and sub tropic regions that can cause illness (Diamond & Pierson, 2015; S. K. Roy & Bhattacharjee, 2021). While the majority of infection leads to asymptomatic or mild disease, 5% of infections can lead to severe illness, with 2.5% of those leading to death (Pang, Mak, & Gubler, 2017). Severe illness is manifested by either a hemorrhagic fever (dengue hemorrhagic fever, DHF) or by shock (dengue shock syndrome, DSS). DHF and DSS are characterized by the onset of capillary leakage and thrombocytopenia, which causes bleeding into the skin and gastrointestinal tract and are often fatal (Halstead, 2007).

Infection caused by these serotypes are a significant public health concern, with 13,500 fatal cases globally and an annual economic burden of 8.89 billion US dollars globally (Shepard, Undurraga, Halasa, & Stanaway, 2016). Elucidating the interactions between the immune cells and flaviviruses may eventually lead to development of effective therapeutics. Understanding the impact of cellular environment on DENV replication, as well as the impact DENV has on cellular homeostasis, is vital to understanding DENV immune evasion and pathogenesis.

### *1.1a DENV genome and proteins*

DENV is a member of the *Flaviviridae* family and is an enveloped single stranded positive-sense RNA virus surrounded by a host-derived lipid membrane, covered by surface envelope proteins. It possesses an 11-kb long genome that encodes a single polyprotein, which is cleaved into 3 structural proteins (C, PrM and E) and 7 nonstructural proteins (NS1, NS2A, NS2B, NS3, NS4A, NS4B and NS5).

The structural proteins are involved in nucleocapsid formation, membrane formation, maturation and envelopment of the virion (Nanaware et al., 2021). The capsid protein is a 12-kDa protein that functions as a homodimer with each monomer possessing 4 alpha helical regions (Byk & Gamarnik, 2016). The main function of the capsid protein is to encapsulate the genome into the virion, creating the nucleocapsid (Byk & Gamarnik, 2016; Oliveira, Mohana-Borges, de Alencastro, & Horta, 2017). This interaction is critical for viral replication, as the reversal is necessary for genome release within the cell (Byk & Gamarnik, 2016).

The precursor M (prM) protein and the envelope protein (E) are associated on the immature virus particle and form 60 trimeric spikes on the capsid (Li et al., 2008). The prM protein is a 26 kDa protein that consists of a N-terminal domain, the predomain, followed by the M domain, a flexible structure that forms the membrane of a mature virus particle (Li et al.,

2008). The predomain contains seven  $\beta$ -strands that conceal the fusion loop of the E protein and prevent fusion of the immature virus particle with the host membrane in the trans-Golgi network and exosomes (Yu et al., 2009; Yu et al., 2008). Inside the Golgi apparatus, the prM protein is cleaved by the host furin protein (Yu et al., 2009). After cleavage, the pr protein is no longer attached to the viral particle, while the M protein is still associated, but not exposed on the surface. The rearrangement of the M protein causes the E protein to form homodimers, giving the mature virion its characteristic “smooth” shape (Yu et al., 2009; Yu et al., 2008). The E protein (53 kDa) will form a trimer once it binds onto to cells surface receptors (Bressanelli et al., 2004; Modis et al., 2004). Once inside an endosome, the low pH causes the E protein to reveal a fusion peptide, which becomes inserted into the cell membrane and releases the viral genome into the cytoplasm (Bressanelli et al., 2004).

Nonstructural (NS) proteins are responsible for viral replication and evasion of anti-viral responses. NS1 is a 48 kDa glycosylated protein that is the only DENV protein to be secreted from the cell. NS1 is secreted as a hexamer (H. R. Chen, Lai, & Yeh, 2018), which is composed of three dimers and resembles a high-density lipoprotein (Gutsche et al., 2011). The similarity between NS1 and a high-density lipoprotein is thought to disrupt coagulation by interfering with the synthesis of endogenous lipoproteins (Gutsche et al., 2011). NS1 has been shown to induce vascular leakage (Malavige & Ogg, 2017), either through interaction with toll like receptor 4 (TLR-4) (Modhiran et al., 2015), which releases inflammatory cytokines, or through disruption of the endothelial glycocalyx by induction of heparanase-1 (Glasner et al., 2017; Puerta-Guardo, Glasner, & Harris, 2016). Intracellular NS1 is also required for viral replication (Płaszczycya et al., 2019) and infectious particle assembly (Fan, Liu, & Yuan, 2014; Songprakhon et al., 2020).

NS2A is a 22kDa endoplasmic reticulum (ER) associated transmembrane protein, with 5 transmembrane regions, spanning from the N-terminal domain in the ER lumen to the C terminal domain in the cytosol (Xie et al., 2013). NS2A recruits structural proteins, a protease complex and the viral genome to sites of virion assembly where the encapsulation of the genome and assembly of the virion take place (Xie et al., 2019).

NS2B is a 15 kDa protein with four transmembrane regions, with both the N and C termini located in the cytoplasm. The hydrophilic domain of NS2B is a cofactor for the NS2B/NS3 serine protease, where it cleaves the DENV polyprotein between NS2A/NS2B, NS2B/NS3, NS3/NS4A, NS4A/NS4B and internal cleavage at C protein, NS2A, NS3 and NS4A (Gopala Reddy et al., 2018). The NS2B/NS3 protease targets the stimulator of the interferon gene (STING) protein, preventing a type I interferon response in infected cells (Aguirre et al., 2012). This protease also targets cyclic GMP/AMP synthase (cGAS) for proteolysis to avoid detection by mitochondrial DNA sensors (Aguirre et al., 2017). The NS2B/NS3 protease has been shown to cleave host mitofusions, which alters mitochondrial function and inhibits anti-viral response to infection (Yu et al., 2015) .

NS3 is the second largest DENV nonstructural protein at 70 kDa. NS3 functions as a protease with NS2B and a single stranded RNA (ssRNA)-activated NTPase and helicase (Cui et al., 1998; Li et al., 1999). It associates with NS2B at the N terminal domain and is a NTPase-helicase for the remaining 70% of the protein (Matusan et al., 2001; Swarbrick et al., 2017). NS3 has also been shown to induce shifts in cellular metabolism. NS3 recruits fatty acid synthase (FASN) to the site of replication to increase fatty acid synthesis for ER remodeling (Heaton et al., 2010). It also binds to glyceraldehyde-3-phosphate dehydrogenase (GAPDH) and reduces glycolytic activity and shifts cellular metabolism to non-glycolytic pathways (Silva et al., 2019).

NS4A is a 16 kDa protein that associates with the ER through three transmembrane regions. The C terminal domain is located in the ER, where it acts as a signal for translocation of NS4B into the ER (Miller et al., 2007). NS4A creates replication complexes by inducing membrane rearrangement through oligomerization with a host protein, reticulon 3.1 (Aktepe & Mackenzie, 2018; S. Miller & Krijnse-Locker, 2008; Stern et al., 2013). Furthermore, NS4A forms replication complexes by interacting with a host scaffolding protein, vimentin (Teo & Chu, 2014). NS4A also interacts with ancient ubiquitous protein 1 (AUP1), an ER-associated protein correlated with increased levels of lipid droplets, to increase its acetyltransferase activity and trigger lipophagy (Jingshu Zhang et al., 2018), which has been shown to be advantageous for viral replication (Jordan & Randall, 2017).

Only a 2-kDa region separates NS4A and NS4B (referred to as 2K). Though this region is not involved in the formation of the replication complexes, the cleavage of the 2K region is important for the induction of membrane alterations (Miller et al., 2006; Zou et al., 2015). The 2K region also defines the C terminal region of NS4A and the N terminal region of NS4B (Zou et al., 2015). NS4B is a 27-kDa protein that is associated with the ER membrane through five transmembrane domains (Gopala Reddy et al., 2018; Zou et al., 2015). NS4B forms a homodimer and associates with NS1 and NS4 to modulate virus replication (Giraldo et al., 2018; Gopala Reddy et al., 2018; Płaszczycyca et al., 2019). Furthermore, NS4B associates with NS3 in the perinuclear region of cells, where it dissociates NS3 from ssRNA, enhancing NS3 helicase activity (Umareddy et al., 2006). As seen with other DENV nonstructural proteins, NS4B alters mitochondrial function; it enhances mitochondrial elongation and decreases mitochondrial fission, which promotes viral replication (Barbier, Lang, Valois, Rothman, & Medin, 2017; Chatel-Chaix et al., 2016).

NS5 is the most conserved and largest nonstructural protein at 103 kDa. The C-terminal domain mainly functions as an RNA-dependent RNA polymerase (RdRp), which replicates the viral genome (Iglesias, Filomatori, & Gamarnik, 2011; Kapoor et al., 1995; Klema et al., 2016). The N-terminal domain functions as a methyl transferase that caps viral RNAs during transcription (Issur et al., 2009; Klema et al., 2016; L. Liu et al., 2010). NS5 also associates with NS3 to form a replicase complex in the ER (Kapoor et al., 1995). Though it replicates viral mRNA in replication complexes in the ER, NS5 is primarily found in the nucleus (Kapoor et al., 1995; S. Miller et al., 2006), and while the full significance of this localization remains unclear, NS5 has been shown to disrupt splicing by interacting with host spliceosomes in the nucleus (De Maio et al., 2016) and has been associated with an increase in IL-8 production, a cytokine that has been correlated with severe dengue cases (Medin et al., 2005; Rawlinson et al., 2009; Soo et al., 2019). NS5 also antagonizes polymerase associated factor 1 complex (PAF1C) to restrict an anti-viral immune response (Petit et al., 2021). In addition, NS5 blocks the type I interferon response by binding the signal transducer and activator of transcription 2 (STAT2) and targeting it for proteasomal degradation (Ashour et al., 2009).

### *1.1b DENV life cycle*

The first step in DENV replication is the binding of the virus onto cellular receptors on the cell surface. The DENV E glycoprotein interacts with cell surface receptors. Multiple cell factors have been identified as receptors for DENV entry. The receptor type is serotype and host cell dependent (Cruz-Oliveira et al., 2015), but adhesion molecule of dendritic cells (DC-SIGN), CD14, heat-shock proteins 70 and 90 (HSP 70/90), as well as mannose receptors have been identified as receptors in monocytes and macrophage (Chen, Wang, & King, 1999; Miller et al., 2008; Reyes-del Valle et al., 2005; Tassaneeritthep et al., 2003;) Pokidysheva et al., 2006).

After DENV attaches to receptors, the virus particle is endocytosed via clathrin-mediated endocytosis (Acosta, Castilla, & Damonte, 2012; Krishnan et al., 2007). Once inside the cell, the endosome carrying the virus is delivered to early endosomes (Smit, Moesker, Rodenhuis-Zybert, & Wilschut, 2011). The exposure to an acidic endosomal environment causes the E protein to undergo conformational change and reveal a fusion peptide (Bressanelli et al., 2004; Modis et al., 2004). The fusion peptide fuses the viral membrane with the endosomal membrane, creating a pore and releasing the nucleocapsid into the cytoplasm (Pierson & Kielian, 2013).

Once in the cytoplasm, the capsid protein dissociates from the genome, which frees the RNA for direct viral translation (Byk & Gamarnik, 2016). Viral translation takes place on the rough ER by host ribosomes. Translation is usually initiated by the recognition of a m<sup>7</sup>GpppN cap structure at the 5' end of mRNAs, but DENV also exhibits the ability to undergo cap independent translation (Edgil et al., 2006). This cap independent translation is internal ribosomal entry site (IRES) independent and involves both the 3' and 5' untranslated regions (UTR) (Edgil et al., 2006). Translation is carried out by ER associated host proteins and results in a polyprotein (Reid et al., 2018). This polyprotein is cleaved into the 10 viral proteins by the NS2A/NS3 protease (Gopala Reddy et al., 2018).

The prM and E protein assemble on the ER lumen, while the nonstructural proteins rearrange the surface of the ER to create replication complexes. The replication complexes are made of viral and host protein which come together within vesicles in the endoplasmic reticulum, near the nucleus (Den Boon & Ahlquist, 2010). During replication the viral genome takes on two forms, a linear form, and a circular form (Gamarnik & Andino, 1998). The linear form is for translation and protein synthesis, while the circular form is solely for replication (Gamarnik & Andino, 1998). NS3 forms a complex with NS5 and unwinds RNA while NS5

transcribes RNA (Kapoor et al., 1995). Replicating in these vesicle packets is beneficial to the virus because the intermediary dsRNA is shielded from the innate immune response (Morrison, Aguirre, & Fernandez-Sesma, 2012).

Structural proteins are recruited to the ER by NS2A, where the capsid protein encapsulates the genome, creating the nucleocapsid (Byk & Gamarnik, 2016). The immature viral particle buds from the ER, containing a host lipid membrane embedded prM and E proteins (Kuhn et al., 2002). Once in the slightly acidic golgi network, the E protein dimerizes, exposing the pr protein for furin mediated cleavage (Bressanelli et al., 2004). The M protein undergoes a conformational change and shifts cells from spiky appearance to a smooth one, which is a sign of a mature viral particle (Yu et al., 2009; Yu et al., 2008). The cleavage of the pr protein exposes the fusion loop on the E protein, which allows the virion to bud be secreted from the cell (Li et al., 2008).

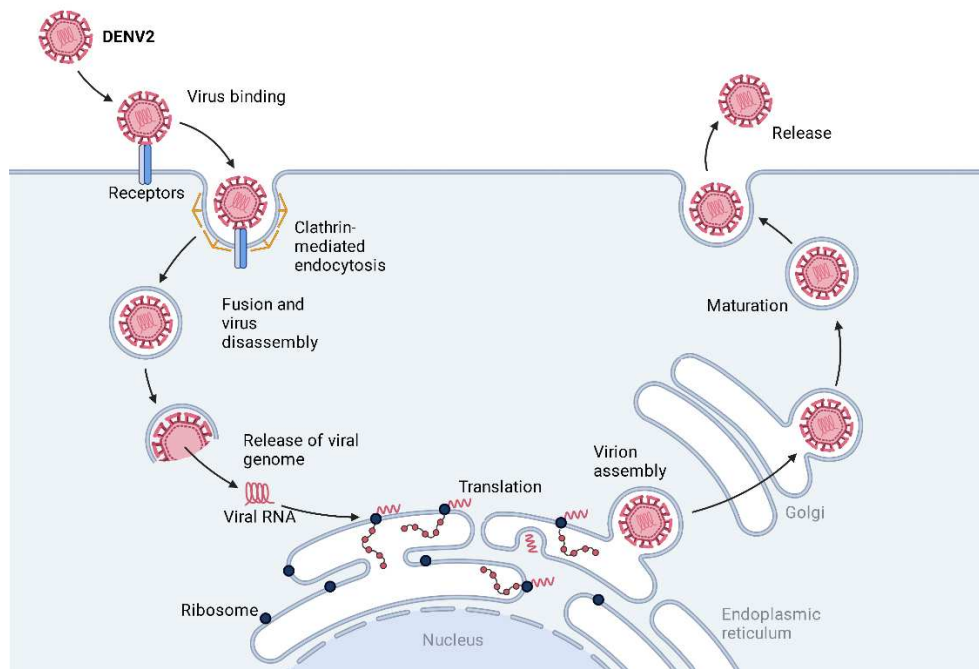


**Figure 1.1: DENV replication cycle.** DENV binds onto cell receptors and enters the cell via clathrin-mediated endocytosis. Once the pH in the endosome drops, the virion undergoes a confirmational changes. These confirmational changes allow the membrane of the virion to fuse

to the endosomal membrane and release the viral genome into the cytoplasm. The viral genome traverses to the endoplasmic reticulum, where it undergoes translation of viral proteins. These viral proteins are assembled into an immature virion and translocate through the golgi network, where it matures. Then the virus is released into the extracellular space. Adapted from image on BioRender.com.

### *1.1c Cellular metabolism*

Glucose is one of the main carbon sources used for glycolysis and is transported into the cell via glucose transporters (GLUT 1-4). Once inside the cell, glucose is phosphorylated by hexokinase enzymes (HKI-IV) and converted into glucose- 6- phosphate (G-6-P). G-6-P can either be shuttled into the pentose phosphate pathway (PPP) or continue through glycolysis (DeBerardinis et al., 2008). If G-6-P is diverted to the PPP, it will undergo a series of oxidations and will ultimately fuel and aid in the synthesis of ribose-5-phosphate and erythrose 4-phosphate, precursors for nucleotides and amino acids, respectively (DeBerardinis et al., 2008). If G-6-P continues through glycolysis, it will eventually be converted into two ATP molecules and two pyruvates. The pyruvate molecules undergo dehydrogenation, which results in one molecule CO<sub>2</sub>, one molecule NADH and one molecule acetyl CoA. The acetyl CoA will be shuttled into the TCA cycle by carnitine palmitoyltransferase 1A (CPT1a).

The TCA cycle occurs within the inner membrane of the mitochondria and is responsible for the majority of cellular oxidation (Akram, 2014). When acetyl CoA enters the TCA cycle, the acetyl group is transferred to oxaloacetate, creating citric acid. Citric acid is dehydrogenated to form a-Ketoglutarate, which also undergoes dehydrogenation to form succinate. Succinate is converted back into oxaloacetate, which can accept the acetyl group from acetyl CoA, finishing the cycle (Akram, 2014; Martínez-Reyes & Chandel, 2020). The eight steps of the TCA cycle result in three NADH molecules, one GTP and one FADH<sub>2</sub> molecule. NADH and FADH<sub>2</sub> transfer the electrons to the electron transport chain where they pass through a series of electron

acceptor and donor molecules (Martínez-Reyes & Chandel, 2020). As the electrons pass through these molecules, they fall into lower energy states. The energy loss pumps protons across the membrane, generating a proton gradient. The proton gradient generates energy for ATP synthetase to phosphorylate ADP to ATP.

Fatty acids support the creation of lipid material in the cell and is crucial for the formation of cellular membranes. Fatty acid synthesis starts when acetyl-CoA and malonyl-CoA, intermediates from the TCA cycle, are converted into palmitate by FASN. Palmitate can be metabolized into long chain fatty acids that can be used for membrane synthesis or converted into lipid droplets (Sanchez & Lagunoff, 2015). Cells can utilize the fatty acids in these lipid droplets for energy. Fatty acid oxidation is the process in which fatty acids in lipid droplets can be broken down for membrane generation or for energy acquisition (Sanchez & Lagunoff, 2015). Each molecule of fatty acid undergoes beta oxidation, a process in which carbons are removed from the carboxyl end of fatty acids, resulting in a molecule of acetyl CoA. Acetyl CoA is transported to the mitochondria by CPT1a where it enters the TCA cycle.

### *1.1d DENV induced metabolism shifts*

Viruses trigger metabolic reprogramming in host cells to access macromolecules needed for viral replication and virion production (Goodwin, Xu, & Munger, 2015; Thaker, Ch'ng, & Christofk, 2019). Virus infected cells increase the rate of glycolysis, which produces increased levels of macromolecules for virion biosynthesis (Sanchez & Lagunoff, 2015; Thaker et al., 2019). Viruses also regulate rates of lipid metabolism to increase availability of ATP, which aids in viral replication (A. P. Bhatt et al., 2012; Syed, Amako, & Siddiqui, 2010).

Increased glucose metabolism increases ATP and biosynthetic precursors for virus genome replication (Sanchez & Lagunoff, 2015). Upon infection, DENV2 upregulates the

expression of glycolytic enzymes, GLUT1, HKI and HKII (Fontaine et al., 2015; Butler et al., 2020). The increased expression of these genes is correlated with increases in viral replication, indicating that glycolysis is necessary for viral replication (Butler et al., 2020; Fontaine, 2015). Furthermore, inhibition of glycolysis decreases viral RNA synthesis and infectious particle production (Fontaine et al., 2015). DENV also increases glucose metabolism for an energy source for oxidative phosphorylation (Fernandes-Siqueira et al., 2018).

DENV2 increases lipid metabolism to aid in viral replication, virion production and packaging (Butler et al., 2020; Fernandes-Siqueira et al., 2018; Heaton & Randall, 2010). DENV2 alters fatty acid oxidation and synthesis by control of FASN (Heaton et al., 2010). Specifically, DENV2 NS3 recruits FASN to sites of viral replication to stimulate fatty acid synthesis. This leads to a remodeling of membranes and establishment of replication complexes (Heaton et al., 2010). Furthermore, loss of acyl-CoA thioesterase, an enzyme that processes fatty acyl CoA, results in decreased DENV RNA and infectious particle production (St Clair et al., 2022). DENV2 induces lipophagy to release free fatty acids from lipid droplets for beta-oxidation and membrane production for ER expansion and the energy demands of replication (Jordan & Randall, 2017; Zhang et al., 2018). To respond to increased energy demands, DENV also increases oxidative phosphorylation and mitochondrial respiration (Butler et al., 2020).

## **1.2 Host response to infection**

The inflammatory response is one of the first lines of defense the body mounts against a pathogen. Inflammation is initiated once DENV single stranded RNA is recognized by cellular sensors, mitochondrial antiviral signaling protein (MAVS) and retinoic acid-inducible gene

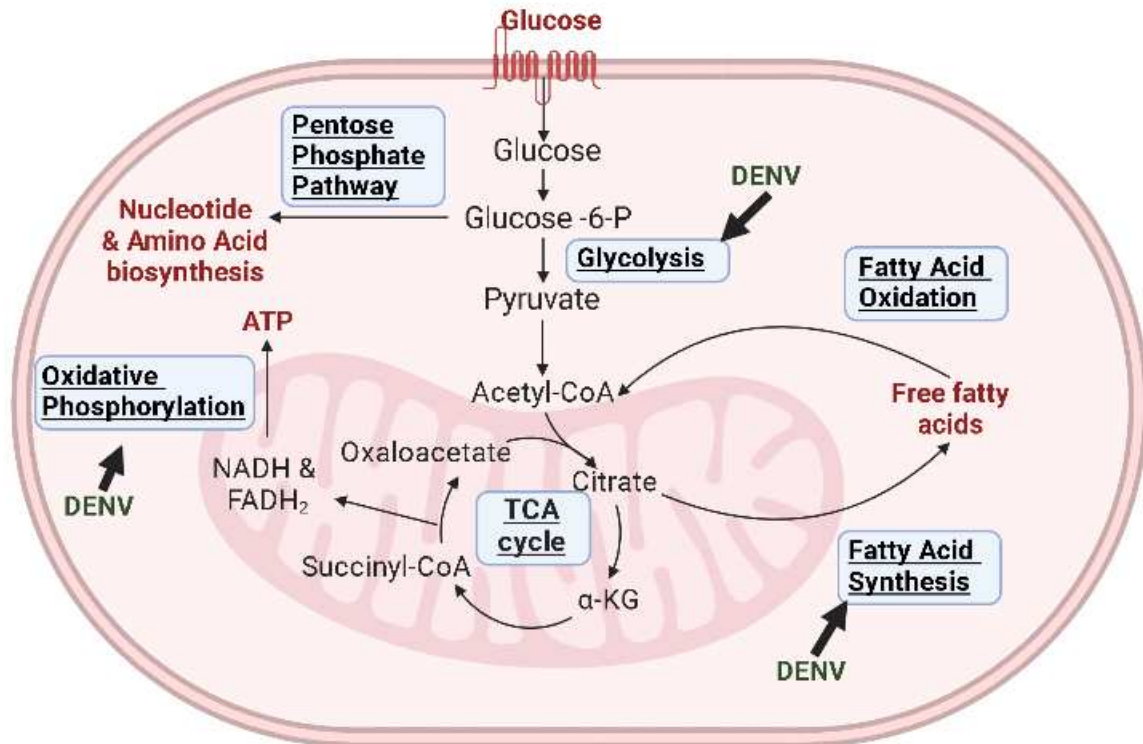


**Figure 1.2: An overview of cellular metabolism.** Glucose enters the cell through a glucose transporter and is converted into Glucose -6-phosphate by hexokinase enzymes. From here it can enter the pentose phosphate pathway, where it will fuel the synthesis of amino acid and nucleotides. If the G-6-P molecule continues through glycolysis, it will ultimately be converted into acetyl CoA. Once inside the mitochondria, the acetyl group is transferred to oxaloacetate to create citrate during the TCA cycle. Citrate will be broken down through a series of decarboxylation and oxidations, which result in NADH and FADH<sub>2</sub>. These molecules will donate their electrons electron transport chain, which will create a proton gradient, that can provide energy to reactions like the phosphorylation of ADP to ATP. DENV has been shown to alter glycolysis, fatty acid synthesis and oxidative phosphorylation during infection. Figure made using BioRender.com.

1(RIG-I) (Nanaware et al., 2021). This detection leads to the activation of monocytes, and macrophages, which secrete pro-inflammatory mediators, such as tumor necrosis factor alpha (TNF $\alpha$ ) and C-X-C motif chemokine ligand 10(CXCL10) (Bennett et al, 2018). Natural killer (NK) cells, which lyse infected cells, are recruited to the site of infection by TNF $\alpha$  and CXCL10. NK cells are critical in preventing DENV replication by initiating the interferon response early in

infection (Nanaware et al., 2021; Vivier et al., 2008). Neutrophils are recruited to the site of infection by the secretion of interleukin 8 (IL-8), TNF $\alpha$  and interferon beta (IFN $\beta$ ). These cells phagocytize pathogens, produce reactive oxygen species (ROS) that kill pathogens and clear infected cells (Rosales, 2018). Inflammatory cytokines and chemokines, as well as the recognition of PAMPS, activate inflammatory macrophage and dendritic cells (DCs) (Mosser & Edwards, 2008; Murray, 2017). These cells are antigen presenting cells (APCs) whose main function during inflammation is to phagocytose, process and present pathogens to T cells in the lymph nodes (Barker et al., 2002). Macrophage and DCs will migrate to the lymph nodes from the site of infection and present antigens to CD4 $^+$  T cells through MHC class II molecules (Barker et al., 2002). In addition to antigen presentation, macrophage and DCs secrete interferon gamma (IFN $\gamma$ ) to aid in the activation of effector T cells. The antigen presentation, coupled with binding of MHC class II and the binding of IFN $\gamma$  onto the interferon gamma receptor (IFN $\gamma$ R) on T cells, activate naive CD4 $^+$  T cells to effector CD4 $^+$  T cells (Castro et al., 2018).

Effector T cells secrete interleukin 2 (IL-2) and IFN $\gamma$ . IFN $\gamma$  further activates macrophage (in a positive feedback loop) and activates cytotoxic T cells (CTLs) in combination with IL-2 (Castro et al., 2018). CTLs recognize infected cells via binding of MHC class I and respond to infected cells by secreting perforins and granzymes, which induce apoptosis (Ito & Seishima, 2010). The secretion of IL-2 and IFN $\gamma$  by effector CD4 $^+$  T cells also activates B cells. Upon activation, B cells produce nonspecific IgM, which can activate the complement pathway and lead to opsonization and death of infected cells (Quartier et al., 2005). Next, DENV specific IgGs, secreted by B cells, bind to the DENV NS1, E and prM proteins (Nanaware et al., 2021). Macrophage recognize the bound antigen-antibody complex via the Fc region of the IgG molecule and phagocytose the complex (Modhiran, Kalayanarooj, & Ubol, 2010).

Clearance of apoptotic cells by neutrophils and macrophage initiates the resolution of inflammation (Ortega-Gómez et al., 2013). During this resolution, cells are shifting from a pro-inflammatory state to an anti-inflammatory state. Pro-inflammatory chemokine and cytokine gene expression is being inhibited, while chemokines in the extracellular space are being sequestered (Ortega-Gómez et al., 2013; Sugimoto et al., 2016). Importantly, during resolution macrophage are reprogramed from an inflammatory phenotype to an anti-inflammatory phenotype (Ortega-Gómez et al., 2013; Sugimoto et al., 2016).

### *1.2a Macrophage role during infection*

Macrophage have three main functions in inflammation: phagocytosis, antigen presentation and immunosuppression (Fujiwara & Kobayashi, 2005). The first two functions are primarily carried out by classically activated macrophage (M1), while immunosuppression is carried out by alternatively activated macrophage (M2) (Sica & Mantovani, 2012).

M1 macrophage are pro-inflammatory macrophage involved in the initiation of inflammation. These inflammatory macrophage combat viral and bacterial infection by producing ROS, phagocytosing pathogens and inducing the type 1 and type 2 interferon response (Murray, 2017; Nikonova et al., 2020). M1 macrophage are activated by inflammatory mediators  $IFN\gamma$  and TNF in combination with the binding of PAMPS on TLRs (Mosser & Edwards, 2008; Murray, 2017).  $IFN\gamma$  leads to the activation of the Janus kinase (JAK)-STAT pathway, which is required for phagosome maturation and phagocytosis (Albieri et al., 2005; Zhu, Zhou, Jiang, & Zhang, 2015). In addition to phagocytosis,  $IFN\gamma$  stimulates monocyte chemoattractant protein-1 (CCL2)-dependent migration to lymph nodes (Hu, Park-Min, Ho, & Ivashkiv, 2005). Once in the lymph node, M1 macrophage present antigens to T cells via MHC-II receptors and activate naïve T cells to effector T cells (Murray, 2017). Within the context of DENV infection, an influx

of M1 macrophage in the brains of infected mice is associated with severe viral encephalitis (Jhan et al., 2021). Furthermore, CXCL10, a chemokine secreted by M1 macrophage, can decrease viral infection of cells by competing for a co-receptor DENV uses for cell entry. (Ip & Liao, 2010).

M2 macrophage are immunosuppressive macrophage involved in the resolution of inflammation. These anti-inflammatory macrophage aid in inhibiting the production of inflammatory mediators, suppression of antigen presenting M1 macrophage and promotion of wound healing (Gordon & Martinez, 2010; Yu et al., 2022). M2 macrophage are activated by interleukin 4 (IL-4) and interleukin 13 (IL-13) (Gordon & Martinez, 2010; Murray, 2017). M2 macrophage have 4 subtypes; M2a, M2b, M2c and M2d. Briefly, M2a macrophage exert immunomodulatory functions; M2b macrophage functions are involved in the Th2 response and aid in the encapsulation of parasites; M2c are involved in tissue repair; and M2d are tumor associated macrophage that is associated with the tumor microenvironment (Sica & Mantovani, 2012; Yao, Xu, & Jin, 2019). Treating cells with IL-4 induces the expression of both TGF $\beta$  and IL-10, two key regulators of the anti-inflammatory response. TGF $\beta$  promotes M2 polarization by inducing the expression of anti-inflammatory genes, such as *arg1* (Gong et al., 2012). TGF $\beta$  also suppresses the macrophage inflammatory phenotype by suppressing expression of inflammatory cytokines like TNF $\alpha$  and IL-12 (Zhang et al., 2015). IL-10 decreases inflammatory cytokine gene expression and decreases MHC class II on the surface of DC, halting the activation of T effector cells (Murray, 2006; Saraiva & O'Garra, 2010). Due to the strong immunosuppressive role in inflammation, many viruses promote M2 polarization during infection (Yu et al., 2022). M2 macrophages have also been associated with increasing levels of bleeding in patients infected with DENV (Lee et al., 2018). IL-10 is also associated with severe dengue illness and is

considered a biomarker for severe illness (Pé Rez et al., 2004; K.-M. Soo et al., 2017; Tsai et al., 2013).

### *1.2b Antibody dependent enhancement and vascular leakage*

One of the unique features of DENV pathogenesis is that infection with one serotype does not provide lifelong immunity against another serotype. In fact, infection with subsequent serotypes is a risk factor for disease severity (Halstead, 2007). During DENV clearance and resolution of disease, antibodies bind to DENV, and facilitate cell entry by Fc gamma receptor (FcγRII) mediated endocytosis (Diamond & Pierson, 2015). Since the virus is neutralized, the macrophage can target the viral particle for degradation. In an antibody dependent enhancement (ADE) model, the antibodies that bind DENV are non-neutralizing or sub-neutralizing and cannot effectively inhibit replication in macrophage (Lee et al., 2020). Once inside, the virus can subvert detection and degradation by negatively regulating the TLR pathway (Modhiran et al., 2010; Narayan & Tripathi, 2020). DENV also upregulates the production of IL-10 and IL-6, which inhibits the JAK/STAT pathway and blocks the interferon response (Chareonsirisuthigul, et al, 2007; Tsai et al., 2014). The overproduction of IL-10 in ADE is associated with increased vascular leakage in patients and can lead to tissue damage and multiple organ failure (Nanaware et al., 2021).

### *1.2c Interferon response to infection*

After infection following mosquito bite, DENV will interact with keratinocytes and resident dendritic cells, called Langerhans cells, and macrophage (Cerny et al., 2014; S. J. L. Wu et al., 2000). Since dendritic cells and macrophage are cell targets for DENV, the virus will bind cell receptors and be endocytosed (Nikitina et al., 2018). Within the endosome, infected cells recognize PAMPs from the virus particle. Toll-like receptors 3 and 7 (TLR3/7) are pattern

recognition receptors (PRR) that reside in the endosomal compartment and recognize viral RNA and double stranded RNA (dsRNA)(Liang et al., 2011; Urcuqui-Inchima, Cabrera, & Haenni, 2017). The recognition of viral RNA by TLR 3, 7 and 8 activates adaptor proteins, myeloid differentiation primary response gene 88 (MyD88) and Toll/IL-1 receptor domain-containing adapter-inducing interferon- $\beta$  (TRIF), which ultimately trigger the transcription of type 1 interferon mediators (Liang et al., 2011; Sariol et al., 2011). These mediators are secreted by the infected cells and bind onto the type 1 interferon  $\alpha/\beta$  receptor (IFNAR) on nearby cells, which activates the tyrosine kinase 2 (TYK2) and JAK1 subunits on the cytoplasmic side of the receptors. The TYK2 and JAK1 kinases phosphorylate STAT 1 and 2, which then form a heterodimer. This heterodimer then forms a complex with IFN-regulatory factor 9 (IRF9) (the complex is called the IFN-stimulated gene factor 3 (ISGF3)) and translocates to the nucleus. In the nucleus, ISGF3 binds to IFN-stimulated response elements (ISREs) on DNA to initiate transcription of interferon stimulated genes (ISGs) (Behrmann et al., 2004; Plataniias, 2005; Seif et al., 2017).

Infection of macrophage also triggers the type 2 interferon response, which is similar to the type 1 response. IFN $\gamma$  binds to a type 2 interferon receptor (IFNGR) which has two JAK subunits (Plataniias, 2005). The JAK kinases phosphorylate STAT1, which then forms a homodimer. The STAT homodimer translocates to the nucleus, where it binds IFN- $\gamma$ -activated sites (GAS) on the DNA and initiates transcription of ISGs (Plataniias, 2005). The binding of IFN $\gamma$  can also cause STAT1 and STAT2 to dimerize and undergo the same signaling cascade and binding of ISREs as in the type 1 response (Schroder, Hertzog, Ravasi, & Hume, 2004). Transcription of IFN $\gamma$  is not only important for regulating intracellular anti-viral mechanisms, but it also primes type 1 T cells (Schroder et al., 2004). Within the context of macrophages, IFN $\gamma$

induces nitric oxide (NO) and ROS production and increases receptor mediated phagocytosis (A. J. Lee & Ashkar, 2018; Schroder et al., 2004)

Since the interferon response is so potent, DENV has multiple mechanisms to subvert and decrease interferon signaling. DENV NS5 binds STAT2 and targets it for proteolytic degradation (Ashour et al., 2009). NS4A and NS4B prevent activation of STAT1 (Muñoz-Jordán et al., 2005). The degradation of STAT2, as well as the inactivation of STAT1, disrupts the formation of IRF9 and prevents the transcription of ISGs (Ashour et al., 2009). The NS2B/NS3 protease disrupts the cGAS–STING pathway. cGAS doesn't detect DENV RNA directly, but instead detects the mitochondrial DNA leaked into the cytoplasm by damaged mitochondria during infection (Tremblay, Freppel, Sow, & Chatel-Chaix, 2019; West et al., 2015). cGAS then produces the second messenger cyclic GMP-AMP (cGAMP), which activates the STING protein. STING activates TANK-binding kinase 1 (TBK1), which will ultimately lead to the transcription of interferon genes (Decout, Katz, Venkatraman, & Ablasser, 2021). By targeting STING for degradation, the virus inhibits the induction of ISGs (Aguirre et al., 2012).

### *1.2d Macrophage immunometabolism*

Once activated, immune cells shift their metabolism to fuel inflammatory or anti-inflammatory functions. The process of changing cellular metabolism in response to environment is referred to as immunometabolism (Buck, Sowell, Kaech, & Pearce, 2017). Inflammatory cells upregulate glycolysis to produce inflammatory chemokines and cytokines, while anti-inflammatory cells upregulate oxidative phosphorylation (O'Neill, Kishton, & Rathmell, 2016).

In response to infection, inflammatory macrophage (M1) rapidly shift their metabolism to produce inflammatory chemokines and cytokines. While glycolysis only produces 2 ATPs per glucose molecule, it is a metabolic pathway that can quickly provide energy and byproducts for

inflammatory mediators (Nagy & Haschemi, 2015). Furthermore, glycolytic enzymes play dual roles in immunometabolism; they convert glucose to pyruvate, but also help regulate the inflammatory immune response. HK1, the first enzyme in glycolysis, promotes inflammasome activation/ IL-1 $\beta$  secretion through an mTOR-dependent pathway or by acting as a PRR (Moon et al., 2015; Wolf et al., 2011). Glycolytic enzymes have also been shown to regulate anti-viral responses. For example, 6-phosphofructo-2-kinase/fructose-2,6-biphosphatase (PFKFB) induces the phagocytosis and removal of VSV infected cells (Jiang et al., 2016). Late glycolytic enzymes also play a role in inflammation. Enolase (ENO), the penultimate glycolytic enzyme, is expressed on inflammatory macrophages and contributes to the production of inflammatory cytokines (Bae et al., 2012; Guillou et al., 2016). Pyruvate kinase M2 (PKM2), the last enzyme in glycolysis, forms a complex with hypoxia-inducible factor-1 alpha (HIF1 $\alpha$ ), stabilizing the protein. HIF1 $\alpha$  induces the expression of interleukin-1 beta (IL-1 $\beta$ ) and aids in macrophage migration (Semba et al., 2016; Van den Bossche, O'Neill, & Menon, 2017).

M1 macrophage also upregulate the PPP, which generates NADPH. NADPH will provide electrons to molecular oxygen, creating ROS (Sedeek, Nasrallah, Touyz, & Hébert, 2013). In addition, NADPH also helps to generate nitric oxide, another anti-microbial product secreted by M1 macrophage (Palmieri et al., 2020).

M1 macrophage have a dysregulated TCA cycle. The TCA cycle in M1 macrophage is disrupted in two places: after citrate and after succinate (Van den Bossche et al., 2017). Increased citrate levels aid in nitric oxide production (Infantino et al., 2011). In addition, the accumulation of citrate generates itaconate via immune responsive gene 1. Itaconate is suggested to have anti-microbial properties (Michelucci et al., 2013; O'Neill, 2015). Itaconate accumulation further dysregulates the TCA cycle by inhibiting succinate dehydrogenase, leading to an accumulation

of succinate. Succinate is an inflammatory signal that induces IL-1 $\beta$  expression by stabilizing HIF1 $\alpha$  (Tannahill et al., 2013). Lastly, M1 macrophage have a reverse electron transport chain at complex 1, which drives the production of ROS (Mills et al., 2016).

In contrast to M1, M2 anti-inflammatory processes are very energy intense and require increased ATP (Shyh-Chang et al., 2013). Therefore, M2 macrophage primarily utilize oxidative phosphorylation, a process that produces around 30 molecules of ATP per glucose (Van den Bossche et al., 2017). Anti-inflammatory cells are thought to fuel oxidative phosphorylation through fatty acid oxidation. While the exact mechanisms remain unclear, increased fatty acid oxidation plays a role in regulating the anti-inflammatory functions in M2 cells. For example, overexpression of fatty acid transport protein 1, an enzyme in fatty acid oxidation, leads to decreases in inflammation (Johnson et al., 2016). Furthermore, increases in CPT1a are associated with the anti-inflammatory properties of M2 cells. Constitutive expression of CTP1a reduced the generation of inflammatory cytokines (Malandrino et al., 2015). In contrast, blocking CPT1a enzyme activity by using etomoxir, prevents cells from polarizing to M2 macrophage (Divakaruni et al., 2018). Although increased glycolysis is a hallmark of M1 macrophage, M2 macrophage depend on glycolysis to fuel the TCA cycle and mitochondrial respiration (O'Neill et al., 2016). Furthermore, blocking glycolysis reduces gene expression of M2 markers, suggesting glycolysis is required for M2 function (Van den Bossche et al., 2017).

### **1.3 CDK8 and CDK19**

Cyclin dependent kinase 8 (CDK8) and its activating cyclin, Cyclin C, are components of the Mediator complex (Soutourina, 2018). The mediator complex is a large complex required for transcription of RNA polymerase II (RNAP II) genes. The mediator complex does this by

transducing signals from transcription activators bound to the enhancer regions of DNA to RNAP II complexes (Rovnak & Quackenbush, 2022; Soutourina, 2018). CDK8, Cyclin C and

### Classically activated macrophage (M1) Alternatively activated macrophage (M2)

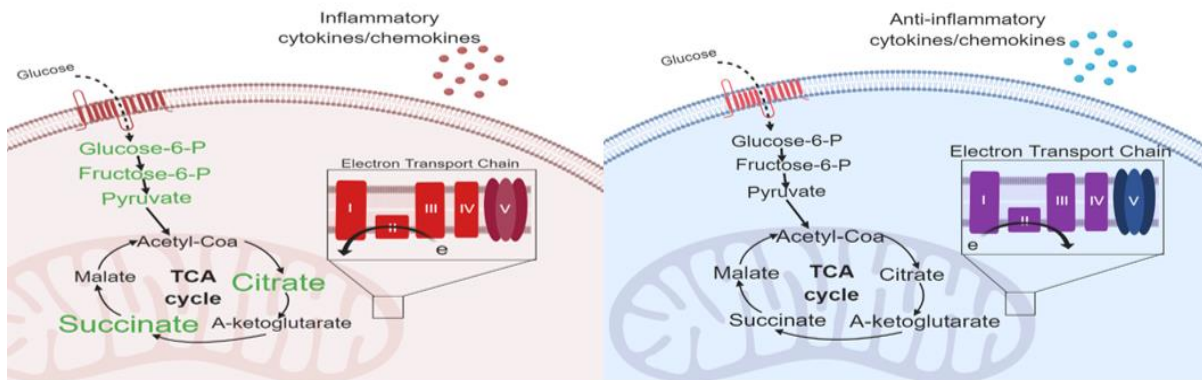


**Figure 1.3: Macrophage phenotypes.** The left side of the figure depicts M1 metabolism, which is defined by an increase in glycolysis and a broken TCA cycle, both of which produce an increase in anti-inflammatory chemokines and cytokines. The right side of the figure depicts M2 metabolism, defined by an increase oxidative phosphorylation, which results in the production and secretion of anti-inflammatory chemokines and cytokines. Figure made using BioRender.com

two other mediator proteins, Med12 and Med13, make up the CDK8 kinase module. The CDK8 module is required for the induced expression of a subset of genes in response to a disruption in cellular homeostasis. This module can phosphorylate the Carboxy Terminal Domain (CTD) of RNAP II to control transcriptional pausing and elongation (Conaway & Conaway, 2013). The CDK8 module can reversibly dissociate from RNAPII and phosphorylate transcription factors to initiate transcription (Knuesel et al, 2009). CDK8 kinase module can also regulate chromatin structure by phosphorylating histone H3 at serine 10 (Knuesel et al., 2009). The CDK8 kinase module phosphorylates transcription factors in response to cell stress and reprograms cellular metabolism, cell proliferation and immune signaling (Donner et al., 2010; Galbraith et al., 2017; Steinparzer et al., 2019; Zhao et al., 2012). CDK19, a CDK8 homolog, associates with Med12L and Med13L and has similar function to CDK8 (Daniels et al., 2013). CDK19 shares 91%

homology with CDK8 and only differs at the C terminal tail, suggesting different interaction partners. For example, CDK8, but not CDK19, is required for the induction of HIF1 $\alpha$  genes during hypoxia (Galbraith et al., 2013).

In times of cellular stress, CDK8 is known to have regulatory functions on metabolism, serum response and immune signaling. CDK8 has been identified as an oncogene that plays a role in tumor development in colon and breast cancer (Firestein et al., 2008; Knab et al., 2021; McDermott et al., 2017). Though the exact mechanism remains unclear, CDK8 has been shown to modulate beta catenin activity, and suppression of kinase function leads to inhibition of colon cancer cell proliferation (Firestein et al., 2008). CDK8 kinase activity has been shown to regulate aspects of cellular metabolism (Galbraith et al., 2017a; X. Zhao et al., 2012). CDK8 is a regulator of glycolysis, where kinase activity is required for the transcription of multiple glycolytic genes and inhibition of CDK8 kinase activity decreases glucose uptake and glycolytic capacity (Galbraith et al., 2017a). In contrast, CDK8 is a negative regulator of lipophagy (D. Feng et al., 2015; X. Zhao et al., 2012). CDK8 phosphorylates sterol regulatory-element binding proteins 1c (SREBP1c), a transcription factor that regulates lipid metabolism, targeting it for ubiquitination and degradation (X. Zhao et al., 2012).

### *1.3a CDK8 during virus infection*

Previous work in our lab has investigated the role of CDK8/19 during virus infection. Walleye dermal sarcoma virus (WDSV) is a retrovirus that causes walleye dermal sarcoma, a seasonal tumor in walleye fish (Rovnak & Quackenbush, 2010). WDSV encodes a retroviral cyclin (RV cyclin), a viral protein that has a small amount of homology to cell cyclins and binds to host transcriptional factors like TATA binding protein-associated factor 9 (TAF9) (Brewster et al., 2011; Quackenbush et al., 2009). Binding transcriptional factors allows RV cyclin to alter

host gene expression to promote cell proliferation and tumor development (Brewster et al., 2011; Quackenbush et al., 2009; Rovnak et al., 2012). RV cyclin also binds CDK8 and enhances its kinase activity to increase transcriptional elongation, gene expression and cell proliferation (Birkenheuer et al., 2015; Brewster et al., 2011; Rovnak et al., 2012).

CDK8 kinase activity aids in DENV replication (Butler et al., 2020). CDK8 gene expression is increased throughout DENV replication and correlates with increases in HK2, a marker for glycolysis, and LC3, a marker for lipophagy. Chemical inhibition of CDK8/19 leads to a decrease in viral replication and decreases in HK2 and LC3 gene expression and protein levels (Butler et al., 2020). Furthermore, treatment with Senexin B, a chemical inhibitor of CDK8/19 kinase activity, decreases mitochondrial respiration and glycolysis (Butler et al., 2020).

### *1.3b CDK8 regulates immune function*

CDK8 controls the interferon response and regulates inflammatory cytokine gene induction by phosphorylating STAT1, STAT3 AND STAT5 (Akamatsu et al., 2019; Bancerek et al., 2013; Martinez-Fabregas et al., 2020). Specifically, CDK8 phosphorylates STAT1 at serine 727 in response to IFN $\gamma$  to differentially regulate the transcription of IFN $\gamma$  response genes (Bancerek et al., 2013). CDK8 and CDK19 have been shown to be mechanistically different in response to IFN $\gamma$ , where CDK8 acts in a kinase dependent manner, CDK19 activity is kinase independent, resulting in regulation of different subset of genes (Steinparzer et al., 2019a). In addition to STAT1, CDK8 mediates nuclear factor  $\kappa$ b (NF- $\kappa$ b) induced transcription (Chen et al., 2017). Upon activation of NF- $\kappa$ b, CDK8 is co-recruited with NF- $\kappa$ b to promoters of NF- $\kappa$ b response genes IL-8, CXCL1 and CXCL2, inducing transcription (Chen et al., 2017).

NK immune surveillance and cytolytic function is also regulated by CDK8/19. CDK8 phosphorylates STAT1 within NK cells, which suppresses the production of cytolytic mediators, perforin and granzyme B (Putz et al., 2013). Inhibition of CDK8/19 kinase activity results in an increase in these mediators. The increase in these mediator leads to diminished cancer cell size and an increase in survival in melanoma and leukemia mouse models (Hofmann et al., 2020; Witalisz-Siepracka et al., 2018). Furthermore, knockdown of CDK8 inhibits tumor growth and prevents metastasis in a NK cell mediated fashion (Knab et al., 2021).

In macrophage and Tregs, inhibition of CDK8 kinase activity enhances anti-inflammatory gene expression. CDK8 is a negative regulator of IL-10, where chemical inhibition of CDK8/19 results in an increase in IL-10 protein secretion from macrophage (Johannessen et al., 2017). CDK8/19 phosphorylation of STAT5, prevents it from binding and activating transcription of the *Foxp3* gene (Akamatsu et al., 2019). Inhibition of CDK8/19 kinase activity results in increased retention of STAT5 in the nucleus, leading to induction of *Foxp3* gene expression and suppression of auto immune diseases in mouse models (Akamatsu et al., 2019; Guo, Wang, Lv, Wan, & Zheng, 2019)

## CHAPTER 2: OPTIMIZING MACROPHAGE DIFFERENTIATION AND POLARIZATION IN A THP-1 MONOCYTE CELL LINE

### 2.1 Summary

Macrophage are among the first cells to become infected with DENV2. These cells are crucial in the pathogenesis of DENV infection, as they can either drive a potent anti-viral response early in infection or further enhance pathogenesis. One of the most widely used cell lines to study macrophage, THP-1 cells, are a monocytic cell line that can be differentiated into macrophage and subsequently polarized into two different macrophage phenotypes: M1 macrophage and M2 macrophage. In this study we sought to optimize methods for differentiating and polarizing THP-1 cells. We found that differentiating cells with low concentrations of PMA for a longer duration of time resulted in increased expression of gene of *CD11b*, a marker of macrophage maturity. We also optimized the duration of treatment with interferon gamma (IFN $\gamma$ ) or interleukin 4 (IL-4) to polarize cells towards an inflammatory (M1) or anti-inflammatory (M2) phenotype, respectively. When polarizing cells towards different macrophage phenotypes, a shorter incubation in IFN $\gamma$  resulted in M1-like macrophages, while longer incubation in IL-4 resulted in M2-like macrophage.

### 2.2 Introduction

Dengue virus (DENV) infects monocytes and macrophage, which play a significant role in pathogenesis (Lee et al., 2018; Soo, Tham, Khalid, Basir, & Chee, 2019). In response to DENV infection, macrophage secrete chemokines and cytokines, an excess of which can cause a cytokine storm. Overproduction of cytokines, IL-6 and IL-10, lead to tissue damage and vascular leakage, which can ultimately lead to multiple organ failure and possibly death (Lee et al., 2018;

Soo et al., 2019; Tsai et al., 2013). By disseminating the virus throughout the body, macrophage play an important role in viral pathogenesis.

Macrophage phenotype is also an important factor to consider while studying flavivirus macrophage interactions. The two main subsets of macrophage, classically activated macrophage and alternatively activated macrophage, have different functions during inflammation.

Classically activated macrophages (M1) are pro-inflammatory and are highly phagocytic (O'Neill & Pearce, 2016; Van den Bossche et al., 2017). They secrete pro-inflammatory chemokines and cytokines, such as IL-12, IL-1 $\beta$  and TNF $\alpha$ . Glycolysis is upregulated in M1 cells to produce pro-inflammatory mediators, such as reactive oxygen species and nitric oxide (Buck et al., 2017). Alternatively activated macrophages (M2) are immunosuppressive and resolve inflammation (Gordon & Martinez, 2010; Van den Bossche et al., 2017). They secrete anti-inflammatory proteins and aid in wound healing. Oxidative phosphorylation is upregulated in M2 cells (Buck et al., 2017). Macrophage phenotype has been shown to impact flavivirus dynamics, with cells treated with IL-4 cells supporting DENV replication and M1 cells being more resistant to DENV infection (Diamond & Harris, 2001; Schaeffer et al., 2015).

Cultured cells are an important tool for studying the molecular mechanisms involved in virus-pathogen interactions. The THP-1 monocytic cell line is commonly used as a model system for studying macrophage function and biology. Unlike mouse or human peripheral blood mononuclear cells (PBMC), THP-1 cells do not require the isolation of cells from the blood, making them easier to obtain and culture (Aldo et al., 2013). Importantly, macrophage-like cells can be differentiated from THP-1 monocytic cells. THP-1 cells also have cell markers and secrete cytokines similar to that of monocytes and macrophages isolated from mouse or human donors (Auwerx, 1991; Kohro et al., 2004). To differentiate THP-1 cells from monocytes into

macrophages, cells are treated with  $\alpha$  25- dihydroxy vitamin D3 (vD3), macrophage colony stimulating factor (M-CSF), or phorbol 12-myristate- 13 acetate (PMA), with PMA being the most widely used (Chanput, Mes, & Wichers, 2014). Similar to macrophage obtained from mouse or human donors, PMA differentiated THP-1 macrophage have lower proliferation, higher phagocytic capabilities, and higher expression of the macrophage surface cell markers, CD11b and CD14, compared to their non-differentiated monocytic counterparts (Aldo et al., 2013; Daigneault et al., 2010). Furthermore, the morphology of cells treated with PMA is similar to mature macrophage in terms of adhesion and expansion of lamellipodia than their non-differentiated counterparts (Kawakatsu et al., 2019; McWhorter et al., 2013).

The concentration of PMA used to differentiate THP-1 cells varies greatly, with concentrations ranging from 5-400 ng/ml (Starr et al., 2018). A number of studies use 100 ng/ml of PMA to differentiate THP-1 cells, however, a concentration of 5 ng/ml of PMA is sufficient to differentiate cells while maintaining key macrophage functions, such as detecting and responding to antigens (Park et al., 2007). However, culturing cells in the presence of PMA activates protein kinase C (PKC), which could activate inflammatory signaling (Jiang & Fleet, 2012). Therefore, it is necessary to rest macrophage in media without PMA prior to commencing any manipulations (Baxter et al., 2020; Castrillo et al., 2001). Culturing conditions become more complicated when studying virus-pathogen interactions, where the concentration, duration of PMA and resting period after PMA, as well as the kinetics of viral replication, need to be considered. Therefore, the resting period after PMA varies within published studies, with durations ranging from 24-hours to 6 days (Maeß et al., 2010; Maeß et al., 2014). PMA treated THP-1 cells can be polarized to M1 and M2 cells, with multiple studies having found that treating PMA-differentiated THP-1 cells with 20 ng/ml of IFN $\gamma$  polarizes cells into M1

phenotype, while treatment with 20 ng/ml IL-4 polarizes cells into M2 (Gordon & Martinez, 2010; Tedesco et al., 2018).

Since macrophage play an important role in flavivirus replication and pathogenesis (Nikitina et al., 2018), we sought to develop a working model for virus infection. To investigate replication of flaviviruses in a macrophage model system, we utilized THP cells to establish culture conditions to differentiate monocytes into macrophage and polarize cells towards an M1 or an M2 phenotype. In this study, we investigate the impact of PMA concentration and duration on macrophage differentiation. Furthermore, we optimize duration of polarization towards an M1 or M2 phenotype by measuring inflammatory or anti-inflammatory gene markers and cellular metabolism. We used these data to develop a working model to study ZIKV and DENV replication in THP-1 cells, as well as probe the impact of viral replication on macrophage gene expression and metabolism.

## **2.3 Methods and Materials**

### *2.3a: Cell culture and PMA stimulation*

THP-1 human monocytic cells (TIB-202™, Manassas, VA, US) were cultured in RPMI-1640 media, supplemented with 10% fetal bovine serum (FBS), 1% non-essential amino acids, 1% L-glutamine, 1% penicillin-streptomycin, 25 mM HEPES and 0.05mM 2-mercaptoethanol in a 37°C incubator with 5% CO<sub>2</sub>.  $2 \times 10^6$  cells. Cells were plated in T-25 flasks and treated with indicated concentration of phorbol 12-myristate 13-acetate (PMA) to induce differentiation into macrophages. Cells were incubated with 10 ng/ml of PMA for 0, 24, 48, 72 or 96 hours.

### *2.3b: Polarization of PMA treated THP-1 cells*

THP-1 monocytes plated at  $2 \times 10^6$  cells in T-25 flasks were stimulated with 10 ng/mL PMA. Twenty-four hours later, media with PMA was removed, and cells were washed with D-

PBS. Cells were then treated with either 20 ng/mL interferon gamma (IFN $\gamma$ ) (R & D Systems, Minneapolis, MN, USA) or 20 ng/mL interleukin 4 (IL-4) (R & D Systems, Minneapolis, MN, USA) to polarize them into M1 or M2 phenotypes, respectively.

### *2.3c: DENV infection*

For infection, cells were washed with Dulbecco's phosphate-buffered saline (D-PBS) and incubated with DENV2 (strain 16681) (Kinney et al., 1997) at indicated multiplicities in media for 1 hour at 4°C with rocking. Virus media was removed, cells were washed twice with cold D-PBS, and warmed RPMI-1640 media with 10% FBS was added.

### *2.3d: RNA extraction and qPCR*

At the indicated time points, cells were harvested in TRIzol (Invitrogen, Thermofisher, Waltham, MA, USA), and total RNA was isolated using ZymoGen TRIzol RNA extraction kit according to manufacturer's instructions. cDNA was made using an iScript cDNA synthesis kit (Bio-Rad, Hercules, CA, USA) according to the manufacturer's instructions, and then subjected to qPCR analysis with iQ SYBR green Supermix in a CFX96 real-time PCR system. Primers are listed in Table 1. Relative expression was normalized to a house keeping gene, Ribosomal Protein L37a (RPL37a). For genomic equivalent analysis, Cq values were standardized to ten-fold dilutions of in vitro transcribed DENV2 genomic RNA and subject to qRT-PCR.

### *2.3e Mitochondrial and Glycolytic Stress Tests*

A Seahorse XFe analyzer (Agilent Technologies) was used to measure the oxygen consumption rate (OCR) and extracellular acidification rate (ECAR) based on the mitochondrial stress test (Agilent 103015-100) and glycolysis stress test (Agilent 103020-100), respectively. THP-1 cells were plated at  $4 \times 10^6$  cells in 10 cm<sup>2</sup> dishes with 10 ng/ml PMA. After 24 hours PMA was removed, and cells were polarized with 20 ng/ml IL-4 for 48 hours or 20 ng/ml IFN $\gamma$

**Table 2.1** PCR Primers

Gene	FWD	REV	Source
IL-10	GAC TTT AAG GGT TAC CTG GGT TG	TCA CAT GCG CCT TGA TGT CTG	(X. Huang et al., 2016)
TGFβ1	ACG TGG AGC TGT ACC AGA AAT A	GGC GAA AGC CCT CAA TTT CC	(Shiratori et al., 2017)
CXCL10	CCA GAA TCG AAG GCC ATC AA	CAT TTC CTT GCTAAC TGC TTT CAG	(Qi et al., 2009)
RPL37A	ATTGAAATCAGCCAG CACGC	AGGAACCACAGTGCCAG ATCC	(Maeß et al., 2010)
DC-SIGN	GGATACAAGAGCTTA GCAGGGTG	GCGTGAAGGAGAGGAGT TGC	(Teles et al., 2010)
CD11b	GTGAAGCCAATAACG CAGC	CTCCCATCCGTGATGAC AAC	(Izban, Nowicki, & Nowicki, 2012)
IFNβ	CGCCGCATTGACCAT CTA	GACATTAGCCAGGAGGT TCTCA	(Bender et al., 2015)
DENV2	ACAAGTCGAACAACC TGGTCCAT	GCCGCACCATTGGTCTTC TC	(Butler et al., 2020)

for 12 hours. Cells were then detached from 10 cm<sup>2</sup> dished plates using cell stripper (Corning, Manassas, VA, US), washed with D-PBS, centrifuged at 500g for 5 minutes. Cells were resuspended in 2 ml XF base medium (Agilent Technologies) supplemented with 1 mM pyruvate, 2 mM L-glutamine, and with 10 mM glucose for the mitochondrial stress test. Cells were then counted and plated at a density of  $7.5 \times 10^4$  cells per well in XF96 cell culture microplates with Cell-Tak (Corning, Manassas, VA, US) and spun at 500g for 5 minutes. XF base medium was added for a total amount of 500  $\mu$ l per well. Cells were rested for 20 minutes in a non-CO<sub>2</sub> incubator at 37°C, and then placed in the Seahorse XFe analyzer for analysis. The mitochondrial stress test used sequential injections of oligomycin (1  $\mu$ M), p-trifluoromethoxyphenylhydrazone (FCCP, 1.5  $\mu$ M), and rotenone and antimycin A (0.5  $\mu$ M

each). The glycolysis stress test used sequential injections of glucose (10 mM), oligomycin (1  $\mu$ M), and 2-deoxyglucose (50 mM). Measurements were collected at 5-minute intervals; three times before and after injections and six times after the last injection.

Mitochondrial activity was determined as follows: (1) Basal respiration was calculated using the last rate measurement before injection of oligomycin minus the non-mitochondrial respiration rate (defined as the minimum rate measurement after rotenone/antimycin A injection), (2) ATP production was calculated as the last rate measurement before oligomycin injection minus the minimum rate measurement after oligomycin injection, (3) Maximum respiration was calculated using the maximum rate measurement after FCCP injection minus non-mitochondrial rate, (4) Spare capacity was the maximal respiration minus basal respiration, and (5) Proton leak was the minimum rate measurement after oligomycin injection minus non-mitochondrial respiration. OCR/ECAR ratio based on measurements at basal conditions at 18 minutes.

### *2.3f Statistics*

Statistical analysis was performed on Prism Software version 9.3.1. Statistical significance was calculated using the two-tailed Student's t test or one way ANOVA.

## **2.4 Results**

### *2.4a PMA concentration and timing*

We first wanted to determine the optimal PMA concentration and resting period after treatment to differentiate THP-1 cells. The reported concentration of PMA ranges from 5-400 ng/ml (Park et al., 2007). We sought a concentration of PMA that differentiated the majority of cells but had low levels of cytotoxicity. To determine the amount of PMA needed to differentiate cells, we treated cells with either 10 ng/ml, 50 ng/ml, or 100 ng/ml PMA. Total cellular RNA

was collected at 24 hours post treatment and quantified gene expression by RT-qPCR. We first measured *CD11b*, a gene that encodes a cell surface marker for mature macrophages. An increase of 1.8-fold and 2.0-fold expression of *CD11b* was observed in cells treated with 10 ng/ml of PMA and 50 ng/ml of PMA, respectively, over that measured in untreated cells. Treatment with 100 ng/ml did not change *CD11b* expression (mean fold change over 0 ng/ml = 1.09 +/- 0.11) (Figure 2.1A). Expression of *CD209*, a known receptor for DENV binding and cell entry, followed a similar trend. Treatment with 10 ng/ml and 50 ng/ml resulted in an increase of 3.3-fold and 3.1-fold *CD209* expression, respectively. A slight increase in *CD209* expression (mean fold change over 0 ng/ml = 1.44 +/- 0.18) was measured in cells treated with 100 ng/ml PMA over that of untreated cells. The 10 ng/ml concentration was selected for subsequent experiments.

THP-1 differentiation is also impacted by the length of time cells rest in PMA free media. Longer treatment times have been shown to increase *CD11b* cell surface expression, but also increase cell death (Starr et al., 2018). To determine the best timing for differentiation, we treated cells with 10 ng/ml for 24 hours, then replaced media with PMA free media for 0, 24, 48 or 72 hours. We collected total cellular RNA at the indicated time points post PMA treatment and quantified gene expression by RT-qPCR (Figure 2.1B). *CD11b* and *CD209* gene expression increased throughout the time course, such that there was a 10-fold increase in *CD11b* and a 2.3-fold increase in *CD209* at 72 hours compared to that at 0 hour. (Figure 2.1B).

We used light microscopy to image cells at each collection time point to observe cell morphology throughout treatment. Changes in cell morphology were dependent on resting time, with cells resting for 72 hours exhibiting more extensive differentiation, as defined by the extended cytoplasm and increased adherence (Kawakatsu et al., 2019) (Figure 2.1C). These data

demonstrate that 10 ng/ml of PMA followed by 72 hours of resting in media without PMA is the optimal differentiation protocol.

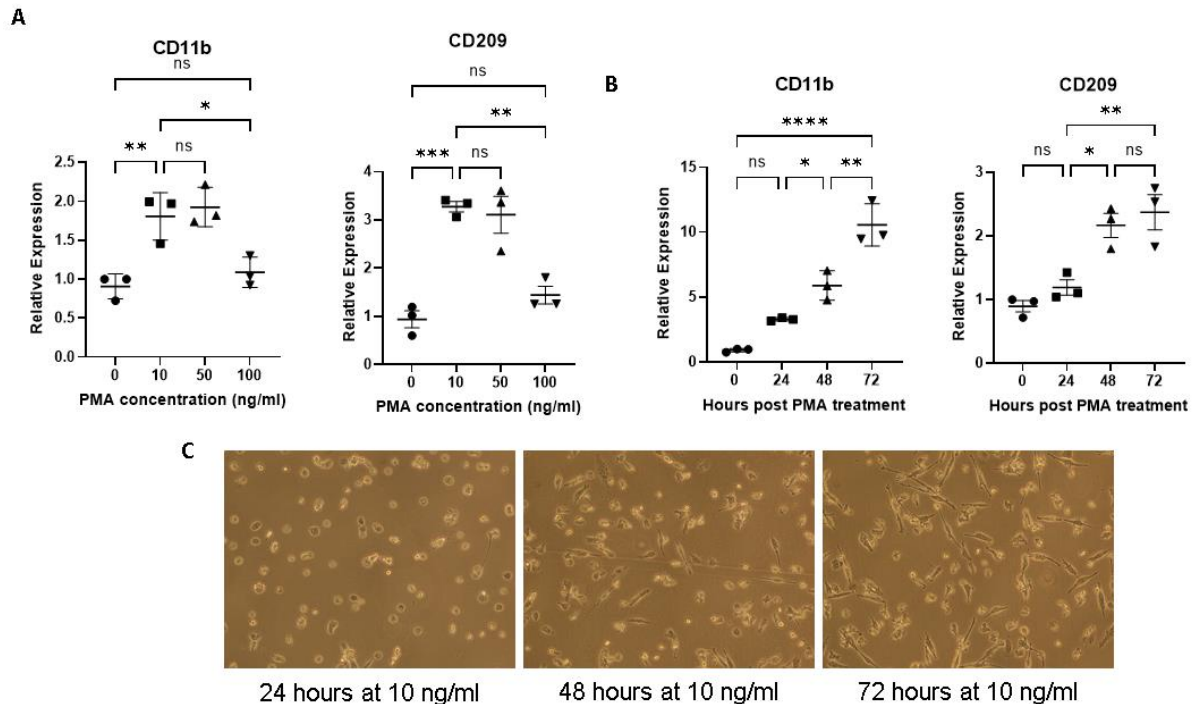


**Figure 2.1: PMA concentration and duration of incubation impact macrophage maturation.** (A) THP-1 cells were treated with indicated PMA concentration; total RNA was collected at 24 hours post treatment. *CD11b* and *CD209* gene expression were measured. (B) THP-1 cells were treated with 10 ng/ml PMA, cellular RNA was collected at specified time points and measured for *CD11b* or *CD209* expression. (C) THP-1 cells treated with 10 ng/ml were imaged at 40x via light microscopy at specified time points. Genes were normalized against reference gene RPL37a. All experiments were n = 3 biological replicates, \*p, 0.05, \*\*p<0.01, \*\*\*p<0.001, \*\*\*\*p<0.0001 unpaired two tailed t tests. Error bars represent mean +/- SEM.

#### 2.4b Polarization of THP-1 cells to M1 phenotype with IFN $\gamma$ treatment

IFN $\gamma$  was used to polarize THP-1 cells to M1 macrophage. To determine the optimal duration of IFN $\gamma$  treatment to polarize cells to an M1 phenotype, we treated cells with 20 ng/ml IFN $\gamma$  for 12, 24, 48, or 72 hours and collected total RNA at indicated time points. We measured gene expression of the chemokine C-X-C motif chemokine ligand 10 (*CXCL10*), and markers for the interferon response: 2'-5'-oligoadenylate synthetase 1 (*OAS1*), and interferon beta (*IFN $\beta$* ).

These genes were chosen because they are upregulated in M1 macrophage and are used as markers for the M1 phenotype (Genin et al., 2015; Nikonova et al., 2020). Expression of *CXCL10* was increased at 12 hours of treatment, then decreased back to baseline levels afterwards (12 hour mean fold change over 0 hour = 2464 +/- 157) (Figure 2.2). In contrast, *IFN $\beta$*  gene expression was elevated later during polarization, with expression increasing at 72 hours (72 hour mean fold change over 0 hour = 6.46 +/- 1.19) (Figure 2.2). The late increase in *IFN $\beta$*  gene expression may be due to an ISG that regulates the late stage interferon response (Smieja, Jamaluddin, Brasier, & Kimmel, 2008). *OAS1*, a type 1 interferon stimulated gene, exhibited an expression pattern similar to *CXCL10*, with expression increasing at 12 hours and decreasing afterwards (12 hour mean fold change over 0 hour = 177.2 +/- 6.98). Interestingly, expression of *OAS1* increased again at 72 hours (72 hour mean fold change over 0 hour = 88.98 +/- 4.24). Since both *IFN $\gamma$*  and *IFN $\beta$*  stimulate *OAS1* expression, the increase at 12 hours could be *OAS1* responding to *IFN $\gamma$*  stimulation, while the increase at 72 hours could be *OAS1* responding to *IFN $\beta$*  induction. Based off of the increase in *CXCL10* expression and *OAS1* expression at 12 hours, we proceeded with a 12-hour *IFN $\gamma$*  treatment for subsequent polarization experiments. The duration of *IFN $\gamma$*  treatment varies in THP-1 cells, with times ranging from 12 hours to 48 hours of treatment (Baxter et al., 2020; Tedesco et al., 2018), so by choosing 12 hours we are still consistent with the literature.

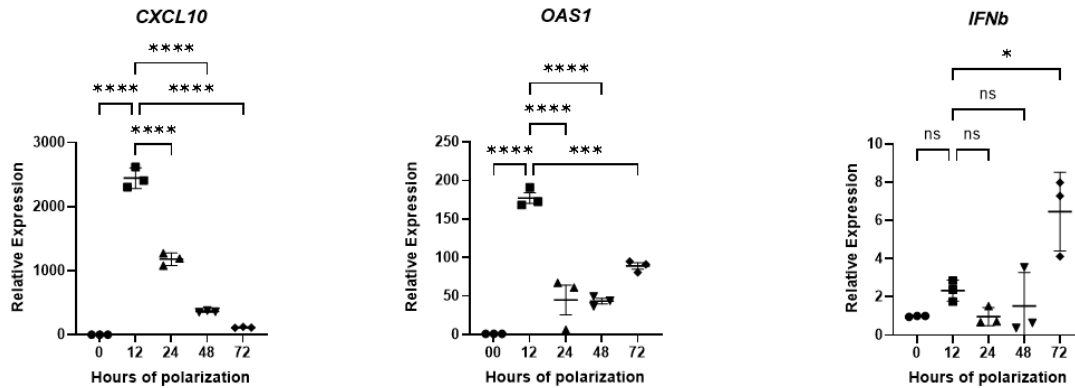


**Figure 2.2: Markers for M1 macrophage peak early in polarization.** PMA treated THP-1 cells were treated with 20 ng/ml IFN $\gamma$ , cellular RNA was collected at specified time points and measured for *CXCL10*, *IFN $\beta$*  or *OAS1* expression. Genes were normalized against reference gene RPL37a. All experiments were n = 3 biological replicates, \*p, 0.05, \*\*p<0.01, \*\*\*p<0.001, \*\*\*\*p<0.0001 unpaired two tailed t tests. Error bars represent mean +/- SEM.

#### 2.4c IFN $\gamma$ increases oxidative phosphorylation and glycolysis early in treatment

The metabolic profile is an important marker for macrophage phenotype. Increased glycolysis is the result of the M1 cell responding to infection (Van den Bossche et al., 2017). The increased rate of glycolysis leads to an accumulation of byproducts such as citrate and succinate, which aid in the production of inflammatory mediators like nitric oxide and IL-1 $\beta$  (Infantino et al., 2011; Tannahill et al., 2013). We sought to determine the point during the M1 polarization time course that would yield the highest rate of glycolysis, as well as produce the most non mitochondrial oxygen consumption rate (OCR), which is an indicator of reactive oxygen species (Chacko et al., 2014). Cells were polarized with 20 ng/ml IFN $\gamma$  for the indicated time points and a Seahorse flux analyzer was used to measure changes in extracellular acidification rate (ECAR) and oxygen consumption (OCR) rates, measures of glycolysis and oxidative phosphorylation, respectively. (Jing Zhang & Zhang, 2019). We measured changes in mitochondrial stress following the addition of oligomycin (ATP synthase inhibitor), FCCP (electron transport chain

uncoupler), rotenone and antimycin A (electron transport chain complex I and III inhibitors). Changes in glycolysis were measured following the addition of glucose, oligomycin (ATP synthase inhibitor), and 2-DG (hexokinase inhibitor).

When we measured ECAR, we found that 12 hours of polarization increased glycolysis and glycolytic reserve, but not glycolytic capacity. Glycolytic capacity is the maximal capacity of a cell to generate ATP from glycolysis, while glycolytic reserve is the difference between basal glycolysis and glycolytic capacity and is the ability of a cell to undergo glycolysis during times of stress (Mookerjee, Nicholls, & Brand, 2016). The increase in glycolysis and glycolytic reserve suggests that 12-hour polarization with IFN $\gamma$  increases a cell's ability to draw on glycolysis to produce ATP in times of stress.

We also considered an increase in reactive oxygen species (ROS) to be an indicator of M1 cells since inflammatory cells increase production of ROS to kill pathogens. When measuring mitochondrial respiration, 12 hours of polarization increased basal respiration, but not maximal respiration. The difference between basal respiration and maximal respiration, known as the spare capacity, decreased at 12 hours of polarization (Figure 2.7B, right). Spare capacity measures the ability of a cell to produce energy under times of increased stress. The decrease in spare capacity suggests that shorter durations of IFN $\gamma$  treatment limits the cell's ability to use oxidative phosphorylation to respond to stress (Figure 2.3). We also observed an increase in ATP production at 12 hours of polarization. This suggests that 12 hours of polarization increases basal respiration for ATP production, possibly to increase fatty acid synthesis, another hallmark metabolic pathway of M1 macrophage (Buck et al., 2017). There was also an increase in proton leak and non-mitochondrial respiration at 12 hours of polarization (Figure 2.3). The increase in both proton leak and non-mitochondrial respiration suggests that cells are generating high levels

of ROS, while also compromising the inner mitochondrial membrane integrity, possibly damaging the mitochondria (Nanayakkara et al., 2020).

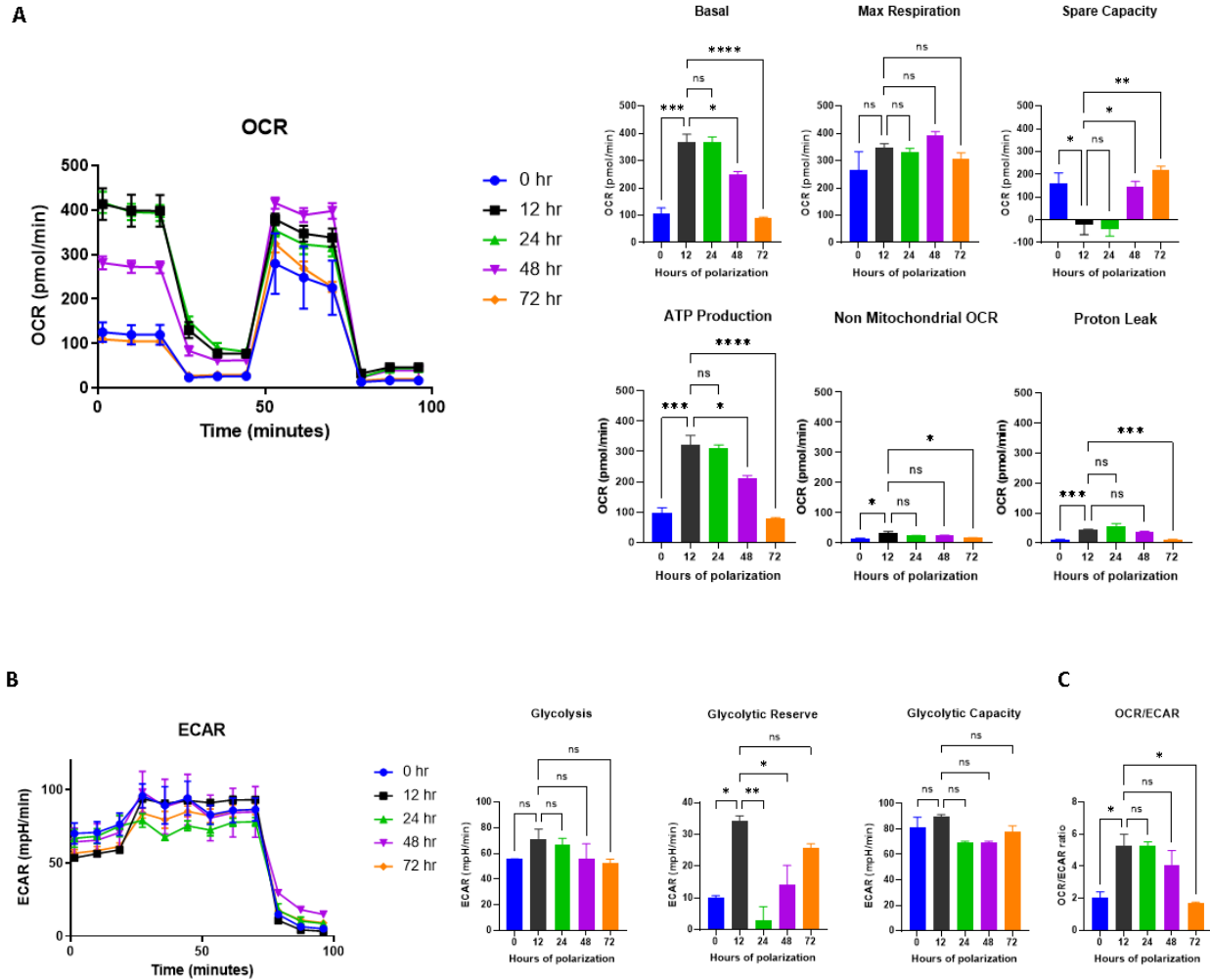


**Figure 2.3: M1 metabolism is upregulated early in polarization.** M1 cells were incubated 20 ng/ml IFN $\gamma$  at indicated time points. Oxygen consumption rate (OCR) was measured during a mitochondrial stress test. Basal rate, Maximum Respiration, Spare Capacity, ATP production, Proton Leak, and Non-Mitochondrial Respiration were calculated. Extracellular acidification rate (ECAR) was measured. Glycolysis, Glycolytic Capacity, and Glycolytic Reserve were measured. (B and D) OCR/ECAR ratio was calculated at basal respiration at 18 minutes. All significant values for OCR and ECAR were calculated using one-way ANOVA with Tukey's multiple comparisons. Significant values for genes calculated using unpaired two tailed t test. \*p, 0.05, \*\*p<0.01, \*\*\*p<0.001, \*\*\*\*p<0.0001. Error bars represent mean +/- SEM.

Lastly, we calculated the OCR/ECAR ratio, to determine which metabolic pathway is dominant during polarization. Cells that are highly glycolytic have lower OCR/ ECAR values, while cells that upregulate oxidative phosphorylation have higher OCR/ ECAR ratios. We found that polarizing cells with IFN $\gamma$  for 12-, 24-, and 48- hours increases the OCR/ECAR ratio. While unexpected, our system still shows an increase in key inflammatory genes and glycolysis at 12 hours polarization. Therefore, we chose to polarize cells for 12 hours for subsequent experiments.

#### *2.4d: IL-4 stimulates anti-inflammatory genes later in polarization*

Schaeffer et al., showed that cells treated with IL-4 were able to sustain DENV replication (Schaeffer et al., 2015). Similar to IFN $\gamma$ , the amount of IL-4 used in literature is consistent, but the timing of treatment varies, with times ranging from 24 hours to 72 hours of IL-4 treatment (Genin et al., 2015; Van den Bossche et al., 2015). To determine the optimal duration of IL-4 treatment to polarize cells to an M2 phenotype, we treated cells with 20 ng/ml IL-4 for 24, 48, 72 or 96 hours and collected total RNA at indicated time points. We measured interleukin 10 (*IL-10*) and tumor growth factor beta (*TGF $\beta$* ) expression, as these markers are key regulators in many anti-inflammatory pathways. There was a 1.9-fold increase in *IL-10* at 72 hours post treatment (72 hour mean fold change over 0 hour = 1.88 +/- 0.06) (Figure 2.4) followed by a decrease at 96 hrs. *TGF $\beta$*  gene expression increased between 0 hours and 48 hours of treatment (48-hour mean fold change over 0 hour = 1.59 +/- 0.14) and leveled off through 96 hrs. *TGF $\beta$*  expression does not significantly change at 72 and 96 hours of treatment (72-hour mean fold change over 0 hour = 1.46 +/- 0.03, 96-hour mean fold change over 0 hour = 1.57 +/- 0.12) (Figure 2.4). These data show that *IL-10* gene expression peaks at 72 hours of IL-4

treatment, while *TGFβ* expression increased until 48 hours of treatment, and does not significantly change afterwards.

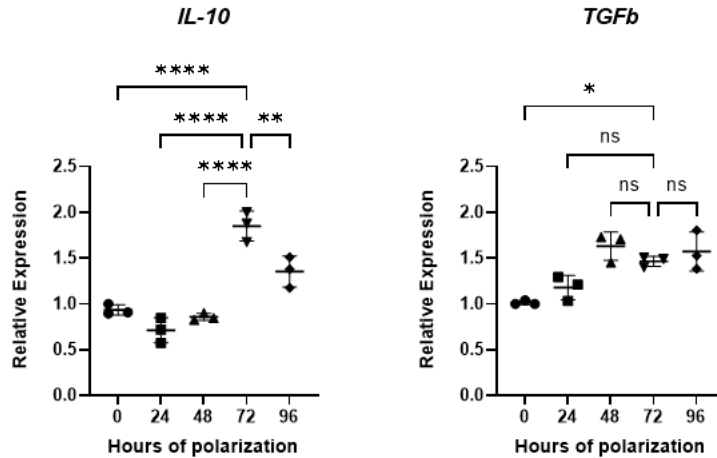


**Figure 2.4: Markers for M2 macrophage peak later in polarization.** PMA treated THP-1 cells were treated with 20 ng/ml IL-4, cellular RNA was collected at specified time points and measured for *IL-10* or *TGFβ* expression. Genes were normalized against reference gene RPL37a. All experiments were n = 3 biological replicates, \*p, 0.05, \*\*p<0.01, \*\*\*p<0.001, \*\*\*\*p<0.0001 unpaired two tailed t tests. Error bars represent mean +/- SEM.

#### 2.4e Longer M2 polarization results in increased mitochondrial respiration

One of the hallmarks of M2 macrophage is an increase in oxidative phosphorylation (Galván-Peña & O'Neill, 2014). We sought to identify the timepoint that would result in the greatest increase in oxidative phosphorylation. PMA-treated THP-1 cells were polarized with 20 ng/ml IL-4 at indicated time points and the Seahorse flux analyzer was used to measure changes in OCR and ECAR, as measures of oxidative phosphorylation and glycolysis, respectively.

Seventy-two hours of IL-4 treatment yielded a metabolic profile most similar to M2 macrophage, as marked by an increase in oxidative phosphorylation parameters (Figure 2.5A). Seventy-two hours of polarization had significantly higher basal respiration compared to the other time points. Interestingly, it did not have a higher max respiration compared to 24- or 48-

hour polarization and had decreased maximal respiration compared to 96 hours of polarization. The spare capacity was markedly lower than the other time points, indicating that either the ability of cells to respond to energy has decreased, or that the basal respiration was already at max (due to too many cells plated for the assay) and there could be no further increase in maximal respiration, resulting in a smaller spare capacity. Seventy-two hours of polarization did increase ATP production, suggesting that longer polarization increases ATP demand. Later polarization increased both proton leak and non-mitochondrial respiration, indicating that longer polarization may have adverse effects on mitochondrial health. Treating cells with IL-4 for 48, 72 and 96 hours increases both glycolysis and glycolytic capacity. However, glycolytic reserve is not impacted by treatment with IL-4. This suggests that polarization towards an M2 phenotype does not impact the ability of cells to use glycolysis in times of stress.

Seventy-two hours of polarization had the highest OCR/ECAR ratio, demonstrating that 72 hours of polarization drives cells to use oxidative phosphorylation as their primary metabolism (Figure 2.5B). Since polarization for 72 hours increased *IL-10* and *TGF $\beta$*  gene expression and increased most oxidative phosphorylation parameters, we selected this polarization duration for future experiments.

## **2.5 Discussion**

THP-1 cells are a widely used model system to study monocyte and macrophage biology, with PMA being the stimulant of choice to differentiate THP-1 monocytes to macrophage (Chanput et al., 2014; Daigneault et al., 2010). However, the concentration and duration of incubation in PMA varies widely throughout published studies. In this study we determined the optimal amount and duration of incubation of PMA for differentiation. Furthermore, we

determined the optimal timing for polarization of PMA treated THP-1 cells towards a M1 or M2 phenotype.

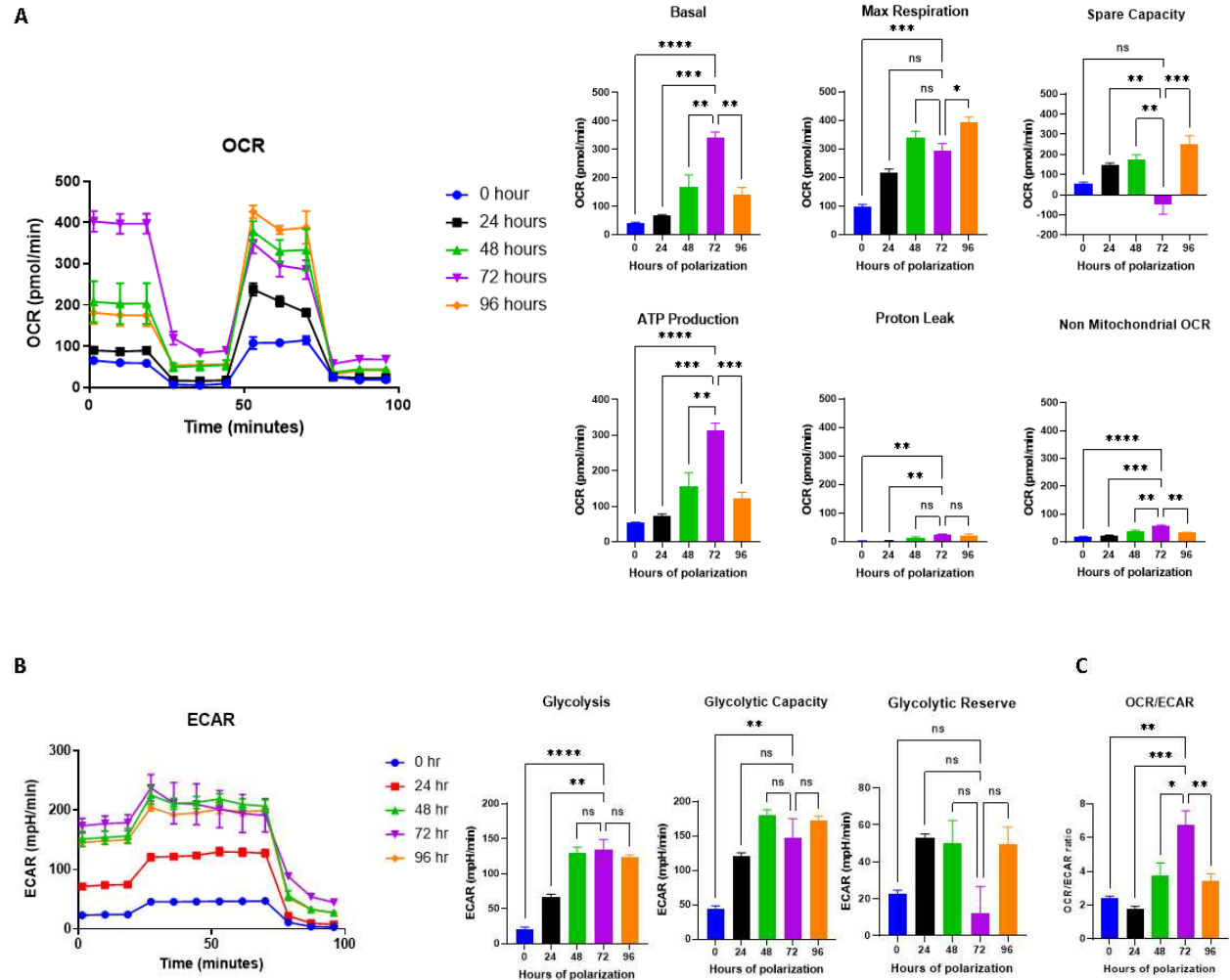


**Figure 2.5: M2 metabolism is upregulated later during polarization.** M2 cells were incubated with 20 ng/ml IL-4 at indicated time points. Oxygen consumption rate (OCR) was measured during a mitochondrial stress test. Basal rate, Maximum Respiration, Spare Capacity, ATP production, Proton Leak, and Non-Mitochondrial Respiration were calculated. Extracellular acidification rate (ECAR) was measured. Glycolysis, Glycolytic Capacity, and Glycolytic Reserve were measured. (B and D) OCR/ECAR ratio was calculated at basal respiration at 18 minutes. All significant values for OCR and ECAR were calculated using one-way ANOVA with Tukey's multiple comparisons. Significant values for genes calculated using unpaired two tailed t test. \* $p$ , 0.05, \*\* $p$ <0.01, \*\*\* $p$ <0.001, \*\*\*\* $p$ <0.0001. Error bars represent mean  $\pm$  SEM.

High concentrations of PMA can lead to unintended outcomes, such as cell death (Starr et al., 2018), or an increase in NF- $\kappa$ B gene clusters (Hellweg et al., 2006), which can upregulate inflammatory genes such as IL-6, and TNF $\alpha$  (Park et al., 2007). Here, we found that concentrations up to 50 ng/ml were sufficient in upregulating *CD11b* and *DC-SIGN*, while 100 ng/ml decreased both *CD11b* and *DC-SIGN* expression. *CD14*, another marker of macrophage maturation, has been shown to have decreased expression with PMA concentrations over 50ng/ml (Park et al., 2007). The decrease in *CD11b* can be considered another adverse effect of using high concentrations of PMA. Higher concentrations have been shown to be cytopathic during intracellular infection (Starr et al., 2018), while lower concentration of PMA allow cells to respond to anti-inflammatory polarizing stimulants such as IL-10 (Baxter et al., 2020; Maeß et al., 2014). Due to this fact, as well as the results of our study, we used 10 ng/ml of PMA for future assays. Resting cells in media without PMA increases macrophage cell markers while decreasing NF- $\kappa$ B gene clusters and secretion of inflammatory cytokines and chemokines (Chanput et al., 2014). We found that longer resting times after PMA increases both *CD11b* and *CD209* expression. However, we based our rest period on the DENV replication cycle in Huh7 cells, a liver cell line commonly used in *in vitro* DENV experiments. Resting cells for 24 hours prior to DENV infection means that 48 hours of DENV infection (peak viral replication in huh7 cells (Butler et al., 2020)) would coincide with 72 hours of post PMA rest. This means that cells express *CD209* and *CD11b*, receptors for DENV, at the same time DENV replication increases.

Since macrophage phenotype impacts viral replication (Sang, Miller, & Blecha, 2015), we tested the optimal timing of IFN $\gamma$  or IL-4 treatment in our system. The concentrations of IFN $\gamma$  and IL-4 are consistent throughout the literature, with studies using 20 ng/ml of IFN $\gamma$  or IL-4 to polarize cells towards M1 or M2 phenotypes, respectively. We first optimized the

duration of incubation with IFN $\gamma$ , measuring both gene expression and cellular metabolism to confirm an M1 phenotype. While an increase in M1 markers have been found to be upregulated at 6 hours of IFN $\gamma$  polarization (Shiratori et al., 2017), these experiments used 100 ng/ml of PMA and may have been measuring off target effects of PMA stimulation (Chanput et al., 2014). Even though our system used a lower concentration of PMA and rested cells for 24 hours in media without PMA, our assays yielded similar results as seen in the literature (Shiratori et al., 2017; Surdziel et al., 2017). We saw an increase in *CXCL10* and *OAS1* at earlier timepoints, and a sharp decrease later in the time course. In contrast, we did not see an increase in *IFN $\beta$*  until 72 hours of polarization. Our data suggest that *IFN $\beta$*  gene expression is not directly regulated by IFN $\gamma$  treatment. A plausible explanation for this is that *IFN $\beta$*  is regulated by an ISG that regulates the late stage interferon response, like interferon regulatory factor 1 (IRF-1) (Smieja et al., 2008). IRF-1 is induced by the binding of the STAT1 homodimer formed during the type II interferon response (Feng et al., 2021). IRF-1 has been shown to upregulate *IFN $\beta$*  at low levels, which is also supported by our data (Feng et al., 2021; Yarilina et al., 2008).

Our study is one of the few to measure changes in metabolism in M1 cells over the course of IFN $\gamma$  treatment. Other studies polarize macrophage with IFN $\gamma$  for 24 hours, then measure glycolysis and oxidative phosphorylation (Jha et al., 2015; Van den Bossche et al., 2015). Our study confirms that many glycolytic and mitochondrial parameters are increased after 24 hours of polarization. Furthermore, we show polarization for 12 hours yields similar results to a 24-hour polarization. Treatment with IFN $\gamma$  for 12 hours leads an upregulation in glycolysis, non- mitochondrial OCR and ATP production. The increase in glycolysis early in polarization support the concept that M1 cells rapidly upregulate the rate of glycolysis for production of anti-microbial products early in infection (Nagy & Haschemi, 2015). The increase in ATP and non-

mitochondrial OCR, an indicator for ROS production, show that a 12 hour time point may lead to the highest energy demand, but also the most production of ROS(Chacko et al., 2014). The rapid increase in ROS and ATP does not come without trade off, as proton leak, an indicator of the loss of mitochondrial membrane integrity, is also increased at 12 hours of polarization (Nanayakkara et al., 2020).

THP-1 cells are notoriously difficult to polarize to an M2 phenotype. THP-1 macrophage do not readily respond to IL-10 (Shiratori et al., 2017) and do not upregulate M2 markers to the same degree as PBMCs (Forrester et al., 2018). Since M2 macrophage play an important role in DENV pathogenesis (Schaeffer et al., 2015; Tsai et al., 2013), we attempted to optimize our system for M2 polarization. The resolution of inflammation is a slower process than the initiation of inflammation, therefore studies treat cells with IL-4 for longer amounts of time than they treat cells with IFN $\gamma$ , with times ranging from 24-72 hours (Genin et al., 2015). We found that longer incubation in IL-4 resulted in increased *IL-10* and *TGF $\beta$*  gene expression. IL-10 decreases the expression of inflammatory chemokines and cytokines and inhibits the activation of T effector cells, while *TGF $\beta$*  promotes the polarization towards an M2 phenotype by upregulating anti-inflammatory genes and suppressing the M1 phenotype (Gong et al., 2012; Murray, 2006; Saraiva & O'Garra, 2010; Zhang et al., 2015). Our metabolism data further substantiate the concept that longer polarization leads to cells that are more M2-like. Longer periods of IL-4 incubation resulted in increased mitochondrial respiration, a hallmark of M2 macrophage (Kelly & O'Neill, 2015). Interestingly, longer incubation also led to increases in glycolysis. While glycolysis is a hallmark of M1 cells, increases in glycolysis supports the increase in oxidative phosphorylation and fatty acid oxidation seen in M2 macrophage (Huang et al., 2016).

Local environment plays a major role in virus-pathogen dynamics, and no in vitro system can fully recapitulate this. However, using THP-1 macrophages can provide insight into the mechanisms of virus-pathogen interactions. We find that these cells can be used to study macrophage polarization and will be used to study flavivirus- macrophage interactions in M1 and M2 macrophage. Our data show that PMA stimulated THP-1 cells are a competent model to study macrophage biology and metabolism.

## CHAPTER 3: DENGUE VIRUS REPROGRAMS MACROPHAGE GENE EXPRESSION AND METABOLISM

### 3.1 Summary

Macrophages are a site of DENV replication, and the imbalance between macrophage pro-inflammatory and anti-inflammatory phenotypes during DENV infection leads to severe disease outcomes. To investigate the effect of macrophage phenotype on DENV serotype 2 (DENV2) replication, we treated THP-1 macrophages with either interferon gamma (IFN $\gamma$ ) or interleukin 4 (IL-4) to polarize them towards an inflammatory (M1) or anti-inflammatory (M2) phenotype, respectively, prior to infection. DENV2 showed preferential replication in M2 compared to M1 or non-treated cells. Infection with DENV2 resulted in increased expression of inflammatory and anti-inflammatory genes in all phenotypes. Macrophage infected with DENV exhibited elevated expression of glycolytic genes and a fatty acid oxidation gene. Furthermore, DENV metabolically reprograms macrophages to utilize resulted in an upregulation of oxidative phosphorylation in M0, M1 and M2 cells. These data suggest that DENV shifts macrophage gene expression and metabolism to support viral replication.

### 3.2 Introduction

Dengue virus (DENV) is the most prevalent mosquito borne virus in the world. DENV is transmitted by *Aedes albopictus* and *Aedes aegypti* mosquitoes, which have a predicted geographical range that includes Europe, Africa, Asia, and the Americas (Kraemer et al., 2015). Therefore, DENV epidemics occur in the Americas, Africa, Asia, and Europe (S. K. Roy & Bhattacharjee, 2021), putting roughly 3.6 billion people at risk (S. Bhatt et al., 2013).

Four distinct serotypes of dengue (DENV1, 2, 3, 4) circulate in tropic and subtropic regions and can cause disease. While 75% of cases with a single serotype are asymptomatic or mild, infection can cause severe illness, such as dengue hemorrhagic fever (DHF) and dengue shock syndrome (DSS) (Diamond & Pierson, 2015). Infection with a single serotype does not confer lifelong immunity against infection with another serotype (Diamond & Pierson, 2015). In fact, infection with two or more serotypes is a leading risk factor for severe disease (Halstead, 2007). These diseases are characterized by hemorrhagic episodes and vascular permeability, which can lead to shock and death (Halstead, 2007).

Virus replication depends on cellular metabolism for energy and metabolic precursors, and infection triggers changes in carbon metabolism and fatty acid synthesis (Thaker et al., 2019). DENV serotype 2 (DENV2), in particular, increases glucose and lipid metabolism to aid in viral replication, virion production and virion assembly (Fernandes-Siqueira et al., 2018; Fontaine et al., 2015; Heaton & Randall, 2010, Butler et al., 2020). Glycolysis and the TCA cycle generate ATP in cells, and intermediates from glycolysis are shuttled into the pentose phosphate pathway for synthesis of nucleotide and amino acid precursors. Increased glucose metabolism increases ATP and biosynthetic precursors for virus genome replication (Sanchez & Lagunoff, 2015). DENV2 increases cellular glucose consumption by upregulating the expression of glycolytic enzymes, hexokinase 1 and 2 (Fontaine et al., 2015; Butler et al., 2020). Inhibition of glycolysis decreases viral RNA synthesis and infectious particle production (Fontaine et al., 2015). Fatty acids can be shuttled into lipid synthesis or into the TCA cycle and oxidative phosphorylation via  $\beta$ -oxidation. DENV2 alters fatty acid oxidation and synthesis by recruiting fatty acid synthetase (FASN) to replication sites (Heaton et al., 2010). DENV2 remodels and expands the endoplasmic reticulum (ER) membrane to establish replication complexes (Gullberg

et al., 2018; Heaton & Randall, 2010; Jordan & Randall, 2017; Perera et al., 2012). Furthermore, DENV2 induces lipophagy to release free fatty acids from lipid droplets for  $\beta$ -oxidation and membrane production for ER expansion and the energy demands of replication (Jordan & Randall, 2017; Jingshu Zhang et al., 2018).

Macrophage are a primary target of DENV infection (Cerny et al., 2014; Jessie et al., 2004; Schmid & Harris, 2014). Macrophage have two major subsets: classically activated macrophage and alternatively activated macrophage, referred to as M1 and M2, respectively (Gordon & Martinez, 2010; Mosser & Edwards, 2008). M1 cells secrete inflammatory mediators, such as  $IFN\gamma$ ,  $IL-1\beta$ ,  $IL-12$ , tumor necrosis factor alpha ( $TNF\alpha$ ), and inflammatory chemokines, such as C-X-C motif chemokine ligand 10 ( $CXCL10$ ) (Murray, 2017). M2 cells secrete immunosuppressive mediators, such as  $IL-10$  and  $TGF\beta$ , which resolve inflammation and aid in wound healing (Murray, 2017; Shapouri-Moghaddam et al., 2018). Infected macrophage disseminate viruses to tissues and organs throughout the body, and inflammatory cytokines and chemokines support viral infection and spread (Nikitina et al., 2018). Patients with severe dengue fever symptoms were shown to have elevated serum concentrations of  $CXCL10$  and  $TNF\alpha$ , while patients that resolved infections had higher concentrations of  $TGF\beta$  (Soo et al., 2017; Soo et al., 2019; Zhao et al., 2016). The balance between inflammatory and immunosuppressive cytokines is crucial in disease severity and resolution.

Macrophage shift their metabolism for rapid macrophage recruitment and proliferation, as well as cytokine production in response to infection (Buck et al., 2017). The macrophage subsets utilize different metabolic pathways: M1 cells upregulate the pentose phosphate pathway to increase in NADPH levels. NADPH oxidase catalyzes the transfer of electrons from NADPH to molecular oxygen to produce anti-microbial reactive oxygen species. Upregulation of

glycolysis results in high levels of succinate, which enhances IL-1 $\beta$  expression by stabilizing HIF-1 $\alpha$ , a transcriptional regulator of IL-1 $\beta$  (Tannahill et al., 2013). M2 cells upregulate oxidative phosphorylation and fatty acid oxidation (Ching-Cheng Huang et al., 2014; Galván-Peña & O'Neill, 2014; Viola et al., 2019) to increase ATP production and fuel bioenergetically intense immunosuppressive functions (Shyh-Chang et al., 2013), such as tissue repair and angiogenesis (S. Yu et al., 2022). While DENV, Zika virus, Hepatitis C virus, and HIV have all been shown to change macrophage phenotype during infection, few studies have investigated the link between viral metabolic reprogramming and shifts in macrophage phenotype (Cassol et al., 2009; Foo et al., 2017; Jhan et al., 2021; Syed, Amako, & Siddiqui, 2010).

In this study, we investigated the impact of DENV2 on macrophage gene expression and metabolism in naïve (M0), M1 and M2 macrophage subsets. We hypothesized that the presence of DENV2 would decrease expression of anti-viral genes, increase expression of immunosuppressive genes, and increase oxidative phosphorylation in all infected macrophage subsets. Our results show that DENV2 infection upregulated both pro-inflammatory and immunosuppressive genes in M0 cells and drove cells towards oxidative phosphorylation, a metabolic pathway utilized by immunosuppressive (M2) immune cells. By reprogramming metabolism, DENV2 polarizes macrophage towards an immunosuppressive phenotype to create a more hospitable environment for replication. We also found that M1 and M2 cells differ in the type 1 interferon response to DENV2, with M1 cells upregulating type 1 interferon stimulated genes to a higher degree than infected M2 cells. Our data suggest that DENV2 metabolic reprogramming is an important mechanism for immune evasion in M2 cells, while the interferon pathway is an important anti-viral mechanism in decreasing DENV2 replication primarily in M1 cells.

### **3.3 Materials and Methods**

#### *3.3a Cells and infection*

THP-1 human monocytic cells (TIB-202™, Manassas, VA, US) were cultured in RPMI-1640 media, supplemented with 10% fetal bovine serum (FBS), 1% non-essential amino acids, 1% L-glutamine, 1% penicillin-streptomycin, 25 mM HEPES and 0.05mM 2-mercaptoethanol in a 37°C incubator with 5% CO<sub>2</sub>.

24 hours prior to infection, 2 x 10<sup>6</sup> cells, plated in T-25 flasks, were treated with 10 ng/mL phorbol 12-myristate 13-acetate (PMA) to induce differentiation into macrophages. For infection, cells were washed with Dulbecco's phosphate-buffered saline (D-PBS) and incubated with DENV2 (strain 16681)(Kinney et al., 1997) at indicated multiplicities in media for 1 hour at 4°C with rocking. Virus media was removed, cells were washed twice with cold D-PBS, and warmed RPMI-1640 media with 10% FBS was added.

#### *3.3b Macrophage polarization and infection*

THP-1 monocytes plated at 2 x 10<sup>6</sup> cells in T-25 flasks were stimulated with 10 ng/mL PMA. 24 hours later, media with PMA was removed, and cells were washed with D-PBS and then treated with either 20 ng/mL interferon gamma (IFN $\gamma$ ) (R & D Systems, Minneapolis, MN, USA) or 20 ng/mL interleukin 4 (IL-4) (R & D Systems, Minneapolis, MN, USA) to polarize them into M1 or M2 phenotypes, respectively. 24 hours later, cells were infected with DENV2 as described above.

#### *3.3c RNA extraction and qPCR*

At the indicated time points, cells were harvested in TRIzol (Invitrogen, Thermofisher, Waltham, MA, USA), and total RNA was isolated using ZymoGen TRIzol RNA extraction kit according to manufacturer's instructions. cDNA was made using an iScript cDNA synthesis kit

(Bio-Rad, Hercules, CA, USA) according to the manufacturer's instructions, and then subjected to qPCR analysis with iQ SYBR green Supermix in a CFX96 real-time PCR system. Primers are listed below. Relative expression was normalized to reference gene, ribosomal protein L37a (RPL37a). For genomic equivalent analysis, Cq values were standardized to ten-fold dilutions of *in vitro*-transcribed DENV2 genomic RNA and subject to qRT-PCR.

**Table 3.1** PCR Primers

Gene	Forward sequence	Reverse sequence	Source
<i>IL-10</i>	GAC TTT AAG GGT TAC CTG GGT TG	TCA CAT GCG CCT TGA TGT CTG	(Shiratori et al., 2017)
<i>CXCL10</i>	CCA GAA TCG AAG GCC ATC AA	CAT TTC CTT GCTAAC TGC TTT CAG	(Qi et al., 2009)
<i>IFN<math>\beta</math></i>	CGCCGCATTGACCATCTA	GACATTAGCCAGGAGGTT CTCA	(Bender et al., 2015)
<i>TGF<math>\beta</math></i>	ACG TGG AGC TGT ACC AGA AAT A	GGC GAA AGC CCT CAA TTT CC	(Shiratori et al., 2017)
<i>IL-1<math>\beta</math></i>	TCT TCG ACA CAT GGG ATA ACG A	TCC CGG AGC GTG CAG TT	(X. Huang et al., 2016)
<i>TNF<math>\alpha</math></i>	CAG CAA GGA CAG CAG AGG A	CCG TGG GTC AGT ATG TGA GA	(X. Huang et al., 2016)
<i>ENO1</i>	GTCTCTTCAGGCGTGCAA GC	GATGAGACACCATGACGC CC	(Galbraith et al., 2017b)
<i>CPT1a</i>	GCACTGTTGACCACTGA GCA	CCGGTCAGCCCAAGATAA CA	(Sinha et al., 2015)
<i>DENV2</i>	ACAAGTCGAACAACCTG GTCCAT	GCCGCACCATTGGTCTTCT C	(Butler et al., 2020)
<i>HK2</i>	CAAAGTGACAGTGGGTG TGG	GCCAGGTCCTTCACTGTCT C	(Butler et al., 2020)
<i>RPL37a</i>	ATTGAAATCAGCCAGCA CGC	AGGAACCACAGTGCCAGA TCC	(Maeß et al., 2010)

### 3.3d Plaque assays

Media were collected at indicated time points and centrifuged at 500g for 10 minutes at room temperature. Plaque assays were performed on baby hamster kidney (BHK) cells (ATCC CCL-10). BHKs, plated at  $3 \times 10^5$  cells per well in MEM with 10%FBS, were incubated with 10-fold

dilutions of the clarified cell supernatants for 2 hours at room temperature with rocking.

Inoculum was removed and cells were overlaid with 3 mL of 2% agarose in MEM supplemented with 5% FBS. After incubation for 7 days, 8% neutral red solution in PBS was added to the agar overlay, and plaques were counted 24 hours after staining.

### *3.3e Metabolic Stress Tests*

A Seahorse XFe analyzer (Agilent Technologies) was used to measure the oxygen consumption rate (OCR) and extracellular acidification rate (ECAR) with the mitochondrial stress test (Agilent 103015-100). Cells plated at  $4 \times 10^6$  cells in  $10 \text{ cm}^2$  dishes were differentiated and polarized as described above with 20 ng/mL IL-4 for 48 hours or 20 ng/mL IFN $\gamma$  for 12 hours and then infected with DENV2 at an MOI of 10 for 1 hour at 4°C. After incubation, virus media was removed, cells were washed twice with D-PBS and RPMI-1640 media with 10% FBS was added. At 36 hours post infection, cells were detached with Cell Stripper (Corning, Manassas, VA, US), washed with D-PBS, centrifuged at 500g for 5 minutes and resuspended in 2 mL XF base medium (Agilent Technologies) supplemented with 1 mM pyruvate, 2 mM L-glutamine, and with 10 mM glucose. Cells were then counted and plated at  $7.5 \times 10^4$  cells per well in XF<sup>24</sup> cell culture microplates with Cell-Tak (Corning, Manassas, VA, US) and spun at 500g for 5 minutes. XF base medium was added for a total amount of 500  $\mu$ l per well. Cells were rested for 20 minutes in a non-CO<sub>2</sub> incubator at 37°C, and then placed in the Seahorse XFe analyzer for analysis. The mitochondrial stress test used sequential injections of oligomycin (15  $\mu$ M), p-trifluoromethoxyphenylhydrazine (FCCP, 15  $\mu$ M), and rotenone and antimycin A (5  $\mu$ M each). Glucose (10 mM), oligomycin (15  $\mu$ M), and 2-deoxyglucose (500 mM) were injected to measure extracellular acidification rate (ECAR). Measurements were collected at 5-minute intervals; three times before and after injections and six times after the last injection.

Mitochondrial activity was determined as follows: (1) Basal respiration was calculated using the last rate measurement before injection of oligomycin minus the non-mitochondrial respiration rate (defined as the minimum rate measurement after rotenone/antimycin A injection), (2) ATP production was calculated as the last rate measurement before oligomycin injection minus the minimum rate measurement after oligomycin injection, (3) Maximum respiration was calculated using the maximum rate measurement after FCCP injection minus non-mitochondrial rate, (4) Spare capacity was the maximal respiration minus basal respiration, (5) Proton leak was the minimum rate measurement after oligomycin injection minus non-mitochondrial respiration, and (6) Non Mitochondrial Respiration was the minimum rate after rotenone and antimycin A injection.

Glycolytic function was determined as follows: (1) Glycolysis was the maximum rate measurement before oligomycin injection minus minimum rate after 2-DG injection, (2) Glycolytic capacity was the maximum rate measurement after oligomycin injection minus the minimum rate after 2DG injection, and (3) Glycolytic reserve was the glycolytic capacity minus glycolysis. OCR/ECAR ratio was calculated with measurements at basal conditions at 18 minutes.

### *3.3f Subcellular Extracts and Protein Analysis*

Nuclear and cytoplasmic extracts were prepared as previously described (Brewster et al., 2011). Briefly, cells were lysed in 0.5% NP-40 in PBS with protease and phosphatase inhibitors (2  $\mu\text{g}/\text{mL}$  leupeptin and aprotinin, 1  $\mu\text{g}/\text{mL}$  pepstatin, 0.2 mM phenylmethylsulfonyl fluoride [PMSF], 0.2 mM sodium orthovanadate, 2 mM sodium pyrophosphate, and 1 mM glycerophosphate). Cells were incubated on ice for 30 minutes then pelleted for 4 minutes at 1,600g. Supernatants were aliquoted into separate tubes and nuclear pellets were washed with

cold PBS, and then incubated with Dignam's buffer for 1 hour on ice. Extracted nuclei were pelleted for 15 min at 21,000g.

Protein concentration of each extract was determined with a Pierce BCA protein assay kit (Thermo Scientific) according to manufacturer's instructions. Equal quantities of total protein were separated by polyacrylamide gel electrophoresis for western blot. Blocked blot segments, separated by molecular weight range, were probed simultaneously with indicated primary antibodies overnight. Antibodies were detected with appropriate horseradish peroxidase-conjugated secondary antibodies and developed with the TMB membrane peroxidase substrate system (3,3',5,5'-Tetramethylbenzidine, KPL). Images were scanned with a Visioneer One touch scanner 9420 at a gamma value of 1.0, and all contrast adjustments were uniformly applied using Adobe Photoshop. List of antibodies can be found in supplemental methods.

### *3.3g Statistics*

Statistical analysis was performed on Prism Software version 9.3.1. Statistical significance was calculated using the two-tailed Student's *t* test or one way ANOVA.

## **3.4 Results**

### *3.4a Inflammatory and immunosuppressive genes are upregulated during DENV2 infection*

To investigate immunometabolic reprogramming during DENV2 infection we utilized THP-1 human monocytic cells. PMA-treated THP-1 macrophage (M0) were infected with DENV2 at a multiplicity of infection (MOI) of 0.1 and total cellular RNA was collected at 0 hrs (bound virus) and at 12-, 24-, and 36- hours post infection (hpi). DENV2 genome equivalents (GE) were quantified by RT-qPCR. Cell supernatants were collected at the same intervals for quantification of infectious virus production by plaque assay. DENV2 genome equivalents steadily increased after 12 hpi, to  $1.70 \times 10^4$  GE  $\pm$   $2.01 \times 10^3$  at 36 hpi (Figure 3.1A, left).

Infectious particles (PFU/mL) followed a similar trend, with infectious particle titers reaching  $1.36 \times 10^3 \pm 1.68 \times 10^2$  PFU/mL at 36 hours post infection (Figure 3.1A, right). Next, we performed the same experiment with a higher MOI (MOI = 5) to assess virus replication in a synchronized infection with minimal bystander cell effects and with measurable virus effects on cellular gene expression. The replication kinetics were similar to those at MOI = 0.1: genome equivalents increased after 12 hpi and reached,  $6.83 \times 10^6 \pm 1.5 \times 10^5$  GE at 36 hpi (Figure 3.1B, left), and infectious particles followed a similar trend, with viral titers reaching  $5.51 \times 10^4 \pm 3.3 \times 10^3$  PFU/mL at 36 hpi (Figure 3.1B, right).

We used RT-qPCR to measure inflammatory and immunosuppressive gene expression at 36 hpi in mock-infected vs. DENV2-infected M0 cells (MOI = 5). Results were normalized to reference gene, *RPL37a*. We measured *IL-12*, *IL-1 $\beta$* , *TNF $\alpha$*  and *CXCL10*, gene expression to evaluate the inflammatory response during infection. *IL-12* gene expression increased 5-fold (M0 DENV mean fold change over M0 mock-infected =  $4.95 \pm 0.32$ ), *IL-1 $\beta$*  was upregulated 1.75-fold (mean =  $1.74 \pm 0.09$ ), *TNF $\alpha$*  was upregulated 5-fold (mean =  $4.96 \pm 0.43$ ), and *CXCL10* was upregulated ten thousand-fold (mean =  $1.13 \times 10^4 \pm 618$ ) in DENV2-infected M0 compared to mock-infected M0 (Figure 3.1C). Next, we measured *IL-10* and *TGF $\beta$*  to investigate the immunosuppressive response during infection. *IL-10* was upregulated 1.75-fold (mean =  $1.75 \pm 0.16$ ) and *TGF $\beta$*  3-fold (mean =  $3.39 \pm 0.63$ ) (Figure 3.1D). We were also interested in *DC-SIGN (CD209)* gene expression, as it is both a marker for the M2 phenotype (Surdziel et al., 2017) and a receptor for DENV cell attachment (Tassaneetrithep et al., 2003). *CD209* was upregulated 1.7-fold (mean =  $1.70 \pm 0.25$ ) in DENV-infected vs. mock-infected M0 cells (Figure 3.1D). These data indicate that DENV2 upregulates expression of both proinflammatory and immunosuppressive genes in M0 macrophage.

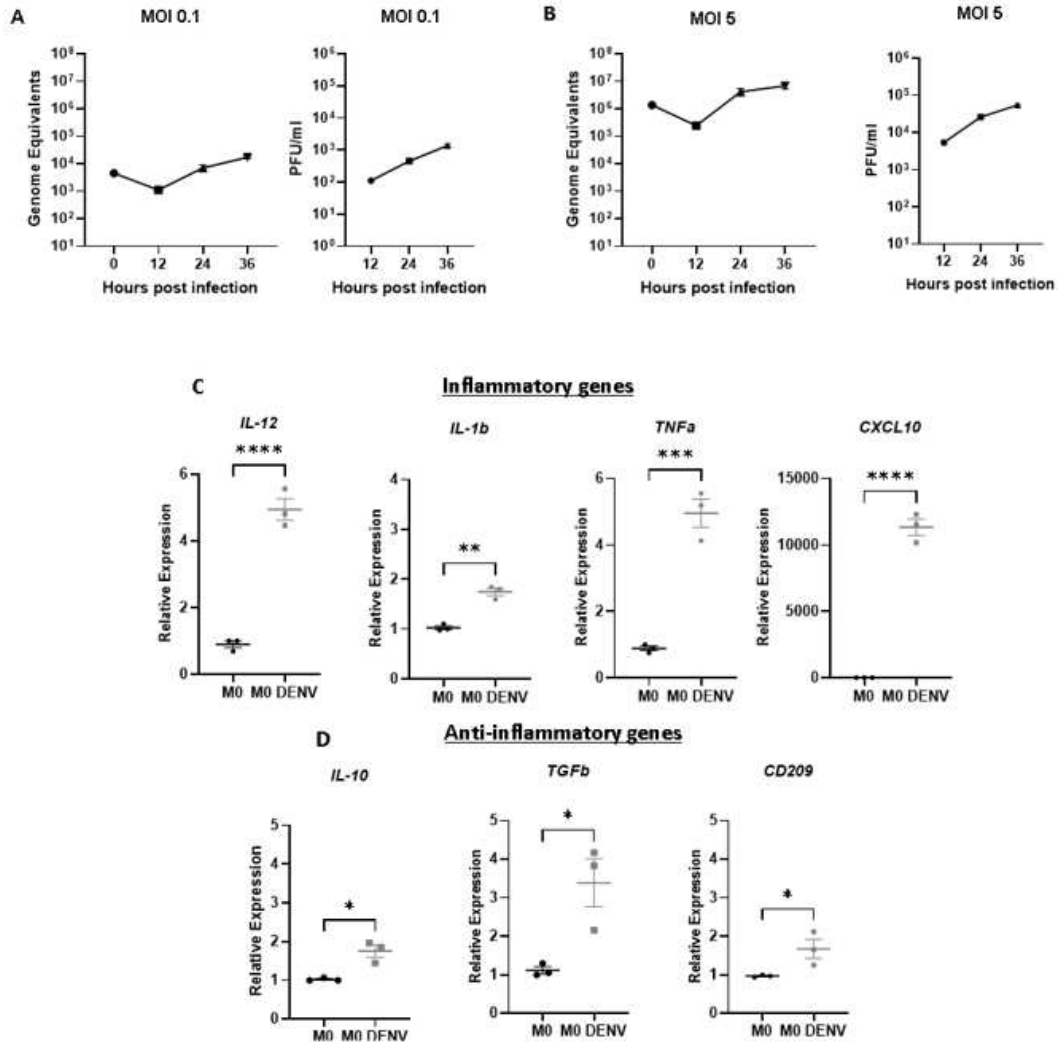


**Figure 3.1: DENV2 upregulates expression of inflammatory and immunosuppressive genes.**

PMA treated THP-1 (M0) cells were infected with an MOI of 0.1 (A) or MOI of 5 (B). Total cellular RNA and supernatant were collected at specified timepoints and analyzed for intracellular DENV2 genome equivalents (left) or infectious particles-PFU/mL (right). M0 cells were infected with an MOI of 5 and total cellular RNA was collected at 36 hpi and analyzed for expression of *IL-12*, *IL-1 $\beta$* , *TNF $\alpha$* , or *CXCL10* (C), or *IL-10*, *TGF $\beta$*  or *CD209* (D). All cellular genes were normalized against reference gene RPL37a. All experiments were n = 3 biological replicates, \*p, 0.05, \*\*p<0.01, \*\*\*p<0.001, \*\*\*\*p<0.0001 unpaired two tailed t tests. Error bars represent mean +/- SEM.

### 3.3b DENV2 infection upregulates cellular metabolism in macrophage

Macrophage undergo metabolic reprogramming during virus infection. To determine the impact of DENV2 infection on macrophage (M0) metabolism, we measured expression of two glycolytic genes, hexokinase 2 (*HK2*) and enolase 1 (*ENO1*). *HK2* encodes the HKII protein, which phosphorylates glucose upon entry into the cell and is a rate limiting enzyme of glycolysis (Wolf et al., 2011). Upon DENV infection, *HK2* was upregulated 2.6-fold (mean = 2.60 +/- 0.22) (Figure 3.2A, left). *ENO1* encodes alpha- enolase ( $\alpha$ -enolase), a glycolytic enzyme that catalyzes 2-phosphoglycerate to phosphoenolpyruvate, the penultimate step in glycolysis.  $\alpha$ -enolase is expressed on the surface of inflammatory macrophage and monocytes. *ENO1* gene expression was upregulated 1.4-fold (mean = 1.39 +/- 0.15) in DENV-infected cells (Figure 3.2A, middle). The increase in both *HK2* and *ENO1* gene expression supports virus-induced glycolysis during DENV2 infection.

To measure an impact of infection on fatty acid oxidation, we measured carnitine palmitoyltransferase 1A (*CPT1a*) gene expression. *CPT1a* encodes CPT1a, an enzyme that transports long chain fatty acids into the mitochondria, where they undergo  $\beta$ -oxidation for efficient ATP generation. *CPT1a* expression was upregulated 1.2-fold (mean = 1.29 +/- 0.06) in infected cells (Figure 3.2A). The modest, but significant increase of *CPT1a* supports the need for fatty acid  $\beta$ -oxidation during DENV2 infection (Jordan & Randall, 2017; Tongluan et al., 2017).

The upregulation of glycolysis and oxidative phosphorylation (OXPHOS) in DENV infected M0 cells at 36 hpi was further corroborated using a Seahorse metabolic flux analyzer. We measured mitochondrial respiration based on oxygen consumption rate (OCR) and measured cellular glycolysis based on extracellular acidification rate (ECAR) (Zhang & Zhang, 2019). OCR and ECAR were measured following injection of oligomycin (ATP synthase inhibitor),

FCCP (uncoupler of oxidative phosphorylation), and rotenone, antimycin A (electron transport chain complex I and III inhibitors) and 2-deoxy-glucose (2-DG) (hexokinase inhibitor). We measured basal respiration, maximal respiration, spare capacity, ATP production, non-mitochondrial respiration, and proton leak (see methods for details regarding calculations of parameters).

There were significant increases in all OCR parameters measured at 36 hpi in DENV2-infected cells when compared to uninfected cells (Figure 3.2B). The increase in basal respiration and maximal respiration shows that DENV2 shifts host cell metabolism to oxidative phosphorylation. The difference between basal respiration and maximal respiration, known as the spare capacity, was higher in infected cells compared to mock infected cells (Figure 3.2B, right). Spare capacity measures the ability of a cell to produce energy under times of increased stress. The increase in spare capacity suggests that mitochondria are responding to the increased stress of viral infection, but still manages to increase energy output, as seen in the increase of ATP production. While DENV2 is increasing mitochondrial respiration, the mitochondria also sustained damage during infection, as seen by an increase in proton leak and non-mitochondrial OCR, two indicators of loss of integrity to the inner mitochondrial membrane and mitochondrial damage (Nanayakkara et al., 2020).

We observed an increase in basal glycolysis, glycolytic capacity, but not glycolytic reserve during DENV infection (Figure 3.2C) Glycolytic capacity is the maximal capacity of a cell to generate ATP from glycolysis, while glycolytic reserve is the difference between basal glycolysis and glycolytic capacity and is the ability of a cell to undergo glycolysis during times of stress (Mookerjee et al., 2016). The increases in both glycolysis and glycolytic capacity indicate that DENV2 is driving the cell to undergo glycolysis at a higher rate, possibly to

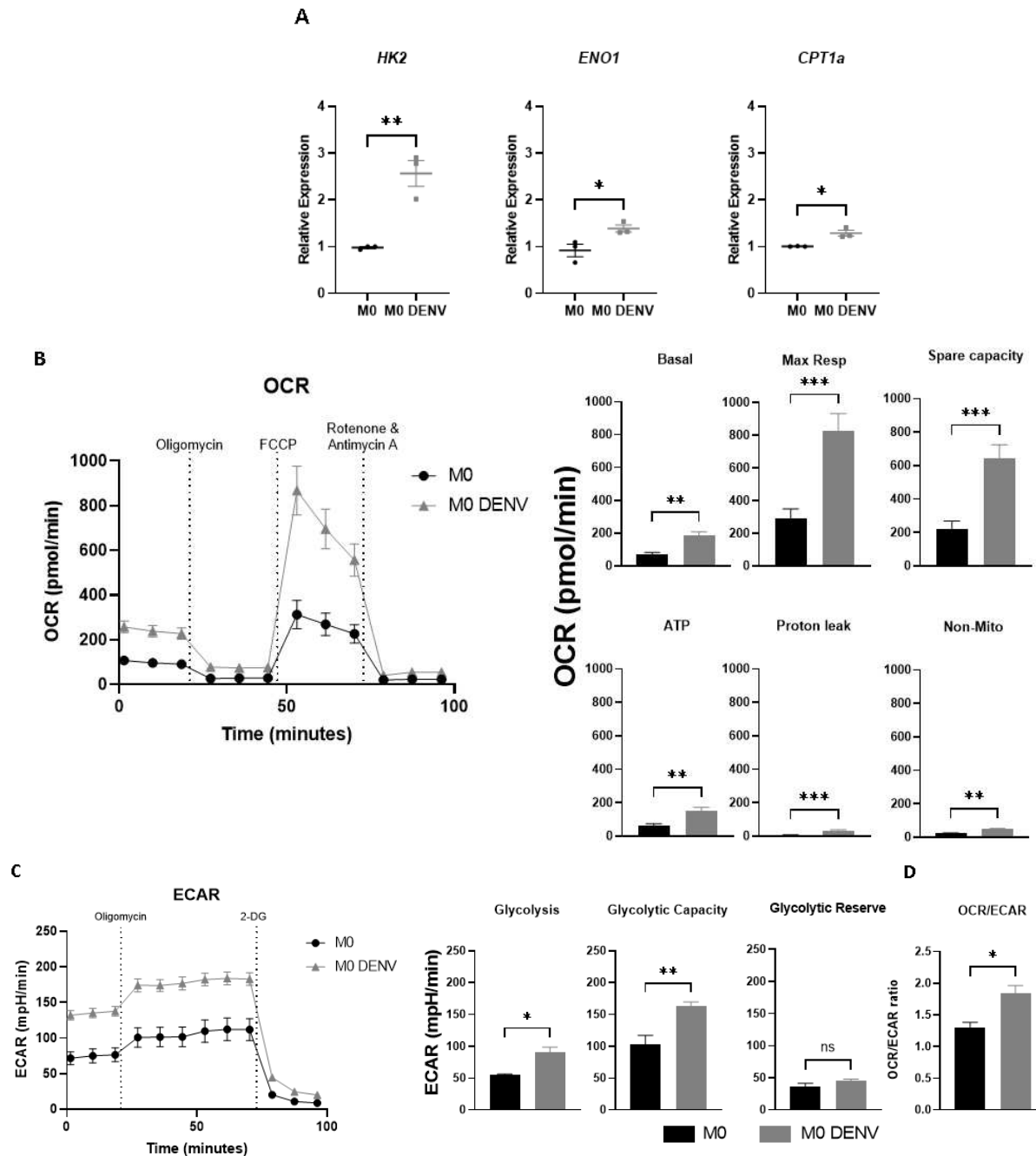


**Figure 3.2: DENV2 drives mitochondrial respiration in M0 cells.** M0 cells were infected with DENV2 at an MOI of 10 (A) Total RNA was analyzed for *HK2*, *ENO1* and *CPT1a* expression (B) Oxygen consumption rate (OCR) was measured during a mitochondrial stress test. Basal rate, Maximum Respiration, Spare Capacity, ATP production, Proton Leak, and Non-Mitochondrial Respiration were calculated. (C) Extracellular acidification rate (ECAR) was measured. Glycolysis, Glycolytic capacity, and Glycolytic reserve were calculated. (D) OCR/ECAR ratio was calculated at 18 minutes. All significant values for OCR and ECAR were calculated using one-way ANOVA with Tukey's multiple comparisons. Significant values for genes calculated using unpaired two tailed t test. \*p, 0.05, \*\*p<0.01, \*\*\*p<0.001, \*\*\*\*p<0.0001. Error bars represent mean +/- SEM.

generate more ATP and funnel glycolytic byproducts into the TCA cycle, and ultimately oxidative phosphorylation. We didn't see any significant difference in glycolytic reserve, suggesting that the ability of a cell to produce ATP from glycolysis is unchanged during times of stress.

Since both OXPHOS and glycolysis were increased, we calculated the OCR/ECAR ratio at basal respiration (Bilz et al., 2018; van der Windt et al., 2012) to determine the dominant metabolic pathway during infection. A high OCR/ECAR indicates cells utilize oxidative phosphorylation for their energy demands, while a low OCR/ECAR ratio suggests cells depend on glycolysis. Infected cells had a higher OCR/ECAR ratio (Figure 3.2D), demonstrating that DENV2 infection drives cells to primarily utilize oxidative phosphorylation for its energy demands.

### *3.3c M2 macrophage support DENV2 infection*

To determine whether macrophage phenotype impacts DENV2 replication, PMA-differentiated M0 were treated with either 20 ng/mL IFN $\gamma$  or 20 ng/mL IL-4 to polarize them into an M1 or M2 phenotype, respectively. M1 and M2 cells were infected with DENV2 at an MOI of 0.1 and total RNA and culture supernatants collected at 0 (virus binding), 6, 12, 18, 24, and 36 hpi to measure viral genome equivalents and plaque forming units. DENV2 genome equivalents decreased in M1 cells throughout infection, with only  $1.4 \times 10^2 \pm 30$  GE remaining at 36 hpi, (Figure 3.3A left). In contrast, viral RNA increased in M2 cells to  $5.36 \times 10^6 \pm 5.5 \times 10^5$  GE at 36 hpi, 4 logs higher than M1 cells (Figure 3.3A, right). The infectious virus titer was also reduced in M1 macrophage when compared to that in M0 and M2 cells at 36 hpi (M0 =  $4.49 \times 10^3 \pm 368$  PFU/mL, M2 =  $3.20 \times 10^3 \pm 409$  PFU/mL, M1 =  $1.55 \times 10^2 \pm 44$  PFU/mL;  $p < 0.001$ ) (Figure 3.3B).

We saw a similar pattern at an MOI of 5, with DENV2 RNA decreasing over time in M1 cells to  $5.10 \times 10^5 \pm 7.0 \times 10^3$  GE at 36 hpi and increasing in M2 cells ( $3.65 \times 10^7 \pm 9.3 \times 10^6$  GE at 36 hpi) (Figure 3.3C). Infectious viral titers were significantly higher in M2 macrophage ( $1.34 \times 10^6 \pm 2.45 \times 10^5$  PFU/mL) and M0 macrophage ( $1.37 \times 10^6 \pm 1.44 \times 10^5$  PFU/mL) when compared to M1 cells ( $2.92 \times 10^3 \pm 7.10 \times 10^2$  PFU/mL) at 36 hpi (Figure 3.3D). Regardless of the MOI, DENV2 did not replicate efficiently in M1 cells, with viral RNA and infectious particles remaining low throughout infection. These data indicate that M2 macrophage provide a supportive cellular environment for DENV2 replication.

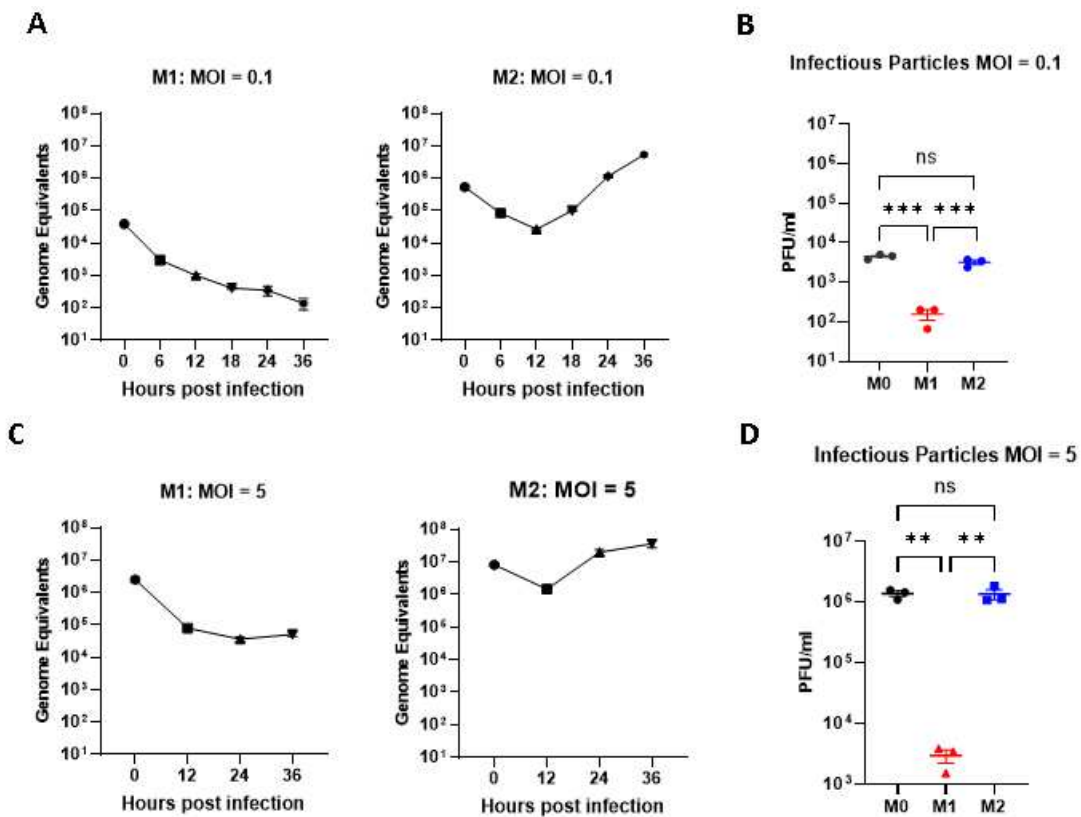


**Figure 3.3: M2 macrophage provide a conducive environment for DENV2 replication.** PMA treated M0 cells were untreated or treated with IFN $\gamma$  or IL4 to polarize to M1 and M2 cells, respectively. Macrophage were infected with a MOI of 0.1 (A and B) or MOI of 5 (C and D). Total cellular RNA and supernatant were collected at specified timepoints and analyzed for intracellular DENV2 genome equivalents (A, C) or infectious particles (PFU/mL) at 36 hours post infection (B, D). All experiments were n = 3 biological replicates, one-way ANOVA with Tukey's multiple comparison's test, \*\*\*p<0.001, \*\*\*\*p<0.0001. Error bars represent mean +/- SEM.

*3.3d DENV2 infection of M2 cells increases immunosuppressive markers but decreases inflammatory cytokines compared to infected M0 cells.*

To further investigate the cellular environment and response to viral infection, we measured the expression of inflammatory and immunosuppressive genes in mock-infected and DENV2-infected M2 cells at 36 hpi. There were no significant differences in the expression of inflammatory genes in M0 and M2 uninfected cells (*IL-12*: M2 mean fold change over M0 = 1.34 +/- 0.21, *IL-1 $\beta$* : M2 fold mean change over M0 = 0.13 +/- 0.03, *TNF $\alpha$* : M2 fold mean change over M0 = 0.66 +/- 0.10, *CXCL10*: M2 fold mean change over M0 = 0.73 +/- 0.10). consider a slightly different format: M2 mean fold change over M0: *IL-12* = 1.34 +/- 0.21, *IL-1 $\beta$*  = 0.13 +/- 0.03, *TNF $\alpha$*  = 0.66 +/- 0.10, *CXCL10* = 0.73 +/- 0.10. Upon infection there was no observed difference in *IL-12* expression levels in M2 cells (M2 DENV mean fold change over M2 = 1.31). However, there was a 0.5-fold increase in *IL-1 $\beta$*  (M2 DENV2 mean fold change over M2 = 0.46), a 6-fold increase in *TNF $\alpha$*  (M2 DENV2 mean fold change over M2 = 6.70) and a 18,000-fold increase in *CXCL10* (M2 DENV2 mean fold change over M2 = 1.83 x 10<sup>4</sup>) in infected M2 cells compared to uninfected M2 cells (Figure 3.4A). When comparing DENV2 infected M2 cells to infected M0 cells, there was a 2.8-fold decrease in *IL-12* (M0 DENV mean fold change over M2 DENV = 2.8), a 5-fold decrease in *IL-1 $\beta$*  (M0 DENV change over M2 DENV2 = 5.84) and a 1.8-fold decrease in *TNF $\alpha$*  (M0 DENV2 mean fold change over M2 DENV2 = 1.83). There was no statistically significant difference in *CXCL10* expression in infected M2 cells compared to infected M0 cells (Figure 3.4A). These data demonstrate that upon infection, the expression of certain inflammatory cytokines, but not *CXCL10*, are reduced in response to DENV2 infection in M2 cells.

While *IL-10* and *TGFβ* are both immunosuppressive genes, they are also master regulators of the anti-inflammatory response and promote activation of M0 cells towards an M2 phenotype (Gong et al., 2012; Saraiva & O'Garra, 2010). To confirm the phenotype of our M2 cells, we measured *IL-10* and *TGFβ* gene expression compared to M0 cells. There was an increase in both *IL-10* and *TGFβ* gene expression in M2 cells compared to that in M0 cells (*IL-10*: M2 mean fold change over M0 = 2.33 +/- 0.06, *TGFβ*: M2 mean fold change over M0 = 2.48 +/- 0.02). Upon infection there was a 3.5-fold increase in *IL-10* (M2 DENV2 mean fold change over M2 = 3.37) and a 1.7-fold increase in *TGFβ* gene expression (M2 DENV2 mean fold change over M2 = 1.69) in infected M2 cells compared to uninfected M2 cells (Figure 3.4B). These data further confirm that DENV2 increases these key regulators of the anti-inflammatory response.

There was an increase in *IL-10* gene expression in infected M2 cells compared to infected M0 cells (M2 DENV2 mean fold change over M0 DENV2 = 1.59). We saw no difference in *TGFβ* gene expression in infected M2 cells versus the infected M0 cells (M2 DENV2 mean fold change over M0 DENV2 = 0.90). DENV2 did increase *IL-10* gene expression (M0 DENV2 mean fold change over M2 = 2.11) and *TGFβ* expression (M2 DENV2 mean fold change over M2 = 1.86) more than the addition of IL-4 alone (Figure 3.4B). This suggests that DENV2 is a stronger trigger for immunosuppressive gene expression than IL-4. The increase of immunosuppressive genes indicates that DENV2 can drive macrophage towards an immunosuppressive phenotype just as strongly as immunosuppressive cytokines, like IL-4.

While *CD209* is a known receptor for DENV2 entry (Tassaneetrithep et al., 2003), it is also a marker for the immunosuppressive macrophage phenotype (Lugo-Villarino et al., 2018). There was a 2.2-fold increase in *CD209* in M2 cells compared to M0 (M2 mean fold change over M0 = 2.23 +/- 0.04). There was also a 1.6-fold increase in infected M2 cells compared to uninfected

M2 cells (M2 DENV2 mean fold change over M2 = 1.58). The increase in *CD209* expression in M2 infected cells compared to M0 infected cells (M2 DENV2 mean fold change over M0 DENV2 = 3.51) (Figure 3.4B) shows that M2 cells not only have a more conducive environment for viral replication, but also upregulates gene expression for one of the receptors DENV2 uses for viral entry.

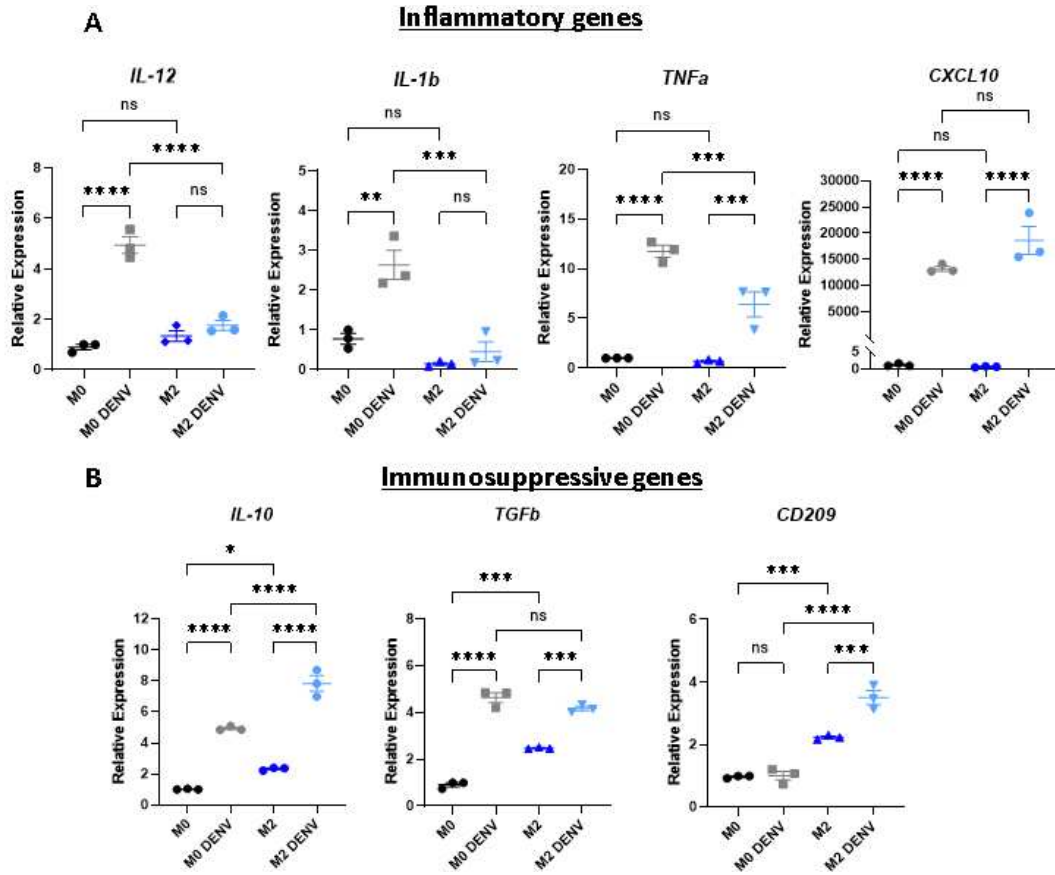


**Figure 3.4: DENV2 infection of M2 cells increases immunosuppressive markers but decreases inflammatory cytokines compared to infected M0 cells.** M2 cells were infected with MOI = 5, total cellular RNA was collected at 36 hours post infection and analyzed for (A) *CXCL10*, *TNF $\alpha$*  or *IL-1 $\beta$* , (B) *IL-10*, *TGF $\beta$*  or *CD209* gene expression. All cellular genes were normalized against reference gene *RPL37a*. All experiments were n = 3 biological replicates, one-way ANOVA with Tukey's multiple comparison's test. \*\*\*p<0.001, \*\*\*\*p<0.0001. Error bars represent mean +/- SEM.

### 3.3e No difference in inflammatory gene expression levels in infected M1 and infected M0 cells

Just as we sought to understand increased DENV2 replication in M2 cells, we measured gene expression of inflammatory genes to evaluate possible outcomes responsible for limited DENV2 replication in M1 cells. We infected M1 cells and collected RNA at 36 hpi to measure *IL-12*, *CXCL10*, *IL-1 $\beta$*  and *TNF $\alpha$*  gene expression. Since *IL-12*, *IL-1 $\beta$*  and *TNF $\alpha$*  are often used to phenotype M1 cells, we used these genes to confirm the M1 phenotype. There was a 1.7- fold increase in *IL-12* (M1 mean fold change over M0 = 1.73 +/- 0.32), a 2.4-fold increase in *IL-1 $\beta$*  (M1 mean fold change over M0 = 2.40 +/- 0.46) and a 10-fold increase in *TNF $\alpha$*  (M1 mean fold change over M0 = 9.98 +/- 0.87) in M1 cells compared to M0 cells. While the increase in *CXCL10* in M1 was not significantly different from M0, M1 cells had 1,000-fold higher expression (M1 mean fold change over M0 =  $1.18 \times 10^3$  +/-  $4.02 \times 10^2$ ) (Figure 3.5).

We measured inflammatory gene expression during infection to determine if an increase in inflammatory gene expression correlated with a decrease in DENV2 replication. DENV2 increased expression of *IL-12*, did not increase the expression of *IL-1 $\beta$*  and increased the expression of *TNF $\alpha$*  and *CXCL10* in M1 infected cells compared to uninfected M1 cells (*IL-12*: M1 DENV2 mean fold change over M1 = 3.09; *IL-1 $\beta$* : M1 DENV2 mean fold change over M1 = 0.95; *TNF $\alpha$* : M1 DENV2 mean fold change over M1 = 1.37; *CXCL10*: M1 DENV2 mean fold change over M1 = 11.22) (Figure 3.5). However, there was not a significant difference in the expression level any of the four inflammatory genes when comparing infected M1 cells and infected M0 cells (*IL-12*: M1 DENV2 mean fold change over M0 DENV = 1.08; *IL-1 $\beta$* : M1 DENV2 mean fold change over M0 DENV2 = 0.87, *TNF $\alpha$* : M1 DENV2 fold change over M0 DENV2 = 1.17, *CXCL10*: M0 DENV2 mean fold change over M1 DENV2 = 1.00) (Figure 3.5). These data indicate that the suppressed DENV2 replication in M1 macrophage was not due to the

increase of these inflammatory genes. Other factors, such as macrophage metabolism or the interferon response, may play an important role in reducing DENV2 replication in M1 cells.

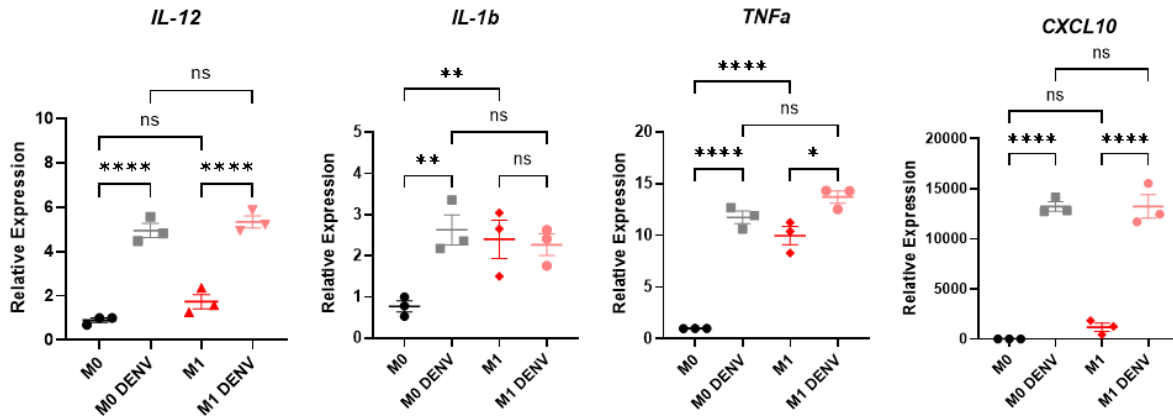


**Figure 3.5: No difference in inflammatory gene expression levels in infected M1 and infected M0 cells.** M1 cells were infected with an MOI = 5, total cellular RNA was collected at 36 hpi and analyzed for *IL-12*, *IL-1β*, *CXCL10*, or *TNFα*. All cellular genes were normalized against reference gene RPL37a. All experiments were n = 3 biological replicates, one-way ANOVA with Tukey's multiple comparison's test (A-D) or unpaired two tailed t tests (D left graph), \*p, 0.05, \*\*p<0.01, \*\*\*p<0.001, \*\*\*\*p<0.0001.). Error bars represent mean +/- SEM.

### 3.4f Expression of glycolytic genes are upregulated in M1 cells upon DENV2 infection, while DENV2 increases expression of both glycolytic and fatty acid oxidation genes in M2 cells

Since inflammatory gene expression did not differ between M0 and M1 macrophage, even though we saw a distinct decrease in DENV2 replication in M1 cells, we wanted to determine if macrophage metabolism impacted replication. The primary pathway used by macrophage differs by phenotype, with M1 utilizing glycolysis and M2 utilizing oxidative phosphorylation and fatty acid oxidation. We investigated the impact of DENV2 infection on metabolic gene expression in M1 and M2 phenotypes at 36 hpi. Since HKII is the first rate limiting enzyme in glycolysis, we measured gene expression changes as a marker for shifts in early glycolysis during polarization and infection. Polarizing cells towards an M2 phenotype did not significantly alter expression levels of *HK2* (M2 mean fold change over M0 = 0.87 +/- 0.06), but infection in M2 cells

increased *HK2* levels 3-fold (M2 DENV2 mean fold change over M2 = 3.10). There was no significant change between M0 DENV and M2 DENV (M0 DENV2 mean fold change over M2 DENV2 = 0.91), meaning that while DENV2 infection increases *HK2* levels, there is no added effect in M2 cells. Next, we measured *HK2* in the M1 phenotype. Since M1 cells upregulate glycolysis, we expected to see an increase in *HK2* upon polarization. As anticipated, *HK2* expression was increased in M1 cells compared to M0 cells (M1 mean fold change over M0 = 2.92 +/- 0.30). We saw a further increase in *HK2* expression levels during DENV2 infection of M1 cells (M1 DENV2 mean fold change over M1 = 1.41), and a significant increase in expression levels in M1 DENV compared to M0 DENV (M1 DENV2 mean fold change over M0 DENV2 = 1.67) (Figure 3.6A).

To determine the impact of DENV2 on late-stage glycolytic genes, we measured *ENO1*.  $\alpha$ -enolase is an enzyme that plays a role in both late glycolysis as well as in the inflammatory response in monocytes. Similar to *HK2*, polarizing cells towards M2 did not significantly change *ENO1* expression levels (M2 mean fold change over M0 = 1.46 +/- 0.20). There was no significant increase in *ENO1* during DENV2 infection of M2 cells (M2 DENV2 mean fold change over M0 = 1.84 +/- 0.07) and no difference in *ENO1* gene expression in M2 DENV compared to M0 DENV (M2 DENV2 mean fold change over M0 DENV2 = 0.96). Next, we measured *ENO1* expression in M1 cells. Since glycolysis is the primary metabolic pathway in M1 cells, we expected *ENO1* expression levels to increase upon polarization. As expected, we saw an increase in *ENO1* expression upon polarization (M1 fold mean change over M0 = 1.73 +/- 0.05). Infection further increased expression (M1 DENV2 mean fold change over M1 = 1.56) and there were significantly higher expression levels in M1 infected cells compared to infected M0 cells (M1 DENV fold change over M0 DENV = 1.490) (Figure 3.6B). These data suggest

that DENV2 induces early glycolytic gene expression in all macrophage phenotypes, but only increases late glycolytic gene expression in naive and inflammatory phenotypes.

Since oxidative phosphorylation plays a major role in M2 macrophage function, we investigated the gene expression of *CPT1a* in M1 and M2 macrophage. While *CPT1a* was not upregulated in M2 cells compared to M0 cells (M2 mean fold change over M0 = 1.06 +/- 0.02), there was a significant increase in expression during infection of M2 cells (M2 DENV2 mean fold change over M0 = 1.83 +/- 0.07). Furthermore, the expression of *CPT1a* was higher in infected M2 cells compared to infected M0 cells (M2 DENV2 mean fold change over M0 DENV2 = 1.31). While *CPT1a* is not upregulated during M2 polarization, the upregulation during infection suggests that DENV2 is driving fatty acid oxidation in M2 phenotypes compared to M0. When we measured *CPT1a* expression in M1 cells, we observed an increase in uninfected M1 cells compared to uninfected M0 cells (M1 mean fold change over M0 = 1.50 +/- 0.10). However, when we measured *CPT1a* in infected M1 cells, we did not see a difference between uninfected and infected M1 cells (M1 DENV2 mean fold change over M1 = 0.93) or between infected M1 cells and infected M0 cells (M1 DENV2 mean fold change over M0 DENV2 = 1.00) (Figure 3.6C). The negligible difference in *CPT1a* gene expression during infection of M1 macrophage compared to M0 cells suggests that DENV2 infection does not increase oxidative phosphorylation in these cells. The differences in glycolytic and fatty acid oxidative gene expression between M1 and M2 infected cells suggests metabolism may play an important role to either enhance or diminish viral replication.

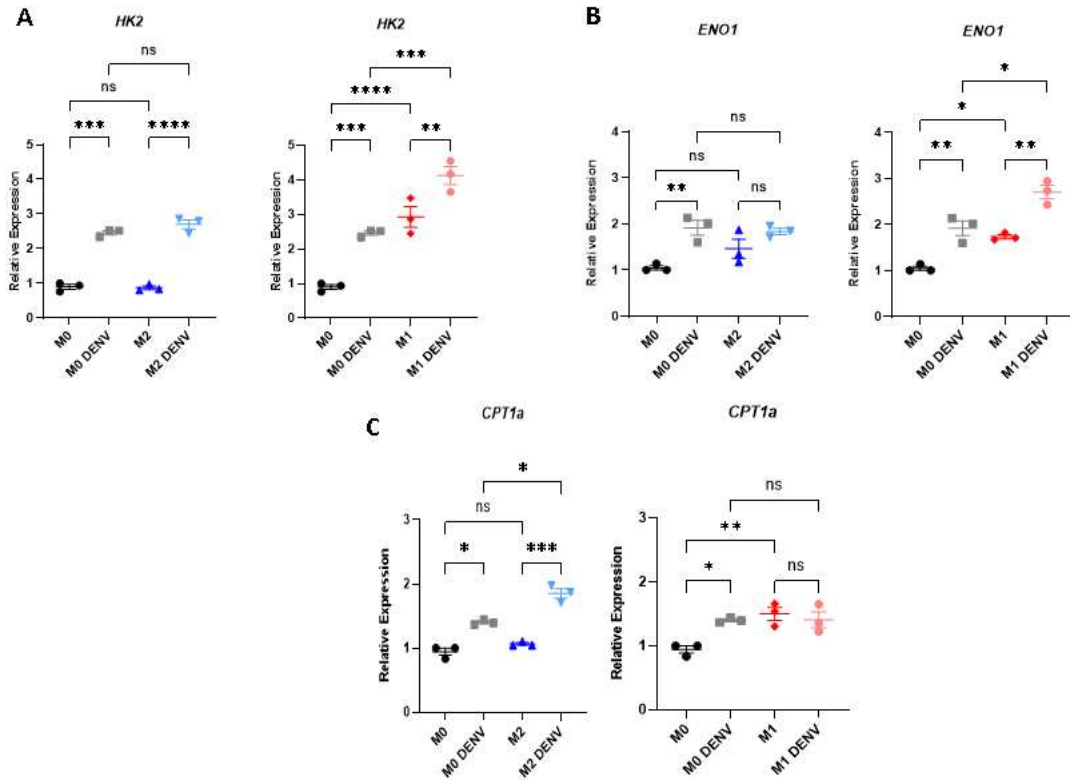


**Figure 3.6: Glycolytic gene expression is upregulated in M1 cells upon DENV2 infection, while DENV2 increases glycolytic and fatty acid oxidation gene expression in M2 cells.** M2 or M1 cells were infected with an MOI of 5, total cellular RNA was collected at 36 hpi and analyzed for *HK2*, *ENO1* or *CPT1a*. All cellular genes were normalized against reference gene RPL37a. All experiments: n = 3 biological replicates, one-way ANOVA with Tukey's multiple comparison's test \*p, 0.05, \*\*p<0.01, \*\*\*p<0.001, \*\*\*\*p<0.0001. Error bars represent mean +/- SEM.

### 3.3g *DENV2* infection increases mitochondrial respiration

To further validate the impact DENV2 has on M1 and M2 metabolism, we used a seahorse flux analyzer to measure oxygen consumption rate (OCR). We measured changes in mitochondrial stress following the addition of oligomycin (ATP synthase inhibitor), FCCP (electron transport chain uncoupler), rotenone and antimycin A (electron transport chain complex I and III inhibitors). We examined mitochondrial respiration in uninfected M0 and M2 cells and M2 cells infected with DENV2 virus. We infected cells with MOI = 10 and performed a seahorse assay at 36hpi.

Our data confirm that M2 cells have higher oxygen consumption than non-polarized cells (Figure 3.7A,B). While M2 cells had higher basal respiration, maximal respiration compared to M0 cells, there was no significant difference in spare capacity, indicating polarization to M2 cells does not impact the cell's ability to produce energy under conditions of increased work. Polarization towards M2 also increased ATP production, suggesting that polarization increases ATP demand, which is a hallmark of this phenotype (Van den Bossche et al., 2017). M2 polarization did not change proton leak, but it did increase non mitochondrial respiration (Figure 3.7B) indicating that there is no damage to the mitochondrial matrix, but possibly an increase in the activity of enzymes associated with inflammation, such as NADPH oxidase or lipoxygenases (Chacko et al., 2014).

Lastly, we compared M2 and M2 DENV2. The only parameters that had a significant difference between M2 and M2 DENV2 cells were maximal respiration and spare capacity. The increase in both of these parameters indicates that DENV2 is not only driving the maximum amount of oxidative phosphorylation mitochondria can sustain but is also increasing the range of potential of substrates the cell can use for respiration, such as lipids or amino acids (Tavakoli et al., 2013). These data suggest that DENV2 increases mitochondrial respiration in M2 cells to create an environment that is beneficial to viral replication (Figure 3.7B).

Next, we measured mitochondrial respiration on M1 macrophage. We measured mitochondrial respiration in uninfected M0 and M1 cells and M2 cells infected with DENV2 virus at an MOI = 10 and performed the seahorse assay at 36hpi. Since M1 macrophage upregulate glycolysis and not oxidative phosphorylation, we did not expect to see a difference in any mitochondrial respiration parameter compared to M0 macrophage. There was no significant difference between M1 and M0 cells when measuring basal respiration, maximal respiration, or

spare capacity (Figure 7C & D). There was an increase in ATP production, proton leak and non-mitochondrial OCR in M1 cells compared to M0 cells. Proton leak and non-mitochondrial OCR are indicators of mitochondrial health but are also associated with inflammation (Chacko et al., 2014). The increase in these parameters could further confirm that M1 cells have increased inflammatory mechanisms compared to M0 cells.

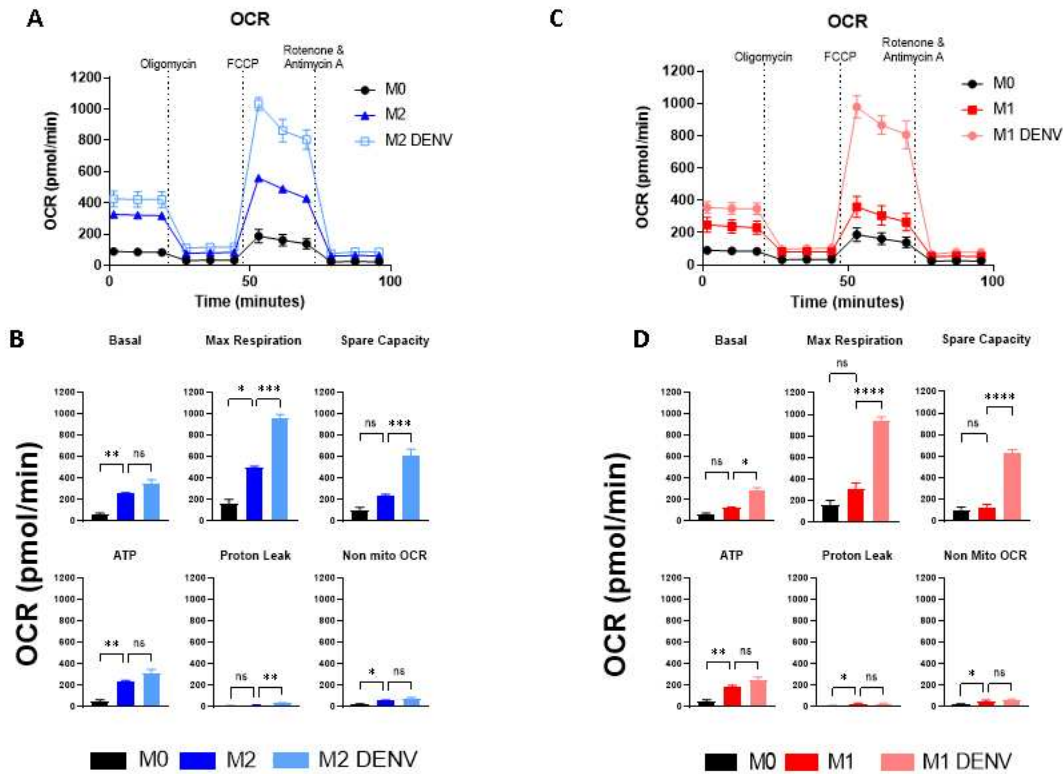


**Figure 3.7: DENV2 drives oxidative phosphorylation in M1 and M2 cells.** M1 and M2 cells were infected with an MOI of 10. (A and B) M2 cells or (C and D) M1 cells were infected with DENV2 at an MOI of 10. Oxygen consumption rate (OCR) was measured during a mitochondrial stress test. Basal rate, Maximum Respiration, Spare Capacity, ATP production, Proton Leak, and Non-Mitochondrial Respiration were calculated. All significant values for OCR and ECAR were calculated using one-way ANOVA with Tukey's multiple comparisons. Significant values for genes calculated using unpaired two tailed t test. \*p, 0.05, \*\*p<0.01, \*\*\*p<0.001, \*\*\*\*p<0.0001. Error bars represent mean +/- SEM.

There was a significant increase in basal and maximal respiration between M1 and M1 DENV. This indicates that the virus is driving cells towards oxidative phosphorylation. The increase in spare capacity, shows that the virus is increasing the cell's ability to utilize energy in times of stress. The insignificant differences between M1 and M1 DENV in ATP production, non-mitochondrial OCR and proton leak suggests infection does not lead to increased ATP synthesis and does not dysregulate mitochondrial function. These data show that even though there is little DENV2 replication, there is still an impact of the virus on cellular metabolism. Regardless of phenotype, DENV2 increases mitochondrial respiration, but is not a sufficient explanation for the differences in virus replication in M1 compared to M0 and M2 cells (Figure 3.7D)

#### *3.4h DENV2 does not increase glycolysis in M1 or M2 cells*

To understand differences in glycolysis between M1 and M2 cells, we measured changes in extracellular acidification rate (ECAR) using a seahorse flux analyzer. We measured changes in glycolysis following the addition of glucose, oligomycin (ATP synthase inhibitor), and 2-DG (hexokinase inhibitor). We measured ECAR in uninfected M0 and M2 cells and M2 cells infected with DENV2 virus. We infected cells with MOI = 10 and performed a seahorse assay at 36 hpi.

Polarization towards M2 cells increased glycolysis, and glycolytic capacity, but did not impact glycolytic reserve (Figure 3.8A). While glycolysis is not the primary metabolism of M2 cells, increasing the rate of glycolysis has the potential to increase the amount of lactate shuttled into the TCA cycle, ultimately increasing oxidative phosphorylation. There was no difference between M2 and M2 DENV in the observed glycolytic parameters, indicating that the binding, uptake, and replication of DENV2 in M2 macrophages has little impact on glycolysis. The

OCR/ECAR ratio is increased once cells are polarized towards an M2 phenotype, which further confirms that these cells utilize oxidative phosphorylation over glycolysis (Figure 3.8B). We measured an increase in the ratio between M2 and M2 DENV cells. Polarization towards M2 increases oxidative phosphorylation and infection with DENV2 increases it further.

Polarization towards M1 cells increased the rate of glycolysis compared to M0 cells, but we saw no difference in glycolytic capacity or glycolytic reserve (Figure 3.8C). The negligible difference in these parameters between M1 and M0 cells confirm our previous results and demonstrates that M1 cells do not utilize glycolysis during cellular stress and will most likely use oxidative phosphorylation. The only significant difference between M1 and DENV-infected M1 cells was the level of glycolytic reserve, an indication that infection increased the cell's ability to use glycolysis in times of stress. This may be beneficial to the virus as it can increase the capacity of a cell to metabolize carbon, via glycolysis, and shuttle byproducts into the TCA cycle. There was no significant difference in OCR or ECAR between M0 and M1 cells (Figure 3.8D). However, infection seems to increase the OCR/ECAR ratio in M1 cells, indicating DENV drives this cell type to upregulate oxygen consumption instead of glycolysis (Figure 3.8D). The increase in oxidative phosphorylation over glycolysis during infection suggests that DENV drives M1 cells towards a metabolic profile distinct from conventional M1 macrophage.

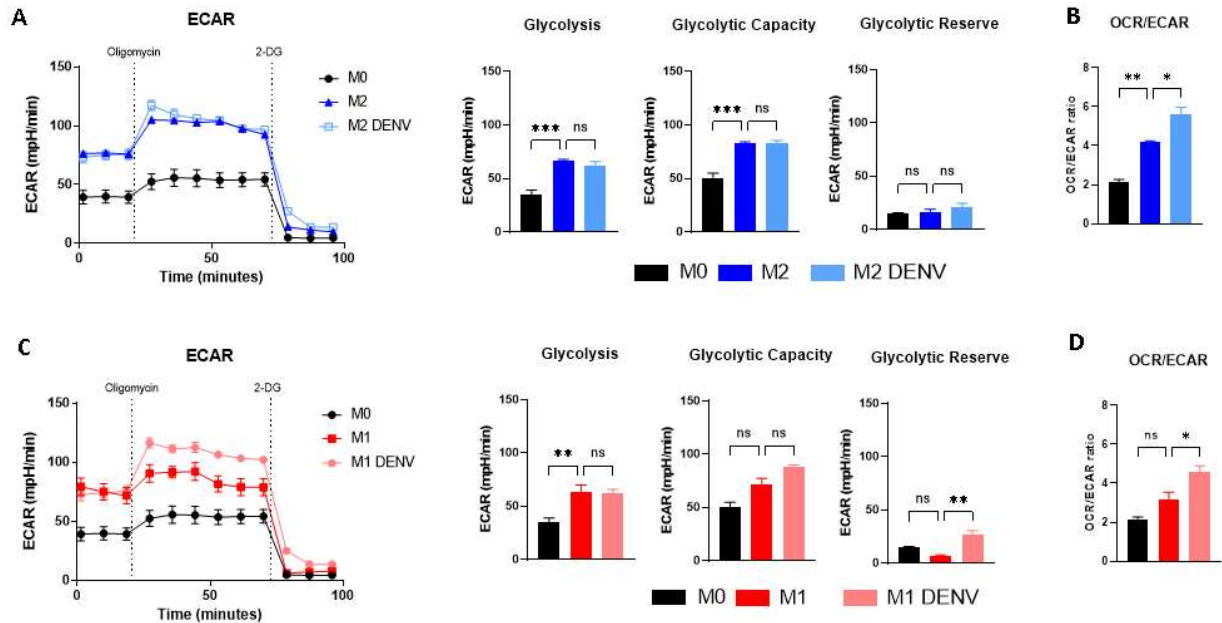


**Figure 3.8: DENV2 does not increase rates of glycolysis in M1 and M2 cells.** M1 and M2 cells were infected with an MOI of 10. (A and B) M2 cells or (C and D) M1 cells were infected with DENV2 at an MOI of 10. Extracellular acidification rate (ECAR) was measured. Glycolysis, Glycolytic Capacity, and Glycolytic Reserve were measured. (B and D) OCR/ECAR ratio was calculated at basal respiration at 18 minutes. All significant values for OCR and ECAR were calculated using one-way ANOVA with Tukey's multiple comparisons. Significant values for genes calculated using unpaired two tailed t test. \*p, 0.05, \*\*p<0.01, \*\*\*p<0.001, \*\*\*\*p<0.0001. Error bars represent mean +/- SEM.

### 3.4i Increases in expression of type I interferon genes during infection correlate with decreases in DENV2 replication in M1 cells

In addition to cellular metabolism, we investigated the impact of the type 1 interferon response on DENV2 replication in M0, M1 and M2 cells. The type 1 interferon response is a potent anti-viral pathway cells use to prevent viral spread (Katze, He, & Gale, 2002). We first measured gene expression of interferons alpha (*IFN $\alpha$* ) and beta (*IFN $\beta$* ). Polarization towards M1 or M2 cells did not impact *IFN $\alpha$*  gene expression compared to M0 cells (M1 mean fold increase over M0 = 0.78 +/- 0.16, M2 mean fold change over M0 = 1.05 +/- 0.21), but infected M0, M1 and M2 cells had elevated levels of *IFN $\alpha$*  compared to mock infected cells. When we compared

infected subsets, infected M2 cells had lower levels of *IFN $\alpha$*  compared to infected M0 cells, but infected M1 cells had higher *IFN $\alpha$*  expression compared to both M0 and M2 infected cells (M2 DENV mean fold change over M0 = 5.8 +/- 0.66, M1 DENV2 mean fold change over M0 = 14.67 +/- 0.229, M0 DENV2 mean fold change over M0 = 10.33 +/- 0.522) (Figure 3.9).

When measuring *IFN $\beta$*  expression, we saw that polarization towards an M1 or M2 phenotype did not impact *IFN $\beta$*  levels (M1 mean fold change over M0 = 1.49 +/- 0.09, M2 mean fold change over M0 = 0.89 +/- 0.11). Upon infection, *IFN $\beta$*  was significantly increased in infected M1 cells, which had a 11-fold increase compared to infected M0 (M1 DENV2 mean fold change over M0 DENV = 11.09). In contrast, infected M2 cells had a lower induction of *IFN $\beta$*  expression compared to M0 cells (M2 DENV mean fold change over M0 DENV2 = 0.18). *IFN $\gamma$*  alone did not significantly increase *IFN $\beta$*  gene expression, so there was a specific induction of *IFN $\beta$*  in response to infection in M1 cells.

To confirm whether type I IFN-mediated mechanisms impact the observed restriction of DENV2 in M1 cells, we measured gene expression levels of 2'-5'-oligoadenylate synthetase 1 (*OAS1*), a known interferon-induced gene. *OAS1* gene expression was increased in M1 cells, but not in M0 or M2 cells (M1 mean fold change over M0 = 24.94 +/- 5.37, M2 fold change over M0 = 1.50 +/- 0.61). DENV2 infection increased *OAS1* gene expression in M0, M1 and M2 cells, with no significant differences between the phenotypes (M1 DENV mean fold change over M0 =  $2.38 \times 10^3$  +/- 55.5, M0 DENV2 mean fold change over M0 =  $2.19 \times 10^3$  +/- 67.1, M2 DENV2 mean fold change over M0 =  $1.74 \times 10^3$  +/- 142). When we measured expression of the IFN-inducible double-stranded RNA-dependent protein kinase R (*PKR*), its expression was increased in M1 cells compared to M0 or M2 cells (M1 mean fold change over M0 = 1.65 +/- 0.06, M2 mean fold change over M0 = 0.93 +/- 0.03) and further increased upon DENV2 infection (M1

DENV2 mean fold change over M0 = 2.27 +/- 0.160, M0 DENV2 mean fold change over M0 = 1.59 +/- 0.084, M2 DENV2 mean fold change over M0 = 1.43 +/- 0.02). There was no difference between M0 and M2 infected cells, but *PKR* expression was significantly increased in infected M1 cells (Figure 3.9). When comparing infected M1 cells and infected M2 cells, we saw higher levels of *IFN $\alpha$* , *IFN $\beta$* , *OAS1*, and *PKR* in infected M1 cells compared to infected M2 cells. These data indicate that the interferon response may play an important role in inhibiting the production of DENV2 infectious virus and possibly increasing the host response against infection in M1 cells.

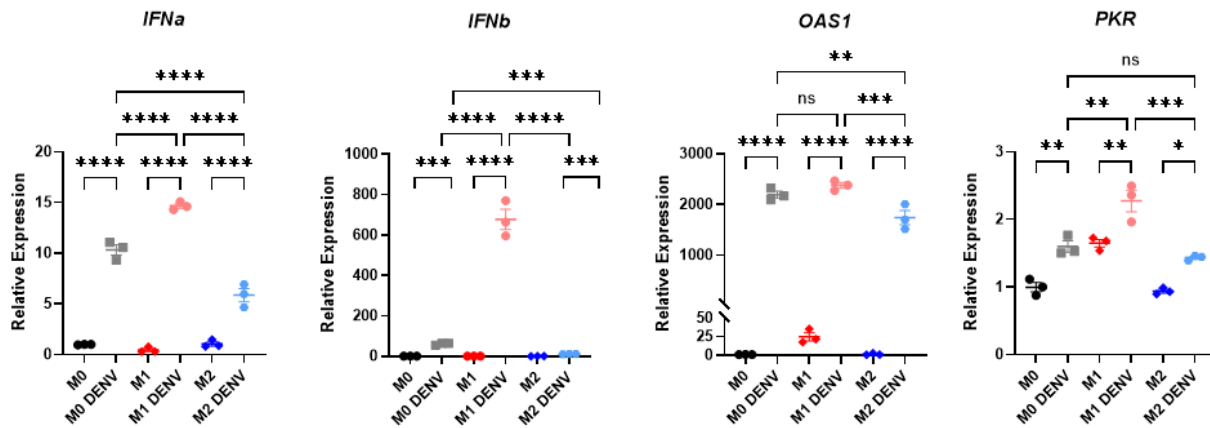


**Figure 3.9: Increase in IFN-stimulated genes leads to a decrease in DENV2 replication.** M1 cells were infected with an MOI = 5, total cellular RNA was collected at 36 hpi and analyzed for *IFN $\beta$* , *IFN $\alpha$* , *OAS1* or *PKR* gene expression. All cellular genes were normalized against reference gene *RPL37a*. All experiments were n = 3 biological replicates, one-way ANOVA with Tukey's multiple comparison's test. \*p, 0.05, \*\*p<0.01, \*\*\*p<0.001, \*\*\*\*p<0.0001.). Error bars represent mean +/- SEM.

### 3.5 Discussion

Together, our data show that regardless of phenotype, DENV2 will attempt to reprogram macrophage gene expression and metabolism to drive cells towards a hospitable environment for replication. DENV infection results in an increase in both inflammatory and anti-inflammatory

genes, suggesting that the virus is driving cells towards a hospitable environment for replication, while the cell is mounting an anti-viral response against the virus. An increase in oxidative phosphorylation combined with an immunosuppressive environment leads to an increase in DENV replication in M2 cells. While DENV did increase oxidative phosphorylation in M1 cells, the interferon response negated any potential benefit an increase in oxidative phosphorylation could have provided for DENV replication.

Macrophage are among the first cells to become infected with DENV2 after a mosquito bite (Schmid & Harris, 2014)(Rathore & St John, 2018). These cells not only initiate inflammation by recruiting inflammatory cells to the site of infection (Fujiwara & Kobayashi, 2005), but they also illicit a strong type I and type II interferon response, which promotes anti-viral mechanisms (McNab, Mayer-Barber, Sher, Wack, & O'Garra, 2015). To evade an anti-viral response some viruses, such as respiratory syncytial virus (RSV), polarize M0 macrophage towards an M2 phenotype, resulting in an environment has an increase in both inflammatory and immunosuppressive genes (Shirey et al., 2010). We observed a similar phenomenon, where M0 macrophage upregulate both inflammatory and immunosuppressive genes in response to DENV2 infection. Our model recapitulates what is seen in severe dengue patients, where severe dengue episodes result in an increase in both inflammatory and anti-inflammatory cytokines and chemokines (Soo et al., 2017; Soo et al., 2019; Zhao et al., 2016). While the immune response to DENV is incredibly complex, our study further confirms that the macrophage is mounting an anti-viral response at the same time the virus is driving the cell to create an immunosuppressive environment.

We observed enhanced replication in M2 macrophage and decreased replication in M1 macrophage. Other viruses, such as HIV and HCV, have altered replication kinetics in different

macrophage phenotypes (D. H. Lee & Ghiasi, 2017). Previous literature has shown that stimulating macrophage with IL-4 increases gene expression of *DC-SIGN (CD209)*, a receptor that is both upregulated in M2 cells and used by DENV2 for cell entry (Schaeffer et al., 2015), which has been correlated with increased DENV RNA during infection. While we did not see an increase in *DC-SIGN* gene expression with IL-4 stimulation on its own, we did see an increase during infection. DENV2 may increase *DC-SIGN* expression as a method to increase entry and viral replication in M2 cells (P. Liu et al., 2017). In contrast, we found that M1 cells were permissive to infection but did not sustain high viral titer or genome equivalents. Cells treated with IFN $\gamma$  have been shown to have limited DENV, most likely due to an increased interferon response (Diamond & Harris, 2001; Sittisombut et al., 1995). Ebola virus exhibits similar replication dynamics, with increased replication in M2 cells and diminished replication in M1 cells (Rhein et al., 2015; Rogers et al., 2019).

M2 cells have an environment more conducive to viral replication. These macrophage have an increase in immunosuppressive genes, such as *IL-10* and *TGF $\beta$* , which allow viruses to replicate while evading strong anti-viral response (Cassol et al., 2009; Mantovani et al., 2004). Expression of inflammatory genes were decreased in infected M2 cells compared to M0 cells, suggesting that a decreased inflammatory response may be beneficial to DENV replication, as seen with HIV (Tricia et al., 2015). The increase in *IL-10* expression during DENV infection alone surpassed the level of IL-10 seen by stimulating cells with IL-4. Many viruses target IL-10 since it is a key regulator in the immunosuppressive response and activation of *IL-10* prevents the release of inflammatory proteins (Saraiva & O'Garra, 2010). Hepatitis C virus, herpesviruses and poxviruses have all adapted a mechanism to increase IL-10 gene or protein expression during infection (Fleming et al., 1997; Kwon et al., 2019; Suzuki et al., 1995). Furthermore, an

increase in IL-10 has been seen in severe dengue illness and is being considered as a marker for severe dengue (Pé Rez et al., 2004). DENV infection also increases *TGFβ* in M0 and M2 macrophage. Increasing the amount of *TGFβ* is also an effective immune evasion strategy. *TGFβ* inhibits iNOS and nitric oxide production (Abd El-Aleem, Mohammed, Saber, Embaby, & Djouhri, 2020), which leads to a dampened anti-viral response and increased survival (Odkhuu et al., 2018).

The M1 phenotype is associated with higher levels of inflammatory genes and our data show *IFNβ*, *IFNα* and *PKR* are particularly important in the M1 phenotype's anti-viral response against DENV2. *IFNα* and *IFNβ* have the highest expression in infected M1 macrophage compared to infected M0 or infected M2 cells. The increase in *IFNα* and *IFNβ* will ultimately lead to the transcription of interferon stimulated genes (ISGs), such as *OAS1* and *PKR*. *OAS1* has been shown to block DENV replication, while the exact role of *PKR* as an anti-viral mechanism against DENV remains to be discovered (Diamond & Harris, 2001; R.-J. Lin et al., 2009). It has been suggested that the decrease in DENV2 replication in *IFNγ/β* treated cells is due to mechanisms that prevent translation of viral proteins necessary for viral replication (Diamond & Harris, 2001). We show that an increase in *PKR* and *OAS1* gene expression are correlated with decreased viral replication in M1 cells. These data suggest that the suppressed replication is due to *IFNγ* priming the type I and type II interferon response in during DENV2 infection (Diamond et al., 2000).

Viral reprogramming of metabolism has dual purposes in macrophage, since shifting metabolism shifts function (O'Neill & Pearce, 2016). We found that DENV2 increases *HK2* gene expression in M0, M1 and M2 macrophage, while *ENO1* was only increased in M0 and M1 cells. *HK2* has been linked as a key enzyme in toll-like receptor (TLR) induced glycolytic burst

and activation of dendritic cells (Everts et al., 2014; Perrin-Cocon et al., 2018), linking its enzyme activity to both the regulation of cellular metabolism and inflammation. Cells cultured in media supplemented with purified  $\alpha$ -enolase protein upregulate proinflammatory gene expression, via binding and activation of TLR-4 (Bae et al., 2012; Guillou et al., 2016), indicating *ENO1* plays an important role in inflammation. Since *ENO1* and *HK2* have both been linked to increase in inflammatory mediators (Bae et al., 2012; Guillou et al., 2016; Hinrichsen et al., 2021; Wolf et al., 2011), an increase in these genes indicates that viral induction of glycolysis for viral replication could be detrimental to DENV2 survival in M1 cells. Since late glycolytic enzymes play a role in production of reactive oxygen species and inflammasomes in macrophage (Van den Bossche et al., 2017), the increase in glycolysis in M1 cells could contribute to the decrease in DENV2 replication. The increases of *HK2* and *ENO1* in M1 infected cells correlate with increased inflammatory chemokines and decreased DENV replication. *CPT1a* is an important protein for oxidative phosphorylation and regulating inflammation (Calle et al., 2019; Lin et al., 2018). We found that *CPT1a* was upregulated in infected M0 and infected M2 macrophage, but not infected M1 cells. The increase in *CPT1a* could be due to the increase in fatty acid oxidation and beta oxidation necessary to sustain infection. Furthermore, since *CPT1a* is important for an anti-inflammatory response, DENV could be upregulating this gene to evade an anti-viral response in the cell.

DENV2 has been shown to enhance the oxidative phosphorylation (Butler et al., 2020; Fernandes-Siqueira et al., 2018) and redistribute fatty acid synthetase to increase fatty acid synthesis (Heaton et al., 2010). We show that DENV2 increases the rate of oxidative phosphorylation in all subsets of infected macrophage. In M0 and M2 cells, the increase in oxidative consumption rate is associated with an increase in DENV2 RNA and infectious

particles. Within these cells the DENV2 is taking advantage of, as well as driving, the increased rate of oxidative phosphorylation to enhance replication and infectious particle production. In contrast, the increased rate of oxidative phosphorylation in M1 cells does not explain the decreased viral replication observed in this phenotype. Increase in mitochondrial respiration may serve a different purpose in M1 cells, as an increase in fatty acid oxidation has been shown to increase IFN $\alpha$  expression, possibly driving an interferon response against the virus (D. Wu et al., 2016). In addition to increasing fatty acid synthesis and oxidative phosphorylation, DENV2 replication also induces glycolysis (Fontaine et al., 2015). We did not observe an increase in glycolysis in infected M2 cells or infected M1 cells, which supports the fact that DENV2 is driving oxidative phosphorylation more than glycolysis in these cells.

Our research shows that DENV infected macrophages exhibit characteristics of both inflammatory and immunosuppressive phenotypes. While infection of inflammatory macrophage leads to an upregulation of oxidative phosphorylation, the strong interferon response leads to diminished replication compared to immunosuppressive macrophage. The differences in cytokine expression levels in acute and chronic dengue infection is correlated with disease severity (K.-M. Soo et al., 2017; K. M. Soo et al., 2019). Understanding the regulation of viral induced inflammatory responses in different phenotypes of macrophage is critical to understanding DENV pathology and disease progression.

## CHAPTER 4: INVESTIGATING THE ROLE OF CDK8 AND CDK19 IN DENV2 INFECTION OF MACROPHAGES

### 4.1 Summary

Dengue virus (DENV) is the most prevalent arthropod borne flavivirus in the world, causing dengue hemorrhagic fever and dengue shock syndrome. To effectively replicate and evade anti-viral responses mounted by infected cells, DENV must block/alter the transcription of inflammatory and anti-inflammatory genes and proteins. Here, we investigate the role of cyclin dependent kinase 8 (CDK8) and its paralog, cyclin dependent kinase 19 (CDK19), during DENV infection of macrophage. CDK8 and CDK19 are host transcriptional co-factors that regulate expression of interferon gamma-stimulated genes and certain cytokines/chemokines. We show that DENV serotype 2 (DENV2) infection induces expression of CDK19, but not CDK8 in THP-1 cells. Treatment with Senexin B, a CDK8/19 inhibitor, was found to increase DENV2 genome equivalents and infectious particles in naïve (M0) macrophages. We also find that inhibition of CDK8/19 kinase activity increases *IL-10* but decreases *CXCL10* gene expression. This suggests dependence upon CDK8/19 activity for virus induction of *CXCL10* and repression of *IL-10*. We present preliminary data assessing the roles of CDK8 and CDK19 during DENV infection of macrophage. Using a shRNA lentiviral knockdown system, we find that CDK8 and CDK19 regulate different pathways within the context of infection. Lastly, we begin to investigate the role of CDK8 and CDK19 within polarized macrophage. Similar to results seen in M0 macrophage, inhibition of CDK8/19 kinase activity increases *IL-10* expression but decreases *CXCL10* gene expression in inflammatory (M1) and anti-inflammatory (M2) macrophage. These preliminary data suggest that CDK8 and CDK19 may play a key role in regulating macrophage

ability to transcribe genes that control polarization and anti-viral immunity during DENV infection.

## **4.2 Introduction**

Cytokines and chemokines are master regulators of the innate and adaptive immune response. These proteins interact with cytokine/chemokine receptors to regulate the immune response, either inducing or suppressing inflammation (Dinarello, 2000; Opal & DePalo, 2000). One of the predominant producers of cytokines and chemokines are macrophage (Tayal & Kalra, 2008), where inflammatory (M1) macrophage secrete inflammatory cytokines and chemokines and anti-inflammatory (M2) macrophage secrete anti-inflammatory cytokines (Sica & Mantovani, 2012). Signal transducer and activator of transcription (STAT) proteins are known to regulate the transcription of cytokines and chemokines genes (Lawrence & Natoli, 2011). During polarization towards an M2 phenotype, the phosphorylation of STAT6 leads to the repression of the inflammasome and inflammatory genes (Czimmerer et al., 2018; T. Yu et al., 2019). In addition, the phosphorylation of STAT3 initiates an anti-inflammatory signaling cascade necessary for M2 function (Weber-Nordtt et al., 1996). In M1 cells, the phosphorylation of STAT1 leads to the induction of various inflammatory genes (Lawrence & Natoli, 2011).

CDK8 is a component of the Mediator complex, which is required for transcription of RNA polymerase II (RNAP II) genes (Soutourina, 2018). CDK8, its activating cyclin, cyclin C, and two other Mediator proteins, Med12 and Med13, make up the CDK8 kinase module. This module can phosphorylate the Carboxy Terminal Domain (CTD) of RNAP II to control transcriptional pausing and elongation of RNAPII dependent genes (Conaway & Conaway, 2013). The CDK8 module can reversibly dissociate from RNAPII and phosphorylate transcription factors in response to cell stress and reprograms cellular metabolism, cell

proliferation and immune signaling (Donner et al., 2010; Galbraith et al., 2017; Knuesel et al., 2009; Steinparzer et al., 2019; Zhao et al., 2012). Since amino acid alignments have shown that the kinase domain is conserved between CDK8 and CDK19, CDK19 is presumed to have similar kinase activity as CDK8. CDK8 and CDK19 differ most at the C terminal tail, suggesting different interaction partners and distinct regulatory functions. For example, CDK8, but not CDK19, is required for the induction of HIF1 $\alpha$  genes during hypoxia (Galbraith et al., 2013). CDK8 and CDK19 have been shown to be mechanistically different in response to interferon gamma (IFN $\gamma$ ), where CDK8 acts in a kinase dependent manner, CDK19 activity is kinase independent, resulting in regulation of a different subset of genes (Steinparzer et al., 2019).

STAT proteins can be phosphorylated by cyclin dependent kinase 8 (CDK8) and its paralog, cyclin dependent kinase 19 (CDK19). CDK8 controls the interferon response and regulates inflammatory cytokine gene induction by phosphorylating STAT1, STAT3 AND STAT5 (Akamatsu et al., 2019; Bancerek et al., 2013; Martinez-Fabregas et al., 2020). Specifically, CDK8 phosphorylates STAT1 at serine 727 in response to IFN $\gamma$  and differentially regulates the transcription of IFN $\gamma$  response genes (Bancerek et al., 2013). Furthermore, inhibition of CDK8 kinase activity enhances anti-inflammatory gene expression. CDK8 is a negative regulator of interleukin 10 (*IL-10*), where chemical inhibition of CDK8/19 results in an increase in *IL-10* protein secretion in macrophage (Johannessen et al., 2017). CDK8/19 phosphorylation of STAT5 prevents the activation of regulatory T cells (Akamatsu et al., 2019). Inhibition of CDK8/19 kinase activity results in increased retention of STAT5 in the nucleus, leading to induction of Foxp3 gene expression and suppression of auto immune diseases in mouse models (Akamatsu et al., 2019; Guo et al., 2019).

Previous work in our lab has investigated the role of CDK8/19 during virus infection. Walleye dermal sarcoma virus (WDSV) is a retrovirus that encodes retroviral cyclin (RV cyclin), a viral protein that has a small amount of homology to cell cyclins and directly binds to CDK8 to enhance its kinase activity resulting in increased transcriptional elongation and cell proliferation (Birkenheuer et al., 2015; Brewster et al., 2011; Rovnak et al., 2012). Dengue virus serotype 2 (DENV2) regulates host metabolism via CDK8 kinase activity (Butler et al., 2020). Furthermore, CDK8 gene expression is increased throughout DENV replication and chemical inhibition of CDK8/19 leads to a decrease in viral replication (Butler et al., 2020).

Here, we present preliminary data investigating the role of CDK8 and CDK19 in the context of DENV2 infection of macrophage. We propose that CDK8/19 regulates the transcription of C-X-C motif chemokine ligand 10 (*CXCL10*) and *IL-10* to provide an environment more conducive to viral replication. In addition, we use a lentivirus knockdown system to characterize the roles of CDK8 and CDK19 individually. We find that CDK8 knockdown has similar effects on *IL-10* and *CXCL10* gene expression as chemical inhibition of kinase activity, suggesting CDK8 kinase regulated *IL-10* and *CXCL10* expression. In contrast, CDK19 knockdown did not yield the same results seen with CDK8 knockdown, indicating CDK19 has a distinct role in transcriptional regulation from CDK8. Our preliminary data suggests that CDK8/19 kinase activity could be a mechanism that plays a role in DENV2 replication.

### **4.3 Methods and Materials**

#### *4.3a: Cell culture and PMA stimulation*

THP-1 human monocytic cells (TIB-202™, Manassas, VA, US) were cultured in RPMI-1640 media, supplemented with 10% fetal bovine serum (FBS), 1% non-essential amino acids, 1% L-glutamine, 1% penicillin-streptomycin, 25 mM HEPES and 0.05mM 2-mercaptoethanol in a 37°C incubator with 5% CO<sub>2</sub>. 2 x 10<sup>6</sup> cells. Cells were plated in T-25 flasks and treated with indicated concentration of phorbol 12-myristate 13-acetate (PMA) to induce differentiation into macrophages. Cells were incubated with 10 ng/ml of PMA for 0, 24, 48, 72 or 96 hours.

#### *4.3b: Polarization of PMA treated THP-1 cells*

THP-1 monocytes plated at 2 x 10<sup>6</sup> cells in T-25 flasks were stimulated with 10 ng/mL PMA. Twenty-four hours later, media with PMA was removed, and cells were washed with D-PBS. Cells were then treated with either 20 ng/mL interferon gamma (IFN $\gamma$ ) (R & D Systems, Minneapolis, MN, USA) or 20 ng/mL interleukin 4 (IL-4) (R & D Systems, Minneapolis, MN, USA) to polarize them into M1 or M2 phenotypes, respectively.

#### *4.3c: DENV2 infection*

For infection, cells were washed with Dulbecco's phosphate-buffered saline (D-PBS) and incubated with DENV2 (strain 16681) (Kinney et al., 1997) at indicated multiplicities in media for 1 hour at 4°C with rocking. Virus media was removed, cells were washed twice with cold D-PBS, and warmed RPMI-1640 media with 10% FBS was added.

#### *4.3d: RNA extraction and qPCR*

At the indicated time points, cells were harvested in TRIzol (Invitrogen, Thermofisher, Waltham, MA, USA), and total RNA was isolated using ZymoGen TRIzol RNA extraction kit according to manufacturer's instructions. cDNA was made using an iScript cDNA synthesis kit

(Bio-Rad, Hercules, CA, USA) according to the manufacturer's instructions, and then subjected to qPCR analysis with iQ SYBR green Supermix in a CFX96 real-time PCR system. Primers are listed in Table 1. Relative expression was normalized to a house keeping gene, Ribosomal Protein L37a (RPL37a). For genomic equivalent analysis, Cq values were standardized to ten-fold dilutions of *in vitro* transcribed DENV2 genomic RNA and subject to qRT-PCR.

**Table 4.1** PCR Primers

Gene	FWD	REV	Source
CDK8	GGGATCTCTATGTCG GCATGTAG	AAATGACGTTTGGATGC TTAAGC	(Galbraith et al., 2013)
CDK19	GCCACGGCTAGGGCC T	GCGAGAACTGGAGTGCT GATAA	(Galbraith et al., 2013)
DENV2	ACAAGTCGAACAACC TGGTCCAT	GCCGCACCATTGGTCTTC TC	(Butler et al., 2020)
CXCL10	CCA GAA TCG AAG GCC ATC AA	CAT TTC CTT GCTAAC TGC TTT CAG	(Qi et al., 2009)
IL-10	GAC TTT AAG GGT TAC CTG GGT TG	TCA CAT GCG CCT TGA TGT CTG	(X. Huang et al., 2016)
RPL37A	ATTGAAATCAGCCAG CACGC	AGGAACCACAGTGCCAG ATCC	(Maeß et al., 2010)

#### 4.3e Plaque assays

Media were collected at indicated time points and centrifuged at 500g for 10 minutes at room temperature. Plaque assays were performed on baby hamster kidney (BHK) cells. BHKs, plated at  $3 \times 10^5$  cells per well in MEM with 10%FBS, were incubated with 10-fold dilutions of the clarified cell supernatants for 2 hours at room temperature with rocking. Inoculum was removed and cells were overlaid with 3 mL of 2% agarose in MEM supplemented with 5% FBS.

After incubation for 7 days, 8% neutral red solution in PBS was added to the agar overlay, and plaques were counted 24 hours after staining.

#### 4.3f *Senexin treatment*

THP-1 monocytes plated at  $2 \times 10^6$  cells in T-25 flasks were stimulated with 10 ng/mL PMA. Twenty-four hours later, media with PMA was removed, and cells were washed with D-PBS. For infection, cells were washed with D-PBS and incubated with DENV2 (strain 16681) (Kinney et al., 1997) at indicated multiplicities in media for 1 hour at 4°C with rocking. Virus media was removed, cells were washed twice with cold D-PBS. Cells were then treated with warmed RPMI-1640 media + 10% FBS, supplemented with 5  $\mu$ M Senexin B. Media supplemented with 5  $\mu$ M Senexin B was left on cells for the remainder of infection.

#### 4.3g *CDK8/19 knockdown*

Lentivirus delivery of short hairpin RNAs (shRNA) (Sigma-Aldrich, St. Louis, MO, USA) was used to knockdown expression of CDK8 and CDK19 as previously described (Butler et al., 2020). THP-1 cells were transduced with shRNA lentiviruses and incubated for 1 hour at 37°C prior to selection with 1  $\mu$ g/mL puromycin for seven days. Selected cells were harvested for gene expression analysis or protein assay. After confirmation of knockdown, cells were plated at  $2 \times 10^6$  cells per T-25 cm<sup>2</sup> flask for DENV2 infection for 36-hour post infection.

**Table 4.2** shRNA sequences

Gene	Designation	Sequence
CDK8	TRCN0000000489	CCGGATGTCCAGTAGCCAAGTTCCACTCGAGTGG AACTTGG C TACTGGACATTTTTT
CDK19	TRCN0000195069	CCGGAGGACTGATAGCTCTTCTTTACTCGAGTAAA GAAGAG CTATCAGTCCTTTTTT
Nontarget	SHC002	CCGGCAACAAGATGAAGAGCACCAACTCGAGTTG GTGCTC TTCATCTTGTTGTTTTT

#### *4.3h Protein analysis*

Nuclear extracts were prepared as previously described (Brewster, Birkenheuer, Vogt, Quackenbush, & Rovnak, 2011). Briefly, cells were lysed in 0.5% NP-40 in PBS with protease and phosphatase inhibitors (2 µg/mL leupeptin and aprotinin, 1 µg/mL pepstatin, 0.2 mM phenylmethylsulfonyl fluoride [PMSF], 0.2 mM sodium orthovanadate, 2 mM sodium pyrophosphate, and 1 mM glycerophosphate). Cells were incubated on ice for 30 minutes then pelleted for 4 minutes at 1,600 g. Supernatants were aliquoted into separate tubes and nuclear pellets were washed with cold PBS, and then incubated with Dignam's buffer for 1 hour on ice. Extracted nuclei were pelleted for 15 min at 21,000 g.

Protein concentrations of each extract were determined with a Pierce BCA protein assay kit (Thermo Scientific) according to manufacturer's instructions. Equal quantities of total protein were separated by polyacrylamide gel electrophoresis for western blot. Blocked blot segments, separated by molecular weight range, were probed simultaneously with indicated primary antibodies overnight. Antibodies were detected with appropriate horseradish peroxidase-conjugated secondary antibodies and developed with the TMB membrane peroxidase substrate system (3,3',5,5'-Tetramethylbenzidine, KPL). Images were scanned with a Visioneer One touch scanner 9420 at a gamma value of 1.0, and all contrast adjustments were uniformly applied using Adobe Photoshop. List of antibodies can be found in supplemental methods.

#### *4.3i Statistics*

Statistical analysis was performed on Prism Software version 9.3.1. Statistical significance was calculated using the two-tailed Student's t test or one-way ANOVA.

## 4.4 Results

### 4.4a *CDK19 is upregulated during DENV2 infection and CDK8/19 kinase inhibition increases DENV2 replication*

Since DENV serotype 2 (DENV2) infection of Huh7 cells results in an increase in CDK8 gene expression (Butler et al., 2020), we hypothesized that within the context of DENV2 infection of macrophage, CDK8 gene expression would be upregulated. We infected cells with a multiplicity of infection of 5 (MOI = 5). Total RNA was collected 36 hours post infection (hpi) and *CDK8* gene expression was analyzed via RT-qPCR. Contrary to our prediction, *CDK8* gene expression was not altered by DENV2 infection (M0 DENV2 mean fold change over M0 = 1.07 +/- 0.06) (Figure 4.1A). Since *CDK8* expression levels did not change during infection, we measured *CDK19* gene expression. CDK19 has a high degree of homology to CDK8, differing only in the C terminal domain, suggesting different interacting partners and different functions (Galbraith et al., 2013; Steinparzer et al., 2019). *CDK19* gene expression was significantly upregulated during infection (M0 DENV2 mean fold change over DENV2 = 2.87 +/- 0.39) (Figure 4.1B). These data suggest that CDK19 may have a distinct role during DENV2 infection in macrophage.

Chemical inhibition of CDK8/19 kinase activity has been shown to decrease DENV2 replication in Huh7 cells, a liver cell line (Butler et al., 2020). To see if we could recapitulate these data in our macrophage system, we treated cells with Senexin B. Senexin B is an active site inhibitor that targets both CDK8 and CDK19 kinase function (McDermott et al., 2017). We pretreated cells 24 hours prior to infection with 5  $\mu$ M dimethyl sulfoxide (DMSO) or 5  $\mu$ M Senexin B dissolved in DMSO. Cells were then infected with DENV2 at a MOI = 0.1. After viral adsorption, cells were treated with media containing DMSO or media containing 5  $\mu$ M of

Senexin B dissolved in DMSO for the duration of the infection. Total RNA was collected at 24 hpi and DENV2 genome equivalents (GE) were quantified by RT-qPCR. Cell supernatants were collected for quantification of infectious virus production via plaque assay. Contrary to previously published data, treatment with Senexin B increased both DENV2 genome equivalents and infectious particle production (Figure 4.1C). Genome equivalents increased 3-fold (DMSO:  $3.68 \times 10^4 \pm 7.82 \times 10^3$  GE, Senexin B:  $1.11 \times 10^5 \pm 1.36 \times 10^4$  GE), while infectious particle production increased 4.4-fold (DMSO:  $1.91 \times 10^3 \pm 4.75 \times 10^2$  PFU/mL, Senexin B:  $8.46 \times 10^3 \pm 4.73 \times 10^2$  PFU/mL) (Figure 4.1C&D). These data suggest that CDK8 and CDK19 gene expression are impacted differently during DENV2 infection.

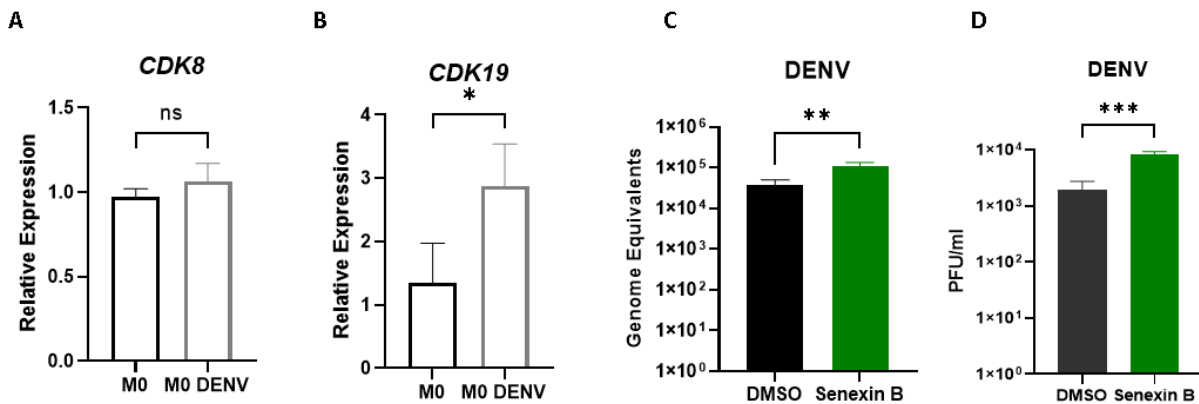


**Figure 4.1: CDK19 expression is increased during DENV2 infection and CDK8/19 kinase inhibition increases DENV2 replication.** M0 macrophage were infected with a MOI = 5 and total cellular RNA was collected at 36 hours post infection. (A) *CDK8* and (B) *CDK19* gene expression was measured. (C & D) M0 macrophage were treated with 5  $\mu$ M Senexin B and infected with a MOI of 0.1 and analyzed for (C) intracellular DENV2 genome equivalents or (D) infectious particles (PFU/mL) at 36 hours post infection. Cellular genes were normalized to housekeeping gene RPL37A. All experiments were n = 3 biological replicates, student's t test, \* p<0.5, \*\* p<0.01, \*\*\*p<0.001. Error bars represent mean  $\pm$  SEM.

#### 4.4b CDK8/19 kinase regulates *CXCL10* and *IL-10* expression during infection

Since CDK8/19 are regulators of gene expression during times of cellular stress, we sought to determine whether CDK8/19 kinase activity regulated *IL-10* and *CXCL10* transcription during infection. Cells were treated for 24 hours prior to infection with DMSO or 5  $\mu$ M Senexin B and infected with an MOI = 5. *CXCL10* and *IL-10* gene expression were measured as inflammatory and anti-inflammatory markers, respectively. DENV2 infection increased *CXCL10* expression in infected Senexin B treated and infected DMSO treated cells compared to uninfected cells (M0 DENV2 DMSO mean fold change over M0 DMSO:  $4.34 \times 10^3 \pm 3.76 \times 10^2$ , M0 DENV2 SB mean fold change over M0 SB:  $3.12 \times 10^3 \pm 1.62 \times 10^2$ ). Treatment with Senexin B decreased *CXCL10* expression 39% compared to DMSO treated cells (M0 DENV2 SB mean fold change over M0 DENV2 =  $0.61 \pm 0.02$ ) (Figure 4.2A, left). *IL-10* expression was only increased in the presence of Senexin B (M0 SB mean fold change over DMSO M0 =  $9.459 \pm 0.36$ ; M0 DENV2 SB mean fold change over M0 DMSO:  $10.44 \pm 1.08$ ). While treatment with Senexin B increased *IL-10* expression, infection did not further enhance gene expression (DENV2 DMSO mean fold change over M0 DMSO:  $1.59 \pm 0.07$ , M0 DENV2 SB mean fold change over M0 SB:  $1.11 \pm 0.07$ ) (Figure 4.2A, right). In concordance with the literature, this indicates that CDK8/19 are positive regulators of *CXCL10* gene expression and negative regulators of *IL-10* expression (Johannessen et al., 2017; Steinparzer et al., 2019).

Since macrophage metabolism impacts macrophage function (Van den Bossche et al., 2017), we investigated the role of CDK8/19 kinase activity on cellular metabolism during infection. Inhibition of CDK8 kinase activity has been shown to decrease expression of glycolytic enzyme hexokinase 2 (*HK2*) and lipophagy protein microtubule-associated protein 1 light chain 3 (*LC3*) during DENV2 infection of Huh7 cells (Butler et al., 2020). In contrast to

previously published data, treatment with Senexin B did not alter gene expression of *HK2* or *LC3* during infection (*HK2*: M0 DENV2 DMSO mean fold change over M0 DMSO: 2.11 +/- 0.06, M0 DENV2 SB mean fold change over M0 DMSO: 2.02 +/- 0.15; *LC3*: M0 DENV2 DMSO mean fold change over M0 DMSO = 0.97 +/- 0.08, M0 DENV2 SB mean fold change over M0 DMSO = 1.36 +/- 0.59) (Figure 4.3B).

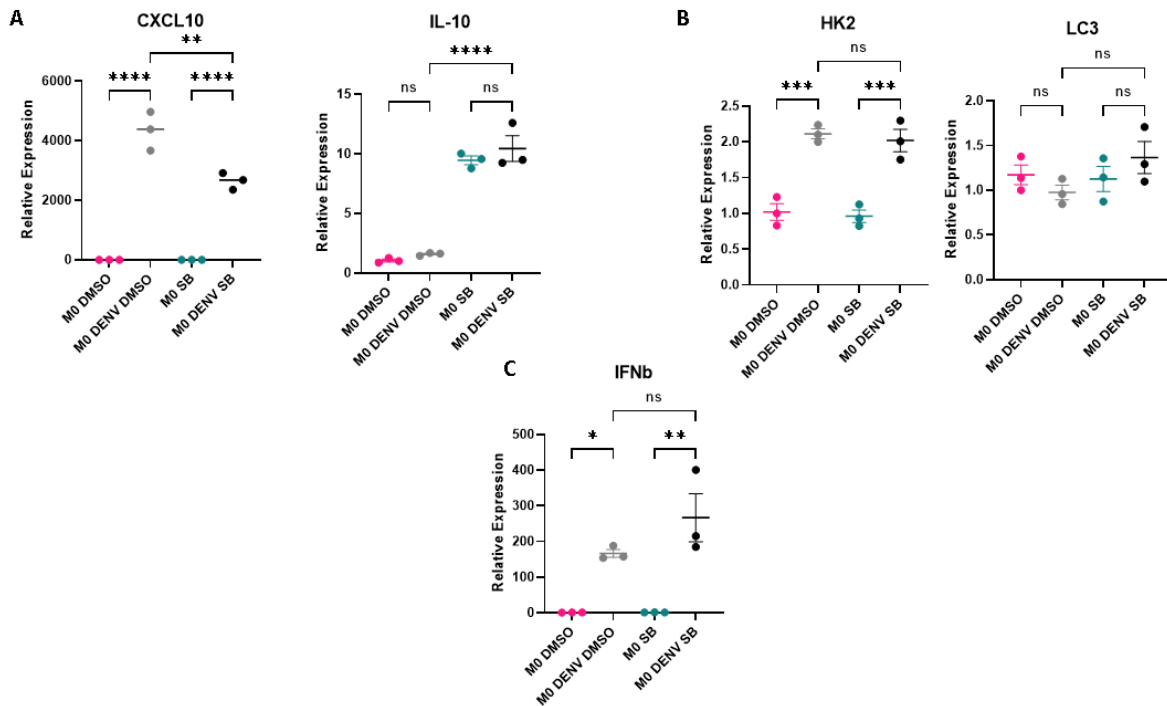


**Figure 4.2: CDK8/19 regulates *CXCL10* and *IL-10* expression.** M0 were infected with a MOI of 5 and total cellular RNA was collected at 36 hours post infection. (A & B) *CXCL10* and *IL-10*, (B) *HK2* and *LC3*, (C) *IFNβ* expression were measured via RT-qPCR. Genes were normalized to housekeeping gene *RPL37A*. All experiments were n = 3 biological replicates, one-way ANOVA with Tukey's multiple comparison's test, \*\*p<0.01, \*\*\*\*p<0.0001. Error bars represent mean +/- SEM.

Since CDK8/19kinase activity has been shown to be regulators of the interferon response (Bancerek et al., 2013; Steinparzer et al., 2019a), we investigated the role for CDK8/19 kinase activity on *IFNβ* gene expression as a marker for the type 1 interferon response. As expected,

*IFN $\beta$*  expression increased during infection (M0 DENV2 DMSO mean fold change over M0 DMSO = 166.6 +/- 10.82, M0 DENV2 SB mean fold change over M0 DMSO = 266 +/- 67.49). When we compared *IFN $\beta$*  gene expression level between infected Senexin B treated and infected DMSO treated cells, we did not see a difference (M0 DENV2 SB mean fold change over M0 DENV2 DMSO = 1.6 +/- 0.06) (Figure 4.3C). These data show that CDK8/19 expression solely regulated inflammatory and anti-inflammatory gene expression in our *in vitro* macrophage model.

#### 4.4c Knockdown of CDK8 increased DENV2 replication

To distinguish the roles of CDK8 and CDK19 during DENV2 infection, we utilized a lentivirus knockdown system to create CDK8/19 shRNA knockdowns in THP-1 cells. THP-1 cells were transduced with non-target shRNA (NT), CDK8 shRNA (CDK8-KD) or CDK19 shRNA (CDK19-KD), then selected with puromycin for 7 days. To evaluate the efficiency of the shRNA knockdown, we measured *CDK8* and *CDK19* gene expression in the knockdown cells. There was a 72% decrease in *CDK8* RNA compared to the non-target cells (CDK8 KD mean fold change over NT = 0.28 +/- 0.02). Interestingly, *CDK8* expression was increased in CDK19-KD cells (CDK19-KD mean fold change over NT = 1.62 +/- 0.03) (Fig 4.3A). Since CDK8 is a lethal knockdown (Westerling et al., 2007), and CDK8 and CDK19 are assumed to be functionally redundant, an increase in *CDK19* expression may be compensating for the decrease in CDK8. To further confirm knockdown of *CDK8*, we measured protein levels in the knockdown lines via western blot. There was a dramatic decrease in CDK8 protein in CDK8-KD cells, verifying the knockdown of CDK8 at the protein level (Figure 4.3B). When *CDK19* expression was measured in the knockdown cells, there was a 79% knockdown in gene expression in the *CDK19* cells (CDK19-KD mean fold change over NT = 0.21 +/- 0.02), and no

decrease in the CDK8 knockdown cells (CDK8-KD mean fold change over NT = 1.00 +/- 0.05) (Fig 4.3C). Protein levels of CDK19 were not measured due to time constraints. Assuming CDK19 protein levels are correlated with *CDK19* RNA levels, as seen with CDK8 knockdowns, we can assume that CDK19 protein levels are decreased in the CDK19 knockdown cells line. These data confirm the knockdown of *CDK8* and *CDK19* gene expression in THP-1 cells.

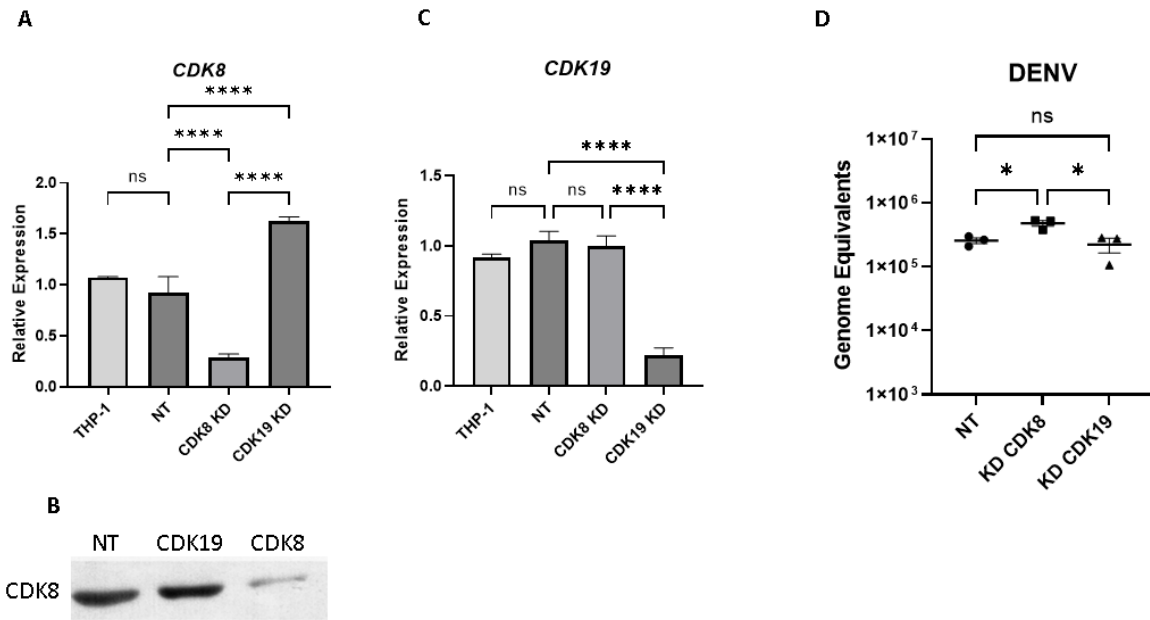


**Figure 4.3: Knockdown of *CDK8* increased DENV2 replication.** M0 cells were transduced with lentivirus mediated nontarget shRNA, CDK8 shRNA, CDK19 shRNA. (A) *CDK8* gene expression was analyzed in knockdown cell lines. (B) CDK8 protein levels were analyzed via western blot analysis. (C) *CDK19* gene expression was analyzed in knockdown cell lines. (D) Knockdown cells were infected with MOI = 5 DENV2 for 36 hours, DENV2 RNA was measured against standard curve. All experiments were n = 3 biological replicates, one-way ANOVA with Tukey's multiple comparison's test, \*\*p<0.01, \*\*\*\*p<0.0001. Error bars represent mean +/- SEM.

We sought to distinguish the roles of CDK8 and CDK19 during DENV2 infection in macrophage. NT, CDK8-KD, and CDK19-KD cells were infected with DENV2 at an MOI of 5 and total RNA was collected at 36 hpi. DENV2 genome equivalents were measured via RT-

qPCR. We found that knockdown of CDK8 increased DENV2 genome equivalents relative to infected NT cells (CDK8 KD =  $4.80 \times 10^5 \pm 4.89 \times 10^4$  GE, NT =  $2.58 \times 10^5 \pm 2.62 \times 10^4$  GE). We did not see a difference in DENV2 GE between NT cells and CDK19-KD cell, but DENV2 genome equivalents were lower relative to CDK8 KD cells (CDK19 KD =  $2.23 \times 10^5 \pm 5.81 \times 10^4$  GE). These results suggest that CDK8 may be the kinase targeted by DENV2 during replication in M0 macrophage.

#### *4.4d CDK8 controls IL-10 and CXCL 10 gene expression*

Next, we determined the role of CDK8 and CDK19 on gene expression during DENV2 infection. There is evidence that CDK8 and CDK19 have distinct mechanisms in regulating the anti-viral interferon response (Steinparzer et al., 2019). To characterize the roles of CDK8 and CDK19 in regulating inflammatory and anti-inflammatory genes during infection, we infected NT, CDK8-KD, and CDK19-KD with DENV2 at a MOI = 5. Total RNA was collected 36 hpi and host gene expression measured by RT-qPCR. *CXCL10* expression, was increased in DENV2 infected NT cells (NT DENV2 mean fold change over NT = 13.39). Infected CDK19-KD cells had an increase in *CXCL10* expression (CDK19-KD DENV2 mean fold change over CDK19-KD = 13.60). Since this expression level is similar to expression levels measured in infected NT cells, this indicates that CDK19 kinase does not play a major role in regulating *CXCL10* gene expression. In contrast, infection did not result in increased *CXCL10* expression in CDK8-KD cells (CDK8- KD DENV2 mean fold change over CDK8-KD = 1.00), suggesting that CDK8 regulates *CXCL10* gene expression (Figure 4.4A).

When we measured *IL-10* expression, there was no significant difference in *IL-10* in NT infected cells compared to uninfected NT cells (NT DENV2 mean fold change over NT = 1.434  $\pm$  0.21). Knockdown of CDK8 increased *IL-10* gene expression (CDK8 KD mean fold change

over NT = 3.364 +/- 0.16). Furthermore, there was no significant difference in *IL-10* expression between infected CDK19-KD cells and uninfected CDK19-KD cells (CDK19-KD DENV2 mean fold change over CDK19- KD = 0.76 +/- 0.09) (Figure 4.4B). In contrast, infected CDK8-KD increased *IL-10* expression 1.5-fold relative to uninfected CDK8-KD cells (CDK8-KD DENV2 mean fold change over CDK8-KD = 1.54 +/- 0.05). While we have not examined the broader array of inflammatory and anti-inflammatory genes, the difference between *IL-10* expression and *CXCL10* expression in CDK8-KD cells and CDK19-KD cells suggests that these paralogs may regulate different genes within the inflammatory response in infected macrophage.

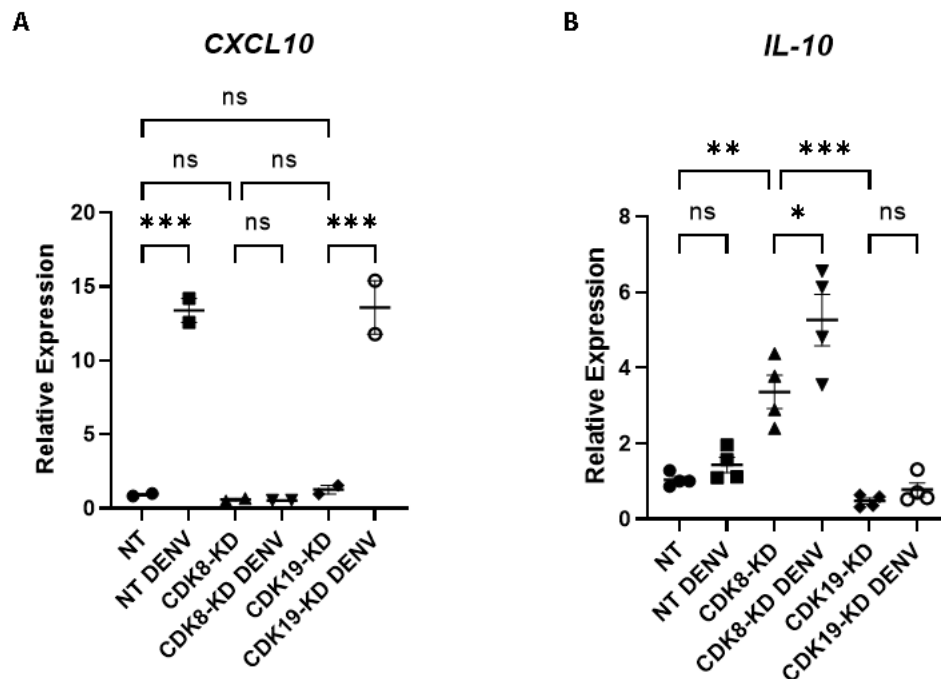


**Figure 4.4: CDK8 controls *IL-10* and *CXCL10* gene expression.** M0 cells were transduced with lentivirus mediated nontarget shRNA (NT), CDK8 shRNA (CDK8-KD), CDK19 shRNA (CDK19-KD) and infected with a MOI of 5. Total cellular RNA was collected at 36 hours post infection. (A) *CXCL10* and (B) *IL-10* expression were analyzed via RT-qPCR. Experiments were either (A) n = 4 or (B) n = 2 biological replicates, one-way ANOVA with Tukey's multiple comparison's test, \*\*p<0.01, \*\*\*\*p<0.0001. Error bars represent mean +/- SEM.

#### 4.4e Regulation by CDK8/19 is not phenotype specific

To determine whether CDK8 inhibition regulates DENV2 replication in M1 and M2 cells, we polarized cells with IFN $\gamma$  or IL-4 and pretreated cells with media containing DMSO or media containing 5  $\mu$ M Senexin B for 24 hours prior to infection. Cells were infected with an MOI = 5 and total RNA and cell supernatants were collected at 36 hours post infection. *CDK8* gene expression was analyzed via RT-qPCR and normalized against reference gene *RP37A*. Similar to the results seen in Figure 4.1A, *CDK8* expression was not significantly increased in any macrophage during infection (Figure 4.5A). Next, we measured *CDK19* gene expression at 36 hpi. We found that *CDK19* was upregulated in M0, M1 and M2 macrophage upon infection (M0 DENV2 mean fold change over M0 = 1.85 +/- 1.90, M1 DENV2 mean fold change over M1 = 1.58 +/- 0.10, M2 DENV2 mean fold change over M2 = 2.02 +/- 0.05) (Figure 4.5B).

To investigate the role of CDK8/19 kinase activity on DENV replication, we measured DENV2 replication in infected M0, M1 and M2 cells treated with DMSO or treated with Senexin B. M0, M1 and M2 cells were pretreated with Senexin B for 24 hours, then infected with DENV2 at an MOI = 5. After infection, fresh media supplemented with DMSO, or Senexin B was added. While Senexin B significantly increased genome equivalents in M0 cells (M0 DENV2 =  $1.37 \times 10^6$  +/-  $1.44 \times 10^5$ , M0 DENV2 SB =  $6.59 \times 10^6$  +/-  $8.6 \times 10^5$ ) (Figure 4.5C), there was no difference in viral genome equivalents in infected M1 or M2 cells (M1 DENV2 =  $2.92 \times 10^3$  +/-  $7.10 \times 10^2$ , M1 DENV2 SB =  $3.19 \times 10^3$  +/-  $5.57 \times 10^2$ ; M2 DENV2 =  $1.34 \times 10^6$  +/-  $2.54 \times 10^5$ , M2 DENV2 SB =  $2.36 \times 10^6$  +/-  $6.05 \times 10^5$ ) (Figure 4.5C). We saw a similar trend for infectious particle production; M0 cells had an increase in infectious particles with Senexin B treatment (M0 DENV2 =  $1.95 \times 10^3$  +/-  $6.6 \times 10^2$ , M0 DENV2 SB =  $8.5 \times 10^3$  +/-  $2.70 \times 10^2$ ) (Figure 4.5D), while Senexin B did not change infectious particles production in

infected M2 cells (M2 DENV2 =  $1.51 \times 10^3 \pm 3.3 \times 10^2$ , M2 DENV2 SB =  $2.66 \times 10^3 \pm 4.01 \times 10^2$ ) (Figure 4.5D). Infected M1 cells failed to produce plaques in this assay (Figure 4.5D). Due to the high error rates of the RNA-dependent RNA polymerase (RdRp) during viral replication (Peck & Lauring, 2018), DENV2 infection often yields higher viral RNA amounts compared to infectious particles (Richardson et al., 2006). A genome equivalent amount of  $10^3$  GE did not yield enough infectious virus to produce plaques in our system. While we did not measure the limit of detection for our plaque assays, this genome equivalent may have been below the limit of detection of these experiments.

Although Senexin B did not change DENV2 replication in M1 or M2 cells, we sought to determine whether Senexin B treatment would impact *IL-10* and *CXCL10* treatment in infected M1 and M2 cells. Total RNA was collected from infected M0, M1 and M2 cells at 36 hpi and analyzed via RT-qPCR. *CXCL10* is only upregulated during infection in M0 cells, so we only observe changes in infected M0 cells. Treatment with Senexin decreased *CXCL10* gene expression in infected M0 cells (M0 DENV2 + SB mean fold change over M0 DENV2 = 0.13). Since IFN $\gamma$  induces *CXCL10* expression (Gotsch et al., 2007), we were able to measure the impact of Senexin B treatment in uninfected and infected M1 cells. In uninfected cells, Senexin B did not significantly decrease *CXCL10* expression (M1 + SB mean fold change over M1 = 0.66). However, in infected M1 cells, Senexin B decreased *CXCL10* expression (M1 DENV2 + SB mean fold change over M1 DENV2 = 0.34). Lastly, Senexin B decreased *CXCL10* expression in infected M2 cells (M2 DENV2 + SB mean fold change over M2 DENV2 = 0.20) (Figure 4.5E). These data show that CDK8/19 are regulators of *CXCL10* expression and inhibition of kinase activity consistently decreases *CXCL10* expression in all macrophage phenotypes.

In contrast to *CXCL10*, inhibition of CDK8/19 kinase activity is found to increase *IL-10* expression (Johannessen et al., 2017). In contrast to previous data, Senexin B did not increase *IL-10* expression in uninfected M0 cells (M0 + SB mean fold change over M0 = 1.14). However, Senexin B treatment did increase *IL-10* expression relative to infected DMSO treated M0 cells (M0 DENV2 + SB mean fold change over M0 DENV2 = 1.32). When measuring *IL-10* expression in M1 cells, we found gene expression remained unchanged for uninfected and infected cells treated with Senexin B (M1 + SB mean fold change over M1 = 1.13, M1 DENV2 + SB mean fold change over M1 DENV2 = 0.73). This may be because M1 cells do not support high levels of *IL-10*, as it dampens the interferon response and inhibits transcription of inflammatory cytokines (Saraiva & O'Garra, 2010). Uninfected M2 cells treated with Senexin B had significantly higher levels of *IL-10* compared to uninfected M2 cells (M2 + SB mean fold change over M2 = 2.02). We saw a similar pattern during infection, where infected cells treated with Senexin B have a higher amount of *IL-10* than infected DMSO treated cells (M2 DENV2 = SB mean fold change over M2 DENV2 = 1.57) (Figure 4.5F). While we did not see an impact of Senexin B on DENV2 replication, we did see an impact on *IL-10* and *CXCL10* expression, indicating that CDK8/19 inhibition regulates immune responses during infection.

#### **4.5 Discussion**

CDK8 and CDK19 have been shown to be important for viral replication in DENV2 infection models of Huh7 cells (Butler et al., 2020). These data add to this body of work by attempting to distinguish distinct roles of CDK8 and CDK19 within the context of macrophage infection. Here, we find that, in contrast to previous work, inhibition of CDK8 kinase activity increases DENV replication. This suggests a distinct mechanism in which DENV utilized CDK8/19 in the context of macrophage infection. Furthermore, we attempt to characterize the

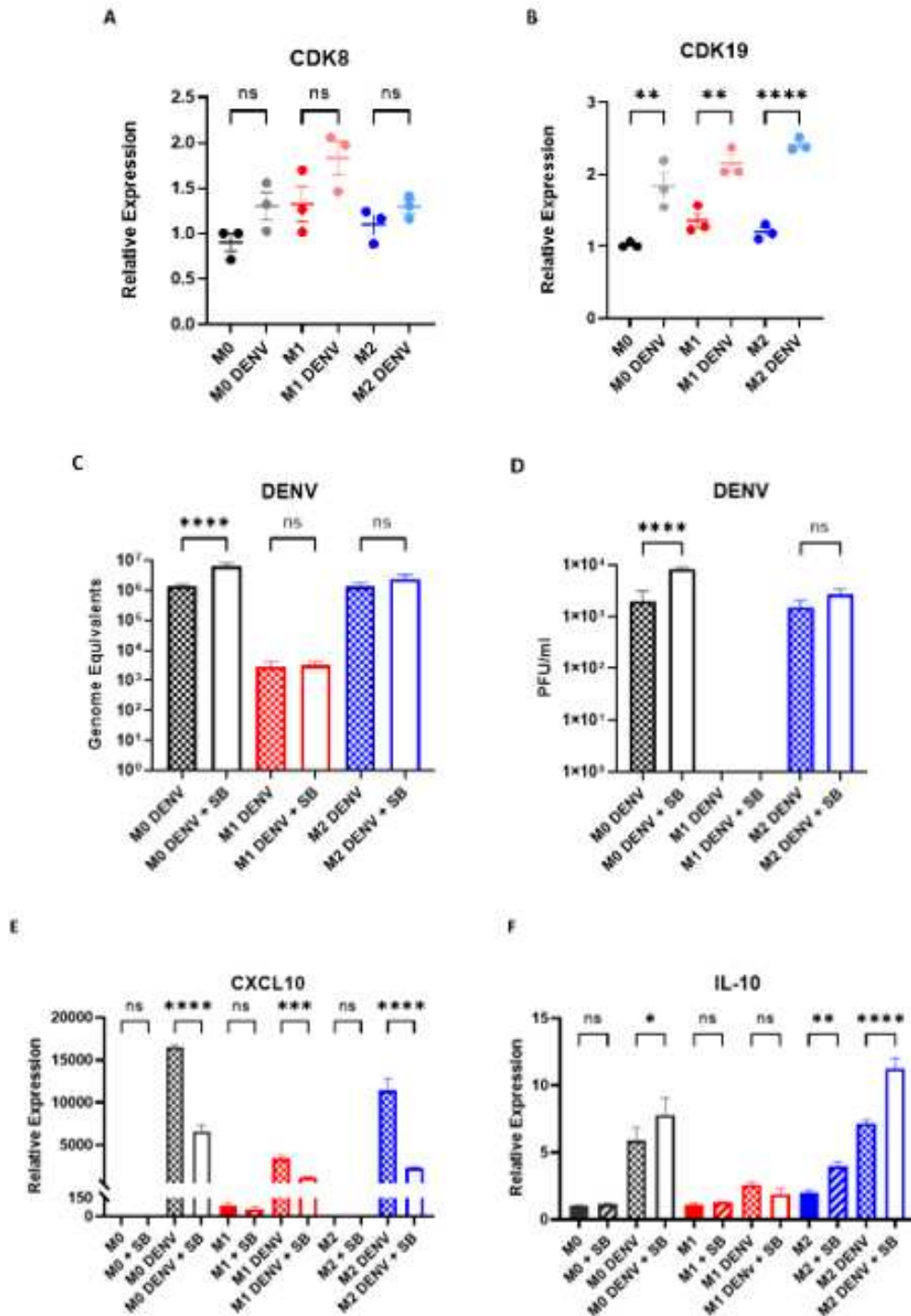


**Figure 4.5: CDK19, not CDK8, is upregulated during infection.** PMA treated M0 cells were untreated or treated with IFN $\gamma$  or IL-4 to polarize to M1 and M2 cells, respectively. Macrophages were infected with a MOI of 5 and total cellular RNA was collected at 36 hours post infection. Genes were normalized to housekeeping gene *RPL37A*. All experiments were  $n = 3$  biological replicates, one-way ANOVA with Tukey's multiple comparison's test, \*\* $p < 0.01$ , \*\*\*\* $p < 0.0001$ . Error bars represent mean  $\pm$  SEM.

roles of CDK8 and CDK19 within DENV2 infection. We find distinct roles for the two paralogs, where CDK8 knockdown shares similar gene expression regulation as treatment with Senexin B. These findings will add to the growing body of literature attempting to distinguish the roles CDK8 and CDK19 regulation of transcription.

Here, we present preliminary data that suggests that these kinases have distinct roles during DENV2 infection of macrophage. For example, CDK19, not CDK8 is upregulated during DENV2 infection of macrophage, suggesting that CDK19 plays a key role in infection. Both CDK8 and CDK19 kinase activity was inhibited during Senexin B treatment due to the fact that their kinase active site is conserved (Porter et al., 2012). When we inhibited CDK8/19 with Senexin B, we found an increase in viral RNA and infectious particles. The increase in DENV2 replication during CDK8/19 inhibition suggests that these kinases are a negative regulator of DENV2 replication, even though CDK19 expression was increased during infection.

CDK8/19 regulate a myriad of host pathways in response to cellular stress, including immune responses to infection and cellular metabolism (Galbraith et al., 2017; Steinparzer et al., 2019). Viruses shift these pathways to aid in viral replication and evasion of the immune response (Sang et al., 2015). We determined the role of CDK8/19 kinase activity in three different pathways: the inflammatory response to infection, cellular metabolism, and the interferon response. A limitation of this study is that these pathways are vastly complex and picking one to two genes from each cannot fully capture the depth of CDK8/19 gene regulation. However, by picking key regulators and comparing our results to published literature, we can begin to determine the role of CDK8/19 kinase activity on the regulation of these cellular pathways during DENV2 infection. We found that Senexin B decreased *CXCL10* expression during infection but did not regulate the expression in any of our other genes during infection.

We observed an increase in *IL-10* expression, but this was due to the inhibition of CDK8/19 and was not impacted by virus infection (Johannessen et al., 2017). In contrast to previous data in the Huh7 model of infection, Senexin B treatment did not change *HK2* or *LC3* expression. This suggests that the mechanisms in which CDK8/19 regulate gene expression in macrophage could be distinctively different from those in liver cells.

We found knockdown of CDK8 yields comparable results to treating cells with Senexin B prior to and during infection. This suggests that CDK8 regulates gene expression in a kinase dependent manner, as shown throughout the literature (Bancerek et al., 2013; Galbraith et al., 2013, 2017b). In contrast, CDK19 knockdown did not mimic Senexin B treatment or CDK8 knockdown. Knockdown of CDK19 slightly decreased DENV replication, while having negligible impact on *IL-10* or *CXCL10* gene expression. This not only confirms that CDK19 is functionally distinct from CDK8, but it also confirms that CDK19 may be regulating transcription in a kinase independent manner. Although CDK8, not CDK19, is the dominant kinase during IFN $\gamma$  directed anti-viral mechanisms, knocking CDK19 down increases the susceptibility of cells to VSV infection (Steinparzer et al., 2019). While CDK19 knockdown slightly decreased DENV replication in our model, contradicting the results seen in the literature (Steinparzer et al., 2019), these data still suggest that CDK19 plays a role in the host response to infection. These data should be interpreted carefully, as there was no evidence of protein knockdown in our model. Further studies are necessary to confirm that protein levels, and therefore kinase activity, are decreased within these cells. In addition, future studies are warranted to elucidate how viruses use CDK19 to regulate gene transcription. For example, transcriptomics could be performed on RNA infected CDK8-KD cells and CDK19-KD cells to show the effects knockdown has on various immune pathways, such as chemotaxis,

phagocytosis, and angiogenesis. The increase in *CDK19* gene expression suggests that CDK19 may play a significant role during DENV2 infection of macrophage. Furthermore, these data suggest that CDK8 and CDK19 have distinct roles during macrophage activation and viral infection.

Polarization is an important part of the macrophage life cycle. For macrophage to be functionally active, cells must polarize to an inflammatory or an anti-inflammatory phenotype (Murray, 2017). Here, we present preliminary data on the impact of CDK8/19 on macrophage polarization and response to infection. While Senexin B treatment did not impact DENV2 replication in M1 or M2 macrophage, it regulated gene expression. In concordance with the literature, inhibition of CDK8/19 kinase activity increased *IL-10* expression, further confirming that CDK8 is a negative regulator of *IL-10* expression (Johannessen et al., 2017). In addition, *CXCL10* gene expression was decreased in Senexin treated cells, indicating CDK8/19 kinase activity regulates *CXCL10* gene expression. We add to these results by measuring the impact of CDK8/19 inhibition in infected polarized cells. Inhibition of CDK8/19 changed *IL-10* and *CXCL10* expression, regardless of phenotype status. The fact that CDK8/19 inhibition does not impact DENV replication but does regulate gene expression of key inflammatory mediators suggests that the influence of inhibition could be more important at an organismal level. For example, as a chemokine, the primary function of *CXCL10* is to attract inflammatory cells to the site of infection (Gotsch et al., 2007). Decreasing the expression of this gene could lead to a dampened inflammatory response at the site of infection. CDK8/19 inhibition has been shown to be important at an organismal level, as inhibition of CDK8/19 enhances the surveillance of natural killer cells during cancer, leading to decreased proliferation of cancer cells and increased survival in mouse models (Knab et al., 2021; Putz et al., 2013).

## CHAPTER 5: INVESTIGATING THE ROLE OF CYCLIN DEPENDENT KINASE 8 AND MACROPHAGE PHENOTYPE IN ZIKA VIRUS PATHOGENESIS

### 5.1 Summary

Zika virus (ZIKV) is a mosquito borne flavivirus that is associated with outbreaks of microcephaly in South America in 2016-2017. ZIKV is linked to cases of Guillain-Barre syndrome, fatal encephalitis, and myelitis as well as other immunological complications. Macrophages play an important role in the pathogenesis of ZIKV, ferrying the virus to different organs throughout the body, such as the testes, the brain, and the placenta. We investigated the role of cyclin dependent kinase 8 (CDK8) on ZIKV replication. CDK8 is a transcriptional co-factor that regulates the transcription of IFN $\gamma$  stimulated genes and the transcription of specific cytokines/chemokines. ZIKV infection in macrophages induced gene expression of *CDK8*, while inhibition of CDK8 kinase activity decreased ZIKV replication. Using the CDK8 inhibitor, Senexin B, we saw an increase in *IL-10* gene expression and decrease in *CXCL10* gene expression. We use a polarized THP-1 macrophage system to explore how macrophage phenotype affects ZIKV replication. We found that ZIKV replicates more efficiently in anti-inflammatory (M2) macrophage versus inflammatory (M1) macrophage. These data suggest that ZIKV uses CDK8 kinase activity as a mechanism to aid in replication and control of host responses to infection.

### 5.2 Introduction

Zika virus (ZIKV) is a mosquito borne flaviviruses that has been associated with outbreaks of microcephaly and Guillain-Barre syndrome in South America and French Polynesia (Cauchemez et al., 2016; Schuler-Faccini et al., 2016). ZIKV can be transmitted by a mosquito

bite from an *Aedes* spp. mosquito, sexual contact, blood transfusion, or vertical transmission to a developing fetus (Lazear & Diamond, 2016). Similar to dengue virus (DENV), infection with ZIKV usually causes an asymptomatic or febrile illness. However, infection with ZIKV during pregnancy can be devastating to developing fetuses, often resulting in congenital abnormalities such as microcephaly, decreased brain tissue and macular scarring of the eyes (Brasil et al., 2016; Cauchemez et al., 2016).

ZIKV is an 11 kb positive sense RNA virus that encodes 3 structural proteins and 7 nonstructural proteins (Pierson & Diamond, 2018). The life cycle of ZIKV is very similar to DENV. Briefly, the E protein binds onto cell surface receptors and is endocytosed (Laureti, Narayanan, Rodriguez-Andres, Fazakerley, & Kedzierski, 2018; Tabata et al., 2016). Once inside the endosome, the shift to a more acidic environment causes the E protein to undergo a conformational change and expose the fusion peptide, which fuses the virion membrane to the membrane of the endosome, creating a pore (Dai et al., 2016; Laureti et al., 2018; Modis et al., 2004). The genome is released into the cytoplasm and is translated by host ribosomes at the rough endoplasmic reticulum by host ribosomes. After the genome has been replicated and structural proteins have been translated, the virion is assembled (Pierson & Diamond, 2012). The newly assembled virion migrates through the golgi network and is released and infects adjacent cells (Pierson & Diamond, 2012). Macrophage are a cell target for ZIKV and are of particular interest in understanding the pathogenesis of the virus (Jurado & Iwasaki, 2017; Michlmayr, Andrade, Gonzalez, Balmaseda, & Harris, 2017).

The transmission route in which ZIKV crosses the placenta is thought to be facilitated by blood monocytes (Jurado & Iwasaki, 2017). Infected monocytes can migrate across the body and disseminate ZIKV to various organs (Jurado & Iwasaki, 2017; Michlmayr et al., 2017).

Furthermore, these infected monocytes can cross the placental barrier and expose various types of cells to the virus (Salinas, Schiavo, & Kremer, 2010). ZIKV has been shown to infect Hofbauer cells, a specialized placental macrophage (El Costa et al., 2016; Quicke et al., 2016). These cells are found at the maternal fetal interface and can migrate between the maternal side and the placental side throughout pregnancy (Gabor, Kim, Reyes, & Golos, 2018). Hofbauer cells have an anti-inflammatory (M2) phenotype, as opposed to an inflammatory phenotype (M1), and are responsible for dampening inflammation at the fetal maternal interface (Gabor et al., 2018). These cells are thought to facilitate vertical transmission of viral agents, such as human cytomegalovirus (HCMV) and HIV (Boily-Larouche et al., 2012; Zulu, Martinez, Gordon, & Gray, 2019). This anti-inflammatory phenotype is especially important during ZIKV infection because infection of M2 macrophages lead to higher viral titer (Foo et al., 2017).

The mechanisms in which ZIKV reprograms macrophage towards an anti-inflammatory phenotype are still being elucidated. We hypothesize that ZIKV is using cyclin dependent kinase 8 (CDK8) to reprogram host gene expression. CDK8 is a part of the Mediator complex and is a transcriptional co-factor that aids in the transcription RNA polymerase II (RNAPII) dependent genes (Soutourina, 2018). CDK8, and its activating partner, Cyclin C, as well as Med12 and Med13 create the CDK8 kinase module. This module can reversibly dissociate from the Mediator complex and phosphorylate transcription factors in response to cellular stress (Rovnak & Quackenbush, 2022; Soutourina, 2018). CDK8 regulates transcription of inflammatory and anti-inflammatory genes (M. Chen et al., 2017; Johannessen et al., 2017; Steinparzer et al., 2019b). CDK8 is used by various viruses for replication and to regulate host transcription in response to infection. Walleye dermal sarcoma virus (WDSV) is retrovirus that encodes retroviral cyclin (RV cyclin), a viral protein that has a small amount of homology to cell cyclins

and binds onto CDK8 and enhances its kinase activity to increase transcriptional elongation, gene expression and cell proliferation (Birkenheuer et al., 2015; Brewster et al., 2011; Rovnak et al., 2012). DENV manipulates CDK8 kinase activity to regulate host metabolism and enhance viral replication (Butler et al., 2020). CDK8 gene expression is increased throughout DENV replication and chemical inhibition of CDK8/19 leads to a decrease in viral replication (Butler et al., 2020). These instances of CDK8 involvement during viral replication indicate a viable mechanism for ZIKV.

In this aim we found that CDK8 kinase inhibition decreased ZIKV replication and decreased *CXCL10* expression, but increased *IL-10* expression. Furthermore, we confirm findings in the literature that M2 cells are more susceptible to infection and that macrophage phenotype impacts ZIKV replication. Our preliminary data that suggests that macrophage phenotype, as well as interactions with CDK8, are a mechanism for ZIKV replication enhancement.

### **5.3 Methods and Materials**

#### *5.3a: Cell culture and PMA stimulation*

THP-1 human monocytic cells (TIB-202™, Manassas, VA, US) were cultured in RPMI-1640 media, supplemented with 10% fetal bovine serum (FBS), 1% non-essential amino acids, 1% L-glutamine, 1% penicillin-streptomycin, 25 mM HEPES and 0.05mM 2-mercaptoethanol in a 37°C incubator with 5% CO<sub>2</sub>. 2 x 10<sup>6</sup> cells. Cells were plated in T-25 flasks and treated with indicated concentration of phorbol 12-myristate 13-acetate (PMA) to induce differentiation into macrophages. Cells were incubated with 10 ng/ml of PMA for 24 hours.

### *5.3b: Polarization of PMA treated THP-1 cells*

THP-1 monocytes plated at  $2 \times 10^6$  cells in T-25 flasks were stimulated with 10 ng/mL PMA. Twenty-four hours later, media with PMA was removed, and cells were washed with D-PBS. Cells were then treated with either 20 ng/mL interferon gamma (IFN $\gamma$ ) (R & D Systems, Minneapolis, MN, USA) or 20 ng/mL interleukin 4 (IL-4) (R & D Systems, Minneapolis, MN, USA) to polarize them into M1 or M2 phenotypes, respectively.

### *5.3c: ZIKV infection*

For infection, cells were washed with Dulbecco's phosphate-buffered saline (D-PBS) and incubated with ZIKV strain PRVABC59 at indicated multiplicities in media for 1 hour at 4°C with rocking. Virus media was removed, cells were washed twice with cold D-PBS, and warmed RPMI-1640 media with 10% FBS was added.

### *5.3d: RNA extraction and qPCR*

At the indicated time points, cells were harvested in TRIzol (Invitrogen, Thermofisher, Waltham, MA, USA), and total RNA was isolated using Zymogen TRIzol RNA extraction kit according to manufacturer's instructions. cDNA was made using an iScript cDNA synthesis kit (Bio-Rad, Hercules, CA, USA) according to the manufacturer's instructions, and then subjected to qPCR analysis with iQ SYBR green Supermix in a CFX96 real-time PCR system. Primers are listed in Table 1. Relative expression was normalized to a house keeping gene, Ribosomal Protein L37a (*RPL37a*). For genomic equivalent analysis, Cq values were standardized to ten-fold dilutions of in vitro transcribed ZIKV genomic RNA and subject to qRT-PCR.

**Table 5.1** PCR Primers

Gene	FWD	REV	Source
ZIKV	CCACTAACGTTCTTTT GCAGACAT	CCGCTGCCCAACACAAG	(Giovanetti et al., 2020)
IL-10	GAC TTT AAG GGT TAC CTG GGT TG	TCA CAT GCG CCT TGA TGT CTG	(X. Huang et al., 2016)
CXCL10	CCA GAA TCG AAG GCC ATC AA	CAT TTC CTT GCTAAC TGC TTT CAG	(Qi et al., 2009)
CDK8	GGGATCTCTATG TCGGCATGTAG	AAATGACGTTTG GATGCTTAAGC	(Galbraith et al., 2013)
CDK19	GCCACGGCTAGG GCCT	GCGAGAACTGGA GTGCTGATAA	(Galbraith et al., 2013)
RPL37A	ATTGAAATCAGCCAG  CACGC	AGGAACCACAGTGCCAG  ATCC	(Maeß et al., 2010)

### 5.3e Plaque assay

Media were collected at indicated time points and centrifuged at 500g for 10 minutes at room temperature. Plaques were performed on Vero cells. Cells were plated at  $3 \times 10^5$  cells per well in DMEM with 10% FBS the day before assay. 10-fold dilutions of clarified supernatant were incubated with cells for 2 hours at room temperature while rocking. The cells were overlaid with 3 mL of 2% agarose in DMEM supplemented with 10% FBS. After incubation for 7 days, 8% neutral red solution in PBS was added to the agar overlay, and plaques were counted 24 hours after staining.

### 5.3f Senexin treatment

THP-1 monocytes plated at  $2 \times 10^6$  cells in T-25 flasks were stimulated with 10 ng/mL PMA. Twenty-four hours later, media with PMA was removed, and cells were washed with D-PBS. For infection, cells were washed with Dulbecco's phosphate-buffered saline (D-PBS) and

incubated with ZIKV strain PRVABC59 at indicated multiplicities in media for 1 hour at 4°C with rocking. Virus media was removed, cells were washed twice with cold D-PBS. Cells were then treated with warmed RPMI-1640 media + 10% FBS, supplemented with 5 µM Senexin B. Media supplemented with Senexin B was left on cells for the remainder of infection.

### 5.3g Statistics

Statistical analysis was performed on Prism Software version 9.3.1. Statistical significance was calculated using the two-tailed Student's t test or one way ANOVA.

## 5.4 Results

### 5.4a: ZIKV infection upregulates *IL-10* and *CXCL10* gene expression

To assess ZIKV replication kinetics in macrophage, THP-1 PMA differentiated (M0) cells were infected with ZIKV at a multiplicity of infection (MOI) = 10. Total cellular RNA was collected at 0 hours (bound virus) and at 24-, 48- and 72- hours post infection (hpi). Genome equivalents steadily increased after 24 hpi, reaching  $4.47 \times 10^4$  GE ( $4.47 \times 10^4 \pm 1.62 \times 10^3$ GE) at 72 hpi (Fig 5.1A). These data confirm that our system supports ZIKV replication and can be used in subsequent experiments.

Transcripts for the C-X-C motif chemokine ligand 10 (*CXCL10*) and interleukin 10 (*IL-10*) were determined using RT-qPCR at 72 hpi. *CXCL10* was used as a marker for host inflammatory response to infection. Furthermore, *CXCL10* gene expression has been shown to be upregulated during ZIKV infection and can be used to confirm infection (Naveca et al., 2018). At 72 hpi, *CXCL10* exhibits a 500-fold (mean fold change =  $498.7 \pm 62.56$ ) increase in gene expression (Fig 5.1B, left). To measure the anti-inflammatory response, we measured *IL-10* gene expression. *IL-10* was upregulated 6-fold (mean fold change =  $6.10 \pm 0.19$ ) at 72 hours post infection (Fig 5.1B, right).

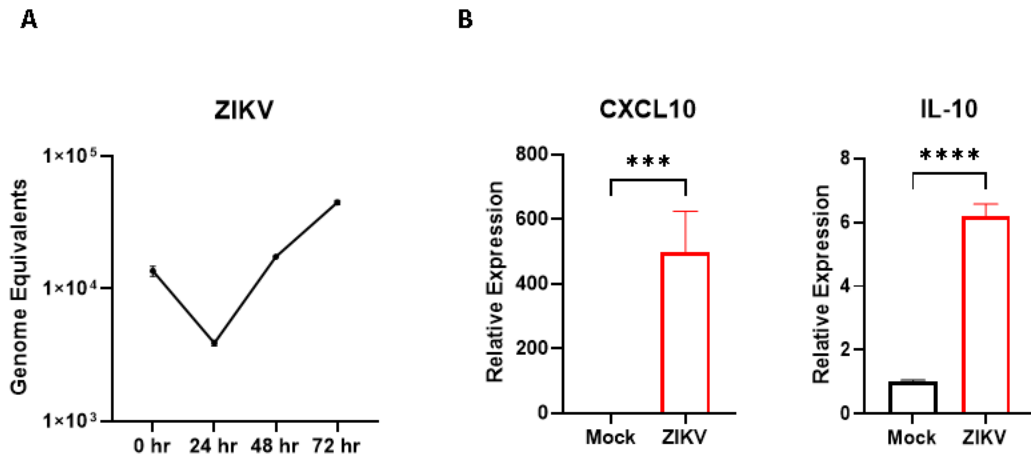


**Figure 5.1: ZIKV upregulates both *IL-10* and *CXCL10* during infection.** PMA treated THP-1 (M0) cells were infected with and MOI of 10 for 72 hours. Total cellular RNA and supernatant were collected at specified timepoints and analyzed for (A) intracellular ZIKV genome equivalents or (B) *IL-10* or *CXCL10* gene expression. All cellular genes were normalized against reference gene *RPL37a*. Time course experiment was 1 biological replicate, *IL-10* and *CXCL10* experiments were n = 4 biological replicates, \*p, 0.05, \*\*p<0.01, \*\*\*p<0.001, \*\*\*\*p<0.0001 unpaired two tailed t tests. Error bars represent mean +/- SEM.

#### 5.4b: Inhibition of CDK8/19 kinase activity decreases ZIKV replication

The mechanism in which ZIKV increases replication and reprograms gene expression is important, and not yet fully understood. CDK8 is a transcriptional co-factor that can regulate immune cell function and is used by DENV to regulate host transcription during infection (Butler et al., 2020; Johannessen et al., 2017; Steinparzer et al., 2019b). To determine the role of CDK8 during ZIKV infection, we measured CDK8 gene expression at 72 hpi. CDK8 gene expression was upregulated 1.8- fold (ZIKV mean fold change over M0 = 1.81 +/- 0.28) (Figure 5.2A). This suggests that CDK8 may play a role during ZIKV infection.

To determine the role of CDK8 kinase activity on ZIKV replication and host gene expression during infection we treated cells with Senexin B, a CDK8/19 kinase inhibitor. Cells were infected with an MOI = 10 for one hour at 4 °C, then treated with media containing

Dimethyl sulfoxide (DMSO) or 5  $\mu$ M Senexin B solubilized in DMSO. We first assessed the impact of CDK8 inhibition on ZIKV replication. Both intracellular RNA and infectious particle production decreased in cells treated with Senexin B (intracellular RNA: Senexin B fold change over DMSO = 0.57 +/- 0.31; infectious particles: DMSO:  $1.46 \times 10^3$  +/- 173 GE, Senexin B:  $2.83 \times 10^2$  +/- 38 GE) (Figure 5.2B). Next, we measured the impact of CDK8 kinase inhibition *CXCL10* and *IL-10* gene expression during infection. *CXCL10* expression was downregulated in infected cells treated with Senexin B (Senexin B fold change over DMSO = 0.47 +/- 0.03). In contrast, *IL-10* was upregulated with Senexin B treatment (Senexin B fold change over DMSO = 3.30 +/- 0.09) (Fig 5.2C). These data show that CDK8 kinase positively regulates *CXCL10* transcription and negatively regulates of *IL-10* transcription during infection. ZIKV may be using CDK8 to increase anti-inflammatory gene expression while dampening proinflammatory gene expression.

#### *5.4c: ZIKV infection upregulates both inflammatory and anti-inflammatory markers in M0, M1 and M2 cells*

When ZIKV first encounters resident tissue macrophage, these macrophages exhibit an M1 or an M2 phenotype (Jenkins & Allen, 2021; Zulu et al., 2019). To better understand how macrophage phenotype can impact ZIKV replication, M0 cells were polarized to either an M1 or M2 phenotype and infected with an MOI = 10. Total RNA was collected at 72 hours post infection and analyzed via RT-qPCR. Infected M1 cells had a lower amount of ZIKV genome equivalents compared to infected M0 cells (M1:  $3.80 \times 10^3$  +/-  $1.0 \times 10^3$  GE, M0:  $3.04 \times 10^4$  +/-  $8.79 \times 10^3$  GE) (Figure 5.2A). In contrast, M2 cells sustained higher amounts of ZIKV genome equivalents compared to M0 (M2:  $8.71 \times 10^5$  +/-  $3.40 \times 10^5$  GE). These data indicate that

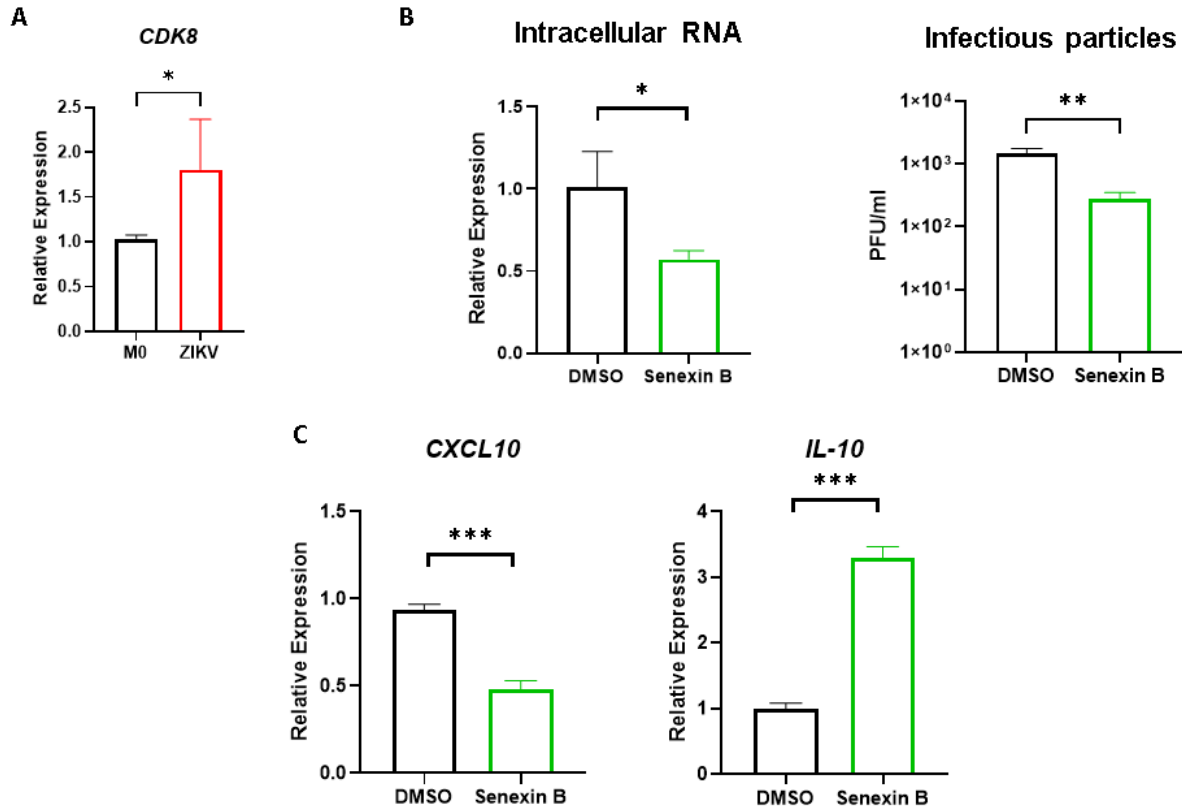


**Figure 5.2: CDK8 kinase activity increases ZIKV replication and regulates *IL-10* and *CXCL10* expression.** PMA treated M0 cells were infected with a MOI of 10 and total RNA was collected at 72 hpi. (A) CDK8 expression was measured (B) intracellular RNA was measured or infectious particle production were measured (C) *IL-10* or *CXCL10* gene expression was measured. All cellular genes were normalized against reference gene *RPL37a*. All experiments were n = 3 biological replicates, \*p, 0.05, \*\*p<0.01, \*\*\*p<0.001, \*\*\*\*p<0.0001 unpaired two tailed t tests. Error bars represent mean +/- SEM.

macrophage that exhibit an M2 phenotype, including Hofbauer cells, are more permissive to ZIKV infection.

To elucidate the differences in ZIKV replication between M1 and M2 cells, *CXCL10* and *IL-10* gene expression was measured at 72 hpi. Since there is only one biological replicate, and ANOVA statistical tests could not be performed, we cannot interpret significant differences in expression levels. *CXCL10* expression was increased in infected M0 cells relative to uninfected M0 cells (M0 ZIKV mean fold over M0 = 895). Polarization towards an M1 phenotype also

increased *CXCL10* relative to uninfected M0 cells (M1 mean fold over M0 = 230). Furthermore, infected M1 cells exhibit a dramatic increase in *CXCL10* expression compared to uninfected M1 cells (M1 ZIKV mean fold change over M0 =  $2.15 \times 10^3$ ) (Figure 5.2B, left). *IL-10* is increased during infection of M0 cells relative to uninfected M0 cells (M0 ZIKV mean fold change over M0 = 5.81) and during M1 polarization (M1 mean fold change over M0 = 1.83). We saw that *IL-10* was also increased during infection of M1 cells (M0 ZIKV mean fold change over M0: 4.69, M1 ZIKV mean fold change over M0 = 3.69) (Figure 5.2B, right).

Similarly, we measured *CXCL10* and *IL-10* gene expression in M2 polarized cells. There was an increase in *CXCL10* expression in infected M0 cells (M0 ZIKV mean fold change over M0 = 530). There was also an increase in *CXCL10* in infected M2 cells (M2 ZIKV mean fold change over M0 =  $969.34 \pm 45.75$ ) (Figure 5.2C, left). Since there is only one biological replicate, the in *CXCL10* expression between infected M0 cells and infected M2 cells cannot be interpreted. When we measured *IL-10* expression we measured an increased in *IL-10* gene expression in M2 cells compared to M0 cells (M2 mean fold change over M0 =  $2.08 \pm 0.19$ ). ZIKV infected M2 cells increased *IL-10* expression compared to infected M0 cells (M2 ZIKV mean fold change over M0 =  $8.57 \pm 0.22$ ) (Figure 5.2C, left).

## 5.5 Discussion

Macrophage are used by ZIKV to disseminate the virus to parts of the body, such as the testes and placenta (Foo et al., 2017; Jurado & Iwasaki, 2017; Quicke et al., 2016; Yang et al., 2020). While it is known that ZIKV can replicate well in these cells, the impact of macrophage phenotype on virus pathogenesis is still being explored. Here, we propose a model in which ZIKV upregulates CDK8 to control host transcription of *CXCL10* and *IL-10*. Furthermore, we began preliminary studies to explore the role of macrophage phenotype on ZIKV replication.

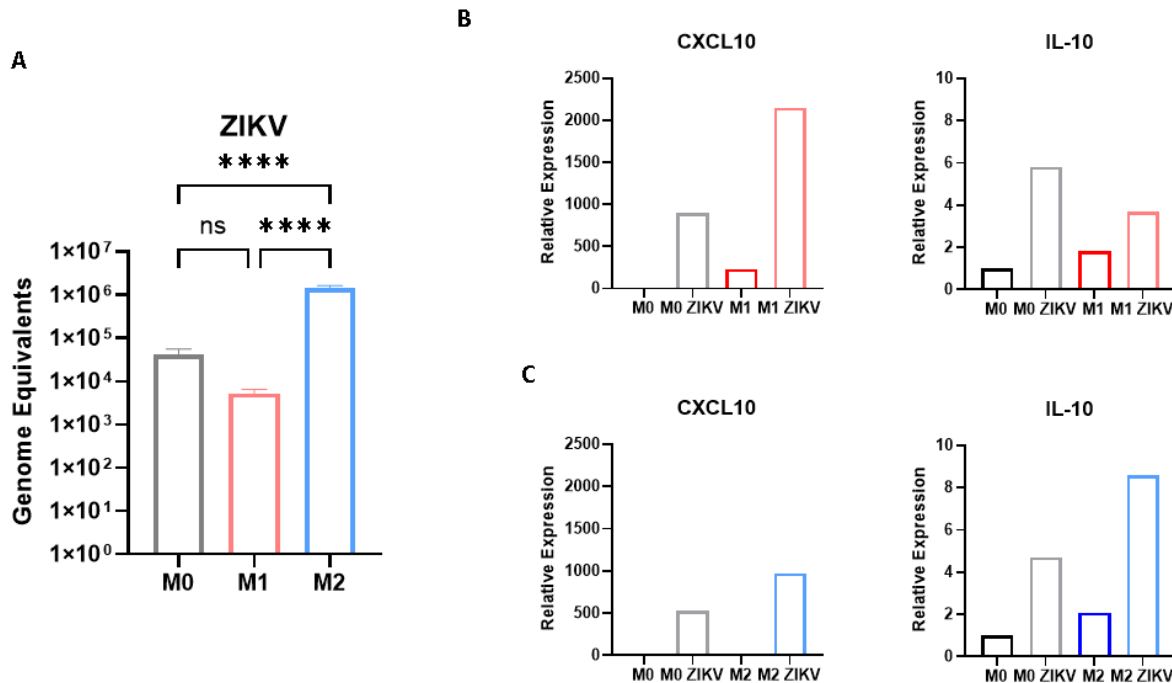


**Figure 5.3: ZIKV upregulates inflammatory and immunosuppressive genes.** (A) M0, M1 and M2 cells were infected with an MOI = 10. *CXCL10* or *IL-10* gene expression was measured in (B) M1 cells or (C) M2 cells. All cellular genes were normalized against reference gene RPL37a. ZIKV GE experiment was n = 3 biological replicates, *CXCL10* and *IL-10* experiments were n = 1 biological replicates, \*p, 0.05, \*\*p<0.01, \*\*\*p<0.001, \*\*\*\*p<0.0001 One way ANOVA. Error bars represent mean +/- SEM.

Recent studies have found that ZIKV can change macrophage gene expression and local environment during infection (Carlin et al., 2018; Foo et al., 2017; Luo et al., 2018). However, few studies examine the mechanism in which ZIKV controls host expression in macrophage. Preliminary data suggest CDK8/19 are the transcriptional regulators ZIKV manipulates during infection. When CDK8/19 kinase activity is inhibited, ZIKV replication decreases. In addition, when kinase activity is inhibited, there is also an increase in *CXCL10* expression and a decrease in *IL-10* expression. While the control of *CXCL10* and *IL-10* transcription by CDK8/19 has been shown in the literature (Bancerek et al., 2013; Johannessen et al., 2017; Steinparzer et al.,

2019b), we are the first to show it within the context of ZIKV infection. We propose that ZIKV manipulates CDK8 to control transcription of key inflammatory and anti-inflammatory genes.

Tissue resident macrophage have distinct functions and phenotypes, depending on the local environment. Hofbauer cells, a maternal macrophage of fetal origin, are important for fetal development and can secrete proinflammatory cytokines (Gabor et al., 2018). Even though these can be proinflammatory, they are often found as an M2-like phenotype and are ineffective in controlling infectious agent spread (Gabor et al., 2018). ZIKV has been shown to target these cells for replication and use these cells for vertical transmission to the placenta (Quicke et al., 2016). In this aim we show that M0, M1, and M2 macrophage phenotype has a profound effect on replication. Cells polarized to an M2 phenotype had significantly more viral RNA compared to cells polarized to an M1 phenotype. These data agree with what is seen by other viruses, such as EBOV and HIV. These viruses have enhanced replication in M2 macrophage, while having restricted replication in M1 macrophage (Denner, 2016; Rhein et al., 2015; Rogers et al., 2019; Tricia et al., 2015). These data also support the theory that ZIKV can be vertically transmitted due to the immunosuppressive environment of the fetal maternal interface (Foo et al., 2017).

The results presented here show a similar expression pattern of *IL-10* and *CXCL10* in both infected M1 and infected M2 macrophage. Expression of both these genes were upregulated during infection, yet the degree of upregulation varied depending on phenotype. The increase of *IL-10* in M1 cells shows that ZIKV works to skew the phenotype towards a more conducive environment for replication, but the dramatic increase in *CXCL10* indicates the cell is mounting a strong enough anti-viral/ inflammatory response to dampen viral replication. M2 cells have a greater increase in *IL-10* expression than M1 cells, showing ZIKV is driving cells towards more of an immunosuppressive phenotype. This further confirms the idea that ZIKV takes advantage

of the anti-inflammatory phenotype of placental macrophage for better replication (Foo et al., 2017). However, this portion of this work is limited by the single biological replicate. Since statistics could not be performed, we cannot assume the differences in gene expression are significant. However, these data are similar to what was measured in a DENV model of infection. This suggests that infection with ZIKV could potentially drive macrophage towards both an inflammatory and anti-inflammatory phenotype. Future work should repeat these infections for at least 3 biological replicates to confirm our results.

## CONCLUSION

Macrophage immunometabolism dictates macrophage function and can be altered by viruses. In this dissertation, we characterize macrophage phenotype and gene expression during DENV and ZIKV infection. We also investigate the role of CDK8/19 kinase activity on the regulation of host genes during infection. We propose a model in which DENV and ZIKV reprogram macrophage gene expression and metabolism via CDK8/19. Few studies investigate the role of polarization during DENV infection, and even fewer examine the reprogramming of macrophage immunometabolism by viruses. This dissertation bridges the gap between immune gene expression and macrophage metabolism during viral infection.

Although the THP-1 monocyte cell line is one of the most widely used cell lines to study monocytes and macrophage biology, the methods in which to differentiate and polarized cells remains inconsistent (Baxter et al., 2020; Genin et al., 2015; Park et al., 2007). In aim 1 we compared different concentrations of phorbol 12-myristate-13-acetate (PMA), paired with different resting periods, to determine the optimal differentiation protocol. We found lower concentrations of PMA, paired with a shorter resting period, were sufficient to differentiate monocytes into macrophages. Since THP-1 macrophage can be polarized into different macrophage subsets, we optimized the duration in which to treat cells with interferon gamma (IFN $\gamma$ ) or interleukin (IL-4). In optimizing polarization of macrophage, we found that a shorter incubation time with IFN $\gamma$  was necessary to polarize cells towards M1 while a longer incubation with IL-4 was sufficient for M2 polarization. Here, we developed a system that can be used to study flavivirus-macrophage interactions in future experiments.

In aim 2, we characterize gene expression and metabolism changes in M0, M1 and M2 macrophage during DENV2 infection. We measured an increase in both inflammatory and anti-inflammatory genes during infection. Gene expression in our infection model mimics cytokine and chemokine profiles seen in severe DENV patients (Soo et al., 2017; Soo et al., 2019; Zhao et al., 2016). The fact that our model is similar to that seen in patients further confirms the use of THP-1 macrophage to study DENV-macrophage interactions. When we measured gene expression in anti-inflammatory macrophage, we found an increase in anti-inflammatory genes compared to naïve macrophage during infection. Furthermore, the upregulation of inflammatory genes was not as strong as that seen in infected naïve or inflammatory cells. This suggests that M2 macrophage are not mounting a strong inflammatory response during infection and is a more conducive environment for replication. In contrast, M1 cells have a higher upregulation of interferon genes compared to M0 and M2 cells. These data, coupled with published literature, indicate that the interferon response is a strong inhibitor of DENV replication (Diamond & Harris, 2001; Diamond et al., 2000; Nanaware et al., 2021; Tremblay et al., 2019). This study is the first to examine gene expression in M2 polarized macrophage during DENV infection and further contributes to knowledge of DENV pathogenesis.

Macrophage have to change phenotypes from inflammatory during the onset of infection to anti-inflammatory during the resolution of infection (Murray, 2017). The shift between these two phenotypes is thought to be regulated by changes in cellular metabolism (Van den Bossche et al., 2015). Since viruses change cellular metabolism in order to obtain precursors for replication (Sanchez & Lagunoff, 2015), we sought to understand whether DENV can change cellular metabolism in polarized cells. We first measured key glycolytic genes hexokinase 2 (*HK2*) and enolase 1 (*ENO1*) and a fatty acid oxidation gene carnitine palmitoyltransferase 1A (*CPT1a*).

*HK2* and *ENO1* were upregulated in infected M1 cells compared to infected M2 cells, while *CPT1a* was upregulated in infected M2 cells compared to infected M1 cells. Furthermore, when we measured infection, we observed increased rates of glycolysis in M1 cells, but not M2. Lastly, the rate of oxidative phosphorylation was similar between M1 and M2 cells. Further studies examining whether metabolic shift correlated with macrophage phenotype, via flow cytometry, are warranted. This study is one of the first to measure changes in polarized macrophages in response to DENV and correlate it to inflammatory and anti-inflammatory gene expression changes. This study contributes to basic knowledge of viral reprogramming of immunometabolism. One of the limitations in this chapter is characterizing phenotype without measuring cells surface markers or cytokine secretion. To fully capture macrophage phenotype and function, multi-panel flow cytometry and ELISA are warranted. Since M2 macrophage have four different subsets, with each having a slightly different function than the other, a panel measuring IL-10 expression, as well as markers specific for each subtype is necessary and included in Table 6.1 below.

**Table 6.1:** A List of Potential Cell Surface Markers for Identifying Different Macrophage Subsets

	M1	M2a	M2b	M2c	M2d
Marker expression	CD86 CD80 CD68 MHC II IL-1R	IL-10 CD163 MHC II CD206	IL-10 CD86 MHC II	IL-10 CD163 TLR1	IL-10 VEGF

Previous work in our lab has identified the role of CDK8 and CDK19 during DENV infection of liver cells (Butler et al., 2020). In aim 3, we investigate the role of CDK8 and

CDK19 in a DENV model of infection in macrophage cells. Unlike liver cells, macrophage regulate the inflammatory response by secreting both inflammatory and anti-inflammatory proteins. Although *CDK19* was upregulated during infection, inhibition of CDK8/19 kinase activity increased viral replication. Furthermore, when we treated infected cells with Senexin B, we saw that CDK8/19 kinase activity regulated interleukin 10 (*IL-10*) and C-X-C motif chemokine ligand 10 (*CXCL10*) expression, but not *HK2* or lipophagy protein microtubule associated light chain 3 (*LC3*) or interferon beta (*IFN $\beta$* ). We also distinguished the roles of CDK8 and CDK19 by utilizing CDK8 and CDK19 knockdown cells. We found that knockdown of CDK8 decreased expression of *IL-10* and increased expression of *CXCL10*, similar to what was observed with Senexin B treatment. This suggests that CDK8 kinase activity is important for regulating expression of these genes (Johannessen et al., 2017; Steinparzer et al., 2019b). These findings contribute to literature attempting to distinguish the roles CDK8 and CDK19 regulation of transcription. This preliminary data is exciting and opens many avenues of exploration. Since CDK8/19 regulate many different cellular pathways, global gene transcription of knockdown cells during infection would yield interesting results. Future experiments should use RNA sequencing to determine the patterns of inflammatory and anti-inflammatory gene expression induced by DENV infection of macrophages in CDK8 and CDK19 knockdown cells.

Macrophage also play an important role in Zika virus (ZIKV) pathogenesis. ZIKV-infected macrophage ferry the virus across the placenta to developing fetal neurons. Once infected, ZIKV stunts the development of these cells, leading to microcephaly and ZIKV congenital syndrome. In aim 4 we present preliminary data investigating the mechanism in which ZIKV reprograms macrophage gene expression. We find that CDK8 gene expression is increased during infection and kinase inhibition via Senexin B decreases viral replication. We also present

preliminary data in which M2 cells are more susceptible to infection than M0 and M1 cells. These data are similar to DENV and suggest that CDK8 can be used as a pan-flavivirus mechanism to reprogram gene expression to create a more conducive environment for replication. Biological replicates are necessary to determine shifts in *IL-10* and *CXCL10* gene expression in M1 cells can be repeated. Future studies analyzing ZIKV induced shifts in cellular metabolism would add to the breath of data on ZIKV-macrophage interactions.

Despite the significant global burden of DENV and ZIKV, there are no effective anti-viral treatments. Immunometabolism is a promising target for host directed therapy during DENV infection. Cancer cells shift metabolism in the tumor microenvironment in a manner similar to DENV reprogramming metabolism in macrophage (Roy et al., 2020; Sanchez & Lagunoff, 2015). Current drugs targeting cancer immunometabolism are showing promising results (Traba et al., 2021). Targeting immunometabolism, in combination with CDK8/CDK19 treatment, could be a promising avenue for host directed anti-viral treatments.

## REFERENCES

- Abd El-Aleem, S. A., Mohammed, H. H., Saber, E. A., Embaby, A. S., & Djouhri, L. (2020). Mutual inter-regulation between iNOS and TGF- $\beta$ 1: Possible molecular and cellular mechanisms of iNOS in wound healing. *Biochimica et Biophysica Acta - Molecular Basis of Disease*, 1866(10), 165850. <https://doi.org/10.1016/j.bbadis.2020.165850>
- Acosta, E. G., Castilla, V., & Damonte, E. B. (2012). Differential Requirements in Endocytic Trafficking for Penetration of Dengue Virus. *PLoS ONE*, 7(9). <https://doi.org/10.1371/journal.pone.0044835>
- Aguirre, S., Luthra, P., Sanchez-Aparicio, M. T., Maestre, A. M., Patel, J., Lamothe, F., ... Fernandez-Sesma, A. (2017). Dengue virus NS2B protein targets cGAS for degradation and prevents mitochondrial DNA sensing during infection. *Nature Microbiology*, 2(March), 1–11. <https://doi.org/10.1038/nmicrobiol.2017.37>
- Aguirre, S., Maestre, A. M., Pagni, S., Patel, J. R., Savage, T., Gutman, D., ... Fernandez-Sesma, A. (2012). DENV Inhibits Type I IFN Production in Infected Cells by Cleaving Human STING. *PLoS Pathogens*, 8(10). <https://doi.org/10.1371/journal.ppat.1002934>
- Akamatsu, M., Mikami, N., Ohkura, N., Kawakami, R., Kitagawa, Y., Sugimoto, A., ... Sakaguchi, S. (2019). Conversion of antigen-specific effector/memory T cells into Foxp3-expressing Treg cells by inhibition of CDK8/19. *Science Immunology*, 4(40), 1–17. <https://doi.org/10.1126/sciimmunol.aaw2707>
- Akram, M. (2014). Citric Acid Cycle and Role of its Intermediates in Metabolism. *Cell Biochemistry and Biophysics*, 68(3), 475–478. <https://doi.org/10.1007/s12013-013-9750-1>
- Aktepe, T. E., & Mackenzie, J. M. (2018). Shaping the flavivirus replication complex: It is curvaceous! *Cellular Microbiology*, 20(8), 1–10. <https://doi.org/10.1111/cmi.12884>

- Albieri, A., Hoshida, M. S., Gagiotti, S. M., Leanza, E. C., Abrahamsohn, I., Croy, A., ... Bevilacqua, E. (2005). Interferon-gamma alters the phagocytic activity of the mouse trophoblast. *Reproductive Biology and Endocrinology*, 3, 1–11.  
<https://doi.org/10.1186/1477-7827-3-34>
- Aldo, P. B., Craveiro, V., Guller, S., & Mor, G. (2013). Effect of culture conditions on the phenotype of THP-1 monocyte cell line. *American Journal of Reproductive Immunology*, 70(1), 80–86. <https://doi.org/10.1111/aji.12129>
- Ashour, J., Laurent-Rolle, M., Shi, P.-Y., & García-Sastre, A. (2009). NS5 of Dengue Virus Mediates STAT2 Binding and Degradation. *Journal of Virology*, 83(11), 5408–5418.  
<https://doi.org/10.1128/jvi.02188-08>
- Auwerx, J. (1991). The human leukemia cell line, THP-1: A multifaceted model for the study of monocyte-macrophage differentiation. *Experientia*, 47(1), 22–31.  
<https://doi.org/10.1007/BF02041244>
- Bae, S., Kim, H., Lee, N., Won, C., Kim, H.-R., Hwang, Y., ... Lee, W. J. (2012).  $\alpha$ -Enolase Expressed on the Surfaces of Monocytes and Macrophages Induces Robust Synovial Inflammation in Rheumatoid Arthritis. *The Journal of Immunology*, 189(1), 365–372.  
<https://doi.org/10.4049/jimmunol.1102073>
- Bancerek, J., Poss, Z. C., Steinparzer, I., Sedlyarov, V., Pfaffenwimmer, T., Mikulic, I., ... Kovarik, P. (2013). CDK8 Kinase Phosphorylates Transcription Factor STAT1 to Selectively Regulate the Interferon Response. *Immunity*, 38(2), 250–262.  
<https://doi.org/10.1016/j.immuni.2012.10.017>

- Barbier, V., Lang, D., Valois, S., Rothman, A. L., & Medin, C. L. (2017). Dengue virus induces mitochondrial elongation through impairment of Drp1-triggered mitochondrial fission. *Virology*, 500(October 2016), 149–160. <https://doi.org/10.1016/j.virol.2016.10.022>
- Barker, R. N., Erwig, L. P., Hill, K. S. K., Devine, A., Pearce, W. P., & Rees, A. J. (2002). Antigen presentation by macrophages is enhanced by the uptake of necrotic, but not apoptotic, cells. *Clinical and Experimental Immunology*, 127(2), 220–225. <https://doi.org/10.1046/j.1365-2249.2002.01774.x>
- Baxter, E. W., Graham, A. E., Re, N. A., Carr, I. M., Robinson, J. I., Mackie, S. L., & Morgan, A. W. (2020). Standardized protocols for differentiation of THP-1 cells to macrophages with distinct M(IFN $\gamma$ +LPS), M(IL-4) and M(IL-10) phenotypes. *Journal of Immunological Methods*, 478(February), 1–11. <https://doi.org/10.1016/j.jim.2019.112721>
- Behrmann, I., Smyczek, T., Heinrich, P. C., Schmitz-Van De Leur, H., Komyod, W., Giese, B., ... Haan, C. (2004). Janus kinase (Jak) subcellular localization revisited: The exclusive membrane localization of endogenous Janus kinase 1 by cytokine receptor interaction uncovers the Jak·receptor complex to be equivalent to a receptor tyrosine kinase. *Journal of Biological Chemistry*, 279(34), 35486–35493. <https://doi.org/10.1074/jbc.M404202200>
- Bender, S., Reuter, A., Eberle, F., Einhorn, E., Binder, M., & Bartenschlager, R. (2015). Activation of Type I and III Interferon Response by Mitochondrial and Peroxisomal MAVS and Inhibition by Hepatitis C Virus. *PLoS Pathogens*, 11(11), 1–30. <https://doi.org/10.1371/journal.ppat.1005264>

- Bennett, J. M., Reeves, G., Billman, G. E., & Sturmborg, J. P. (2018). Inflammation-nature's way to efficiently respond to all types of challenges: Implications for understanding and managing "the epidemic" of chronic diseases. *Frontiers in Medicine*, 5(NOV), 1–30.  
<https://doi.org/10.3389/fmed.2018.00316>
- Bhatt, A. P., Jacobs, S. R., Freemerman, A. J., Makowski, L., Rathmell, J. C., Dittmer, D. P., & Damania, B. (2012). Dysregulation of fatty acid synthesis and glycolysis in non-Hodgkin lymphoma. *Proceedings of the National Academy of Sciences of the United States of America*, 109(29), 11818–11823. <https://doi.org/10.1073/pnas.1205995109>
- Bhatt, S., Gething, P. W., Brady, O. J., Messina, J. P., Farlow, A. W., Moyes, C. L., ... Hay, S. I. (2013). The global distribution and burden of dengue. *Nature*, 496(7446), 504–507.  
<https://doi.org/10.1038/nature12060>
- Bilz, N. C., Jahn, K., Lorenz, M., Lüdtkke, A., Hübschen, J. M., Geyer, H., ... Claus, C. (2018). Rubella Viruses Shift Cellular Bioenergetics to a More Oxidative and Glycolytic Phenotype with a Strain-Specific Requirement for Glutamine. *Journal of Virology*, 92(17), 1–19.  
<https://doi.org/10.1128/jvi.00934-18>
- Birkenheuer, C. H., Brewster, C. D., Quackenbush, S. L., & Rovnak, J. (2015). Retroviral Cyclin Controls Cyclin-Dependent Kinase 8-Mediated Transcription Elongation and Reinitiation. *Journal of Virology*, 89(10), 5450–5461. <https://doi.org/10.1128/jvi.00464-15>
- Boily-Larouche, G., Milev, M. P., Zijenah, L. S., Labbé, A. C., Zannou, D. M., Humphrey, J. H., ... Roger, M. (2012). Naturally-occurring genetic variants in human DC-SIGN increase HIV-1 capture, cell-transfer and risk of mother-to-child transmission. *PLoS ONE*, 7(7).  
<https://doi.org/10.1371/journal.pone.0040706>

- Brasil, P., Pereira, J. P., Moreira, M. E., Ribeiro Nogueira, R. M., Damasceno, L., Wakimoto, M., ... Nielsen-Saines, K. (2016). Zika Virus Infection in Pregnant Women in Rio de Janeiro. *New England Journal of Medicine*, 375(24), 2321–2334.  
<https://doi.org/10.1056/nejmoa1602412>
- Bressanelli, S., Stiasny, K., Allison, S. L., Stura, E. A., Duquerroy, S., Lescar, J., ... Rey, F. A. (2004). Structure of a flavivirus envelope glycoprotein in its low-pH-induced membrane fusion conformation. *EMBO Journal*, 23(4), 728–738.  
<https://doi.org/10.1038/sj.emboj.7600064>
- Brewster, C. D., Birkenheuer, C. H., Vogt, M. B., Quackenbush, S. L., & Rovnak, J. (2011). The retroviral cyclin of walleye dermal sarcoma virus binds cyclin-dependent kinases 3 and 8. *Virology*, 409(2), 299–307. <https://doi.org/10.1016/j.virol.2010.10.022>
- Buck, M. D., Sowell, R. T., Kaech, S. M., & Pearce, E. L. (2017). Metabolic Instruction of Immunity. *Cell*, 169(4), 570–586. <https://doi.org/10.1016/j.cell.2017.04.004>
- Butler, M., Chotiwan, N., Brewster, C. D., Dilisio, J. E., Ackart, D. F., Podell, B. K., ... Rovnak, J. (2020). Cyclin-Dependent Kinases 8 and 19 Regulate Host Cell Metabolism during Dengue Virus Serotype 2 Infection. *Viruses*, 12(654), 1–21.
- Byk, L. A., & Gamarnik, A. V. (2016). Properties and Functions of the Dengue Virus Capsid Protein. *Annual Review of Virology*, 3, 263–281. <https://doi.org/10.1146/annurev-virology-110615-042334>
- Calle, P., Muñoz, A., Sola, A., & Hotter, G. (2019). CPT1a gene expression reverses the inflammatory and anti-phagocytic effect of 7-ketocholesterol in RAW264.7 macrophages. *Lipids in Health and Disease*, 18(1). <https://doi.org/10.1186/s12944-019-1156-7>

- Carlin, A. F., Vizcarra, E. A., Branche, E., Viramontes, K. M., Suarez-Amaran, L., Ley, K., ... Glass, C. K. (2018). Deconvolution of pro- and antiviral genomic responses in Zika virus-infected and bystander macrophages. *Proceedings of the National Academy of Sciences of the United States of America*, *115*(39), E9172–E9181.  
<https://doi.org/10.1073/pnas.1807690115>
- Cassol, E., Cassetta, L., Rizzi, C., Alfano, M., & Poli, G. (2009). M1 and M2a Polarization of Human Monocyte-Derived Macrophages Inhibits HIV-1 Replication by Distinct Mechanisms. *The Journal of Immunology*, *182*(10), 6237–6246.  
<https://doi.org/10.4049/jimmunol.0803447>
- Castrillo, A., Pennington, D. J., Otto, F., Parker, P. J., Owen, M. J., & Boscá, L. (2001). Protein kinase C $\epsilon$  is required for macrophage activation and defense against bacterial infection. *Journal of Experimental Medicine*, *194*(9), 1231–1242.  
<https://doi.org/10.1084/jem.194.9.1231>
- Castro, F., Cardoso, A. P., Gonçalves, R. M., Serre, K., & Oliveira, M. J. (2018). Interferon-gamma at the crossroads of tumor immune surveillance or evasion. *Frontiers in Immunology*, *9*(MAY), 1–19. <https://doi.org/10.3389/fimmu.2018.00847>
- Cauchemez, S., Besnard, M., Bompard, P., Dub, T., Guillemette-Artur, P., Eyrolle-Guignot, D., ... Mallet, H. P. (2016). Association between Zika virus and microcephaly in French Polynesia, 2013-15: A retrospective study. *The Lancet*, *387*(10033), 2125–2132.  
[https://doi.org/10.1016/S0140-6736\(16\)00651-6](https://doi.org/10.1016/S0140-6736(16)00651-6)
- Cerny, D., Haniffa, M., Shin, A., Bigliardi, P., Tan, B. K., Lee, B., ... Fink, K. (2014). Selective Susceptibility of Human Skin Antigen Presenting Cells to Productive Dengue Virus Infection. *PLoS Pathogens*, *10*(12). <https://doi.org/10.1371/journal.ppat.1004548>

- Chacko, B. K., Kramer, P. A., Ravi, S., Benavides, G. A., Mitchell, T., Dranka, B. P., ... Darley-Usmar, V. M. (2014). The Bioenergetic Health Index: a new concept in mitochondrial translational research. *Clinical Science*, *127*(6), 367–373.  
<https://doi.org/10.1042/CS20140101>
- Chanput, W., Mes, J. J., & Wichers, H. J. (2014). THP-1 cell line: An in vitro cell model for immune modulation approach. *International Immunopharmacology*, *23*(1), 37–45.  
<https://doi.org/10.1016/j.intimp.2014.08.002>
- Chareonsirisuthigul, T., Kalayanarooj, S., & Ubol, S. (2007). Dengue virus (DENV) antibody-dependent enhancement of infection upregulates the production of anti-inflammatory cytokines, but suppresses anti-DENV free radical and pro-inflammatory cytokine production, in THP-1 cells. *Journal of General Virology*, *88*(2), 365–375.  
<https://doi.org/10.1099/vir.0.82537-0>
- Chatel-Chaix, L., Cortese, M., Romero-Brey, I., Bender, S., Neufeldt, C. J., Fischl, W., ... Bartenschlager, R. (2016). Dengue Virus Perturbs Mitochondrial Morphodynamics to Dampen Innate Immune Responses. *Cell Host and Microbe*, *20*(3), 342–356.  
<https://doi.org/10.1016/j.chom.2016.07.008>
- Chen, H. R., Lai, Y. C., & Yeh, T. M. (2018). Dengue virus non-structural protein 1: A pathogenic factor, therapeutic target, and vaccine candidate. *Journal of Biomedical Science*, *25*(1), 1–11. <https://doi.org/10.1186/s12929-018-0462-0>
- Chen, M., Liang, J., Ji, H., Yang, Z., Altilia, S., Hu, B., ... Roninson, I. B. (2017). CDK8/19 Mediator kinases potentiate induction of transcription by NFκB. *Proceedings of the National Academy of Sciences of the United States of America*, *114*(38), 10208–10213.  
<https://doi.org/10.1073/pnas.1710467114>

- Chen, Y.-C., Wang, S.-Y., & King, C.-C. (1999). Bacterial Lipopolysaccharide Inhibits Dengue Virus Infection of Primary Human Monocytes/Macrophages by Blockade of Virus Entry via a CD14-Dependent Mechanism. *Journal of Virology*, *73*(4), 2650–2657.  
<https://doi.org/10.1128/jvi.73.4.2650-2657.1999>
- Ching-Cheng Huang, S., Everts, B., Ivanova, Y., Nascimento, M., Smith, A. M., Beatty, W., ... Pearce, E. J. (2014). Cell-intrinsic lysosomal lipolysis is essential for alternative activation of macrophages. *Nature Immunology*, *15*. <https://doi.org/10.1038/ni.2956>
- Conaway, R. C., & Conaway, J. W. (2013). The Mediator complex and transcription elongation. *Biochimica et Biophysica Acta - Gene Regulatory Mechanisms*, *1829*(1), 69–75.  
<https://doi.org/10.1016/j.bbagrm.2012.08.017>
- Cruz-Oliveira, C., Freire, J. M., Conceição, T. M., Higa, L. M., Castanho, M. A. R. B., & Da Poian, A. T. (2015). Receptors and routes of dengue virus entry into the host cells. *FEMS Microbiology Reviews*, *39*(2), 155–170. <https://doi.org/10.1093/femsre/fuu004>
- Cui, T., Sugrue, R. J., Xu, Q., Lee, A. K. W., Chan, Y. C., & Fu, J. (1998). Recombinant dengue virus type 1 NS3 protein exhibits specific viral RNA binding and NTPase activity regulated by the NS5 protein. *Virology*, *246*(2), 409–417. <https://doi.org/10.1006/viro.1998.9213>
- Czimmerer, Z., Daniel, B., Horvath, A., Ruckerl, D., Nagy, G., Kiss, M., ... Nagy, L. (2018). The Transcription Factor STAT6 Mediates Direct Repression of Inflammatory Enhancers and Limits Activation of Alternatively Polarized Macrophages. *Immunity*, *48*(1), 75-90.e6.  
<https://doi.org/10.1016/j.immuni.2017.12.010>

- Dai, L., Song, J., Lu, X., Deng, Y. Q., Musyoki, A. M., Cheng, H., ... Gao, G. F. (2016). Structures of the Zika Virus Envelope Protein and Its Complex with a Flavivirus Broadly Protective Antibody. *Cell Host and Microbe*, *19*(5), 696–704.  
<https://doi.org/10.1016/j.chom.2016.04.013>
- Daigneault, M., Preston, J. A., Marriott, H. M., Whyte, M. K. B., & Dockrell, D. H. (2010). The identification of markers of macrophage differentiation in PMA-stimulated THP-1 cells and monocyte-derived macrophages. *PLoS ONE*, *5*(1).  
<https://doi.org/10.1371/journal.pone.0008668>
- Daniels, D. L., Ford, M., Scwinn, M. K., Benink, H., Galbraith, M. D., Amunugama, R., ... Urh, M. (2013). Mutual Exclusivity of MED12/MED12L, MED13/13L, and CDK8/19 Paralogs Revealed within the CDK-Mediator Kinase Module. *Journal of Proteomics & Bioinformatics*, *01*(S2). <https://doi.org/10.4172/jpb.s2-004>
- De Maio, F. A., Risso, G., Iglesias, N. G., Shah, P., Pozzi, B., Gebhard, L. G., ... Gamarnik, A. V. (2016). The Dengue Virus NS5 Protein Intrudes in the Cellular Spliceosome and Modulates Splicing. *PLoS Pathogens*, *12*(8), 1–29.  
<https://doi.org/10.1371/journal.ppat.1005841>
- DeBerardinis, R. J., Sayed, N., Ditsworth, D., & Thompson, C. B. (2008). Brick by brick: metabolism and tumor cell growth. *Current Opinion in Genetics and Development*, *18*(1), 54–61. <https://doi.org/10.1016/j.gde.2008.02.003>
- Decout, A., Katz, J. D., Venkatraman, S., & Ablasser, A. (2021). The cGAS–STING pathway as a therapeutic target in inflammatory diseases. *Nature Reviews Immunology*, *21*(9), 548–569.  
<https://doi.org/10.1038/s41577-021-00524-z>

- Den Boon, J. A., & Ahlquist, P. (2010). Organelle-like membrane compartmentalization of positive-strand RNA virus replication factories. *Annual Review of Microbiology*, *64*, 241–256. <https://doi.org/10.1146/annurev.micro.112408.134012>
- Denner, J. (2016). Immunosuppressive properties of retroviruses. *European Journal of Immunology*, *46*(1), 253–255. <https://doi.org/10.1002/eji.201545851>
- Diamond, M. S., & Harris, E. (2001). Interferon inhibits dengue virus infection by preventing translation of viral RNA through a PKR-independent mechanism. *Virology*, *289*(2), 297–311. <https://doi.org/10.1006/viro.2001.1114>
- Diamond, M. S., & Pierson, T. C. (2015). Molecular Insight into Dengue Virus Pathogenesis and Its Implications for Disease Control. *Cell*, *162*(3), 488–492. <https://doi.org/10.1016/j.cell.2015.07.005>
- Diamond, M. S., Roberts, T. G., Edgil, D., Lu, B., Ernst, J., & Harris, E. (2000). Modulation of Dengue Virus Infection in Human Cells by Alpha, Beta, and Gamma Interferons. *Journal of Virology*, *74*(11), 4957–4966. <https://doi.org/10.1128/jvi.74.11.4957-4966.2000>
- Dinarello, C. A. (2000). Proinflammatory cytokines. *Chest*, *118*(2), 503–508. <https://doi.org/10.1378/chest.118.2.503>
- Divakaruni, A. S., Hsieh, W. Y., Minarrieta, L., Duong, T. N., Kim, K. K. O., Desousa, B. R., ... Murphy, A. N. (2018). Etomoxir Inhibits Macrophage Polarization by Disrupting CoA Homeostasis. *Cell Metabolism*, *28*(3), 490-503.e7. <https://doi.org/10.1016/j.cmet.2018.06.001>
- Donner, A. J., Ebmeier, C. C., Taatjes, D. J., & Espinosa, J. M. (2010). CDK8 is a positive regulator of transcriptional elongation within the serum response network. *Nature Structural and Molecular Biology*, *17*(2), 194–201. <https://doi.org/10.1038/nsmb.1752>

- Edgil, D., Polacek, C., & Harris, E. (2006). Dengue Virus Utilizes a Novel Strategy for Translation Initiation When Cap-Dependent Translation Is Inhibited. *Journal of Virology*, *80*(6), 2976–2986. <https://doi.org/10.1128/jvi.80.6.2976-2986.2006>
- El Costa, H., Gouilly, J., Mansuy, J. M., Chen, Q., Levy, C., Cartron, G., ... Jabrane-Ferrat, N. (2016). ZIKA virus reveals broad tissue and cell tropism during the first trimester of pregnancy. *Scientific Reports*, *6*(June), 1–9. <https://doi.org/10.1038/srep35296>
- Everts, B., Amiel, E., Huang, S. C. C., Smith, A. M., Chang, C. H., Lam, W. Y., ... Pearce, E. J. (2014). TLR-driven early glycolytic reprogramming via the kinases TBK1-IKKε supports the anabolic demands of dendritic cell activation. *Nature Immunology*, *15*(4), 323–332. <https://doi.org/10.1038/ni.2833>
- Fan, J., Liu, Y., & Yuan, Z. (2014). Critical role of Dengue Virus NS1 protein in viral replication. *Virologica Sinica*, *29*(3), 162–169. <https://doi.org/10.1007/s12250-014-3459-1>
- Feng, D., Youn, D. Y., Zhao, X., Gao, Y., Quinn, W. J., Xiaoli, A. M., ... Yang, F. (2015). mTORC1 down-regulates cyclin-dependent kinase 8 (CDK8) and cyclin C (CycC). *PLoS ONE*, *10*(6), 1–15. <https://doi.org/10.1371/journal.pone.0126240>
- Feng, H., Zhang, Y. B., Gui, J. F., Lemon, S. M., & Yamane, D. (2021). Interferon regulatory factor 1 (IRF1) and anti-pathogen innate immune responses. *PLoS Pathogens*, *17*(1), 1–22. <https://doi.org/10.1371/journal.ppat.1009220>
- Fernandes-Siqueira, L. O., Zeidler, J. D., Sousa, B. G., Ferreira, T., & Da Poian, A. T. (2018). Anaplerotic Role of Glucose in the Oxidation of Endogenous Fatty Acids during Dengue Virus Infection. *MSphere*, *3*(1). <https://doi.org/10.1128/msphere.00458-17>

- Firestein, R., Bass, A. J., Kim, S. Y., Dunn, I. F., Silver, S. J., Guney, I., ... Hahn, W. C. (2008). CDK8 is a colorectal cancer oncogene that regulates  $\beta$ -catenin activity. *Nature*, *455*(7212), 547–551. <https://doi.org/10.1038/nature07179>
- Fleming, S. B., McCaughan, C. A., Andrews, A. E., Nash, A. D., & Mercer, A. A. (1997). A homolog of interleukin-10 is encoded by the poxvirus orf virus. *Journal of Virology*, *71*(6), 4857–4861. <https://doi.org/10.1128/jvi.71.6.4857-4861.1997>
- Fontaine, K. A., Sanchez, E. L., Camarda, R., & Lagunoff, M. (2015). Dengue Virus Induces and Requires Glycolysis for Optimal Replication. *Journal of Virology*, *89*(4), 2358–2366. <https://doi.org/10.1128/jvi.02309-14>
- Foo, S. S., Chen, W., Chan, Y., Bowman, J. W., Chang, L. C., Choi, Y., ... Jung, J. U. (2017). Asian Zika virus strains target CD14 + blood monocytes and induce M2-skewed immunosuppression during pregnancy. *Nature Microbiology*, *2*(11), 1558–1570. <https://doi.org/10.1038/s41564-017-0016-3>
- Forrester, M. A., Wassall, H. J., Hall, L. S., Cao, H., Wilson, H. M., Barker, R. N., & Vickers, M. A. (2018). Similarities and differences in surface receptor expression by THP-1 monocytes and differentiated macrophages polarized using seven different conditioning regimens. *Cellular Immunology*, *332*(April), 58–76. <https://doi.org/10.1016/j.cellimm.2018.07.008>
- Fujiwara, N., & Kobayashi, K. (2005). Macrophages in inflammation. *Current Drug Targets: Inflammation and Allergy*, *4*(3), 281–286. <https://doi.org/10.2174/1568010054022024>
- Gabor, N., Kim, J.-S., Reyes, L., & Golos, T. G. (2018). Hofbauer Cells: Their Role in Healthy and Complicated Pregnancy. *Frontiers in Immunology* | [Www.Frontiersin.Org](http://www.frontiersin.org), *9*, 2628. <https://doi.org/10.3389/fimmu.2018.02628>

- Galbraith, M. D., Allen, M. A., Bensard, C. L., Wang, X., Schwinn, M. K., Qin, B., ... Espinosa, J. M. (2013). HIF1A Employs CDK8-Mediator to Stimulate RNAPII Elongation in Response to Hypoxia. *Cell*, *153*(6), 1327. <https://doi.org/10.1016/j.cell.2013.04.048>
- Galbraith, M. D., Andrysik, Z., Pandey, A., Hoh, M., Bonner, E. A., Hill, A. A., ... Espinosa, J. M. (2017a). CDK8 Kinase Activity Promotes Glycolysis. *Cell Reports*, *21*, 1495–1506.
- Galbraith, M. D., Andrysik, Z., Pandey, A., Hoh, M., Bonner, E. A., Hill, A. A., ... Espinosa, J. M. (2017b). CDK8 Kinase Activity Promotes Glycolysis. *Cell Reports*, *21*(6), 1495–1506. <https://doi.org/10.1016/j.celrep.2017.10.058>
- Galván-Peña, S., & O'Neill, L. A. J. (2014). Metabolic reprogramming in macrophage polarization. *Frontiers in Immunology*, *5*(AUG). <https://doi.org/10.3389/fimmu.2014.00420>
- Gamarnik, A. V., & Andino, R. (1998). Switch from translation to RNA replication in a positive-stranded RNA virus. *Genes and Development*, *12*(15), 2293–2304. <https://doi.org/10.1101/gad.12.15.2293>
- Genin, M., Clement, F., Fattaccioli, A., Raes, M., & Michiels, C. (2015). M1 and M2 macrophages derived from THP-1 cells differentially modulate the response of cancer cells to etoposide. *BMC Cancer*, *15*(1), 1–14. <https://doi.org/10.1186/s12885-015-1546-9>
- Giovanetti, M., Faria, N. R., Lourenço, J., Goes de Jesus, J., Xavier, J., Claro, I. M., ... Alcantara, L. C. (2020). Genomic and Epidemiological Surveillance of Zika Virus in the Amazon Region. *Cell Reports*, *30*(7), 2275-2283.e7. <https://doi.org/10.1016/j.celrep.2020.01.085>

- Giraldo, M. I., Vargas-Cuartas, O., Gallego-Gomez, J. C., Shi, P. Y., Padilla-Sanabria, L., Castaño-Osorio, J. C., & Rajsbaum, R. (2018). K48-linked polyubiquitination of dengue virus NS1 protein inhibits its interaction with the viral partner NS4B. *Virus Research*, 246(September 2017), 1–11. <https://doi.org/10.1016/j.virusres.2017.12.013>
- Glasner, D. R., Ratnasiri, K., Puerta-Guardo, H., Espinosa, D. A., Beatty, P. R., & Harris, E. (2017). Dengue virus NS1 cytokine-independent vascular leak is dependent on endothelial glycocalyx components. *PLoS Pathogens*, 13(11), 1–22. <https://doi.org/10.1371/journal.ppat.1006673>
- Gong, D., Shi, W., Yi, S. ju, Chen, H., Groffen, J., & Heisterkamp, N. (2012). TGFβ signaling plays a critical role in promoting alternative macrophage activation. *BMC Immunology*, 13. <https://doi.org/10.1186/1471-2172-13-31>
- Goodwin, C. M., Xu, S., & Munger, J. (2015). Stealing the Keys to the Kitchen: Viral Manipulation of the Host Cell Metabolic Network. *Trends in Microbiology*, 23(12), 789–798. <https://doi.org/10.1016/j.tim.2015.08.007>
- Gopala Reddy, S. B., Chin, W. X., & Shivananju, N. S. (2018). Dengue virus NS2 and NS4: Minor proteins, mammoth roles. *Biochemical Pharmacology*, 154(April), 54–63. <https://doi.org/10.1016/j.bcp.2018.04.008>
- Gordon, S., & Martinez, F. O. (2010). Alternative activation of macrophages: Mechanism and functions. *Immunity*, 32(5), 593–604. <https://doi.org/10.1016/j.immuni.2010.05.007>
- Gotsch, F., Romero, R., Friel, L., Kusanovic, J. P., Espinoza, J., Erez, O., ... Hassan, S. S. (2007). CXCL10/IP-10: A missing link between inflammation and anti-angiogenesis in preeclampsia? *Journal of Maternal-Fetal and Neonatal Medicine*, 20(11), 777–792. <https://doi.org/10.1080/14767050701483298>

- Guillou, C., Fréret, M., Fondard, E., Derambure, C., Avenel, G., Golinski, M. L., ... Vittecoq, O. (2016). Soluble alpha-enolase activates monocytes by CD14-dependent TLR4 signalling pathway and exhibits a dual function. *Scientific Reports*, 6(March), 1–12.  
<https://doi.org/10.1038/srep23796>
- Gullberg, R. C., Steel, J. J., Pujari, V., Rovnak, J., Crick, D. C., & Perera, R. (2018). Stearoyl-CoA desaturase 1 differentiates early and advanced dengue virus infections and determines virus particle infectivity. *PLoS Pathogens*, 14(8), 1–28.  
<https://doi.org/10.1371/journal.ppat.1007261>
- Guo, Z., Wang, G., Lv, Y., Wan, Y. Y., & Zheng, J. (2019). Inhibition of Cdk8/Cdk19 Activity Promotes Treg Cell Differentiation and Suppresses Autoimmune Diseases. *Frontiers in Immunology*, 10(August), 1–10. <https://doi.org/10.3389/fimmu.2019.01988>
- Gutsche, I., Coulibaly, F., Voss, J. E., Salmon, J., D'Alayer, J., Ermonval, M., ... Flamand, M. (2011). Secreted dengue virus nonstructural protein NS1 is an atypical barrel-shaped high-density lipoprotein. *Proceedings of the National Academy of Sciences of the United States of America*, 108(19), 8003–8008. <https://doi.org/10.1073/pnas.1017338108>
- Halstead, S. B. (2007). Dengue. *Lancet*, 370(9599), 1644–1652. [https://doi.org/10.1016/S0140-6736\(07\)61687-0](https://doi.org/10.1016/S0140-6736(07)61687-0)
- Heaton, N. S., Perera, R., Berger, K. L., Khadka, S., LaCount, D. J., Kuhn, R. J., & Randall, G. (2010). Dengue virus nonstructural protein 3 redistributes fatty acid synthase to sites of viral replication and increases cellular fatty acid synthesis. *Proceedings of the National Academy of Sciences of the United States of America*, 107(40), 17345–17350.  
<https://doi.org/10.1073/pnas.1010811107>

- Heaton, N. S., & Randall, G. (2010). Dengue virus-induced autophagy regulates lipid metabolism. *Cell Host and Microbe*, *8*(5), 422–432.  
<https://doi.org/10.1016/j.chom.2010.10.006>
- Hellweg, C. E., Arenz, A., Bogner, S., Schmitz, C., & Baumstark-Khan, C. (2006). Activation of Nuclear Factor  $\kappa$ B by Different Agents. *Annals of the New York Academy of Sciences*.  
<https://doi.org/10.1196/annals.1378.066>
- Hinrichsen, F., Hamm, J., Westermann, M., Schröder, L., Shima, K., Mishra, N., ... Sommer, F. (2021). Microbial regulation of hexokinase 2 links mitochondrial metabolism and cell death in colitis. *Cell Metabolism*, *33*(12), 2355-2366.e8.  
<https://doi.org/10.1016/j.cmet.2021.11.004>
- Hofmann, M. H., Mani, R., Engelhardt, H., Impagnatiello, M. A., Carotta, S., Kerényi, M., ... Moll, J. (2020). Selective and potent CDK8/19 inhibitors enhance NK-cell activity and promote tumor surveillance. *Molecular Cancer Therapeutics*, *19*(4), 1018–1030.  
<https://doi.org/10.1158/1535-7163.MCT-19-0789>
- Hu, X., Park-Min, K.-H., Ho, H. H., & Ivashkiv, L. B. (2005). IFN- $\gamma$ -Primed Macrophages Exhibit Increased CCR2-Dependent Migration and Altered IFN- $\gamma$  Responses Mediated by Stat1. *The Journal of Immunology*, *175*(6), 3637–3647.  
<https://doi.org/10.4049/jimmunol.175.6.3637>
- Huang, S. C. C., Smith, A. M., Everts, B., Colonna, M., Pearce, E. L., Schilling, J. D., & Pearce, E. J. (2016). Metabolic Reprogramming Mediated by the mTORC2-IRF4 Signaling Axis Is Essential for Macrophage Alternative Activation. *Immunity*, *45*(4), 817–830.  
<https://doi.org/10.1016/j.immuni.2016.09.016>

- Huang, X., He, Z., Jiang, X., Hou, M., Tang, Z., Zhen, X., ... Ma, J. (2016). Folic acid represses hypoxia-induced inflammation in THP-1 cells through inhibition of the PI3K/Akt/HIF-1 $\alpha$  pathway. *PLoS ONE*, *11*(3), 1–15. <https://doi.org/10.1371/journal.pone.0151553>
- Iglesias, N. G., Filomatori, C. V., & Gamarnik, A. V. (2011). The F1 Motif of Dengue Virus Polymerase NS5 Is Involved in Promoter-Dependent RNA Synthesis. *Journal of Virology*, *85*(12), 5745–5756. <https://doi.org/10.1128/jvi.02343-10>
- Infantino, V., Convertini, P., Cucci, L., Panaro, M. A., Di Noia, M. A., Calvello, R., ... Iacobazzi, V. (2011). The mitochondrial citrate carrier: A new player in inflammation. *Biochemical Journal*, *438*(3), 433–436. <https://doi.org/10.1042/BJ20111275>
- Ip, P.-P., & Liao, F. (2010). Resistance to Dengue Virus Infection in Mice Is Potentiated by CXCL10 and Is Independent of CXCL10-Mediated Leukocyte Recruitment. *The Journal of Immunology*, *184*(10), 5705–5714. <https://doi.org/10.4049/jimmunol.0903484>
- Issur, M., Geiss, B. J., Bougie, I., Picard-Jean, F., Despins, S., Mayette, J., ... Bisailon, M. (2009). The flavivirus NS5 protein is a true RNA guanylyltransferase that catalyzes a two-step reaction to form the RNA cap structure. *RNA*, *15*(12), 2340–2350. <https://doi.org/10.1261/rna.1609709>
- Ito, H., & Seishima, M. (2010). Regulation of the induction and function of cytotoxic T lymphocytes by natural killer T cell. *Journal of Biomedicine and Biotechnology*, *2010*. <https://doi.org/10.1155/2010/641757>
- Izban, M. G., Nowicki, B. J., & Nowicki, S. (2012). 1,25-Dihydroxyvitamin D3 Promotes a Sustained LPS-Induced NF- $\kappa$ B-Dependent Expression of CD55 in Human Monocytic THP-1 Cells. *PLoS ONE*, *7*(11). <https://doi.org/10.1371/journal.pone.0049318>

- Jenkins, S. J., & Allen, J. E. (2021). The expanding world of tissue-resident macrophages. *European Journal of Immunology*, 51(8), 1882–1896. <https://doi.org/10.1002/eji.202048881>
- Jessie, K., Fong, M. Y., Devi, S., Lam, S. K., & Wong, K. T. (2004). Localization of dengue virus in naturally infected human tissues, by immunohistochemistry and in situ hybridization. *Journal of Infectious Diseases*, 189(8), 1411–1418. <https://doi.org/10.1086/383043>
- Jha, A. K., Huang, S. C. C., Sergushichev, A., Lampropoulou, V., Ivanova, Y., Loginicheva, E., ... Artyomov, M. N. (2015). Network integration of parallel metabolic and transcriptional data reveals metabolic modules that regulate macrophage polarization. *Immunity*, 42(3), 419–430. <https://doi.org/10.1016/j.immuni.2015.02.005>
- Jhan, M.-K., Chen, C.-L., Shen, T.-J., Tseng, P.-C., Wang, Y.-T., Satria, R. D., ... Lin, C.-F. (2021). Polarization of Type 1 Macrophages Is Associated with the Severity of Viral Encephalitis Caused by Japanese Encephalitis Virus and Dengue Virus \_ Enhanced Reader.pdf. *Cells*, 10, 3181.
- Jiang, Y., & Fleet, J. C. (2012). Effect of phorbol 12-myristate 13-acetate activated signaling pathways on  $1\alpha$ , 25 dihydroxyvitamin D3 regulated human 25- hydroxyvitamin D3 24-hydroxylase gene expression in differentiated Caco-2 cells. *Journal of Cell Biochemistry*, 113(5), 1599–1607. <https://doi.org/10.1002/jcb.24028>.Effect
- Johannessen, L., Sundberg, T. B., O'Connell, D. J., Kolde, R., Berstler, J., Billings, K. J., ... Xavier, R. J. (2017). Small-molecule studies identify CDK8 as a regulator of IL-10 in myeloid cells. *Nature Chemical Biology*, 13(10), 1102–1108. <https://doi.org/10.1038/nchembio.2458>

- Johnson, A. R., Qin, Y., Cozzo, A. J., Freemerman, A. J., Huang, M. J., Zhao, L., ... Makowski, L. (2016). Metabolic reprogramming through fatty acid transport protein 1 (FATP1) regulates macrophage inflammatory potential and adipose inflammation. *Molecular Metabolism*, 5(7), 506–526. <https://doi.org/10.1016/j.molmet.2016.04.005>
- Jordan, T. X., & Randall, G. (2017). Dengue Virus Activates the AMP Kinase-mTOR Axis To Stimulate a Proviral Lipophagy. *Journal of Virology*, 91(11). <https://doi.org/10.1128/jvi.02020-16>
- Jurado, K. A., & Iwasaki, A. (2017). Zika virus targets blood monocytes. *Nature Microbiology*, 2(11), 1460–1461. <https://doi.org/10.1038/s41564-017-0049-7>
- Kapoor, M., Zhang, L., Ramachandra, M., Kusukawa, J., Ebner, K. E., & Padmanabhan, R. (1995). Association between NS3 and NS5 proteins of dengue virus type 2 in the putative RNA replicase is linked to differential phosphorylation of NS5. *Journal of Biological Chemistry*, 270(32), 19100–19106. <https://doi.org/10.1074/jbc.270.32.19100>
- Katze, M. G., He, Y., & Gale, M. (2002). Viruses and interferon: A fight for supremacy. *Nature Reviews Immunology*, 2(9), 675–687. <https://doi.org/10.1038/nri888>
- Kawakatsu, K., Ishikawa, M., Mashiba, R., Tran, N. K., Akamatsu, M., & Nishikata, T. (2019). Characteristic morphological changes and rapid actin accumulation in Serum-MAF-treated Macrophages. *Anticancer Research*, 39(8), 4533–4537. <https://doi.org/10.21873/anticancer.13630>
- Kelly, B., & O'Neill, L. A. J. (2015). Metabolic reprogramming in macrophages and dendritic cells in innate immunity. *Cell Research*, 25(7), 771–784. <https://doi.org/10.1038/cr.2015.68>

- Kinney, R. M., Butrapet, S., Chang, G.-J. J., Tsuchiya, K. R., Roehrig, J. T., Bhamarapravati, N., & Gubler, D. J. (1997). Construction of Infectious cDNA Clones for Dengue 2 Virus: Strain 16681 and Its Attenuated Vaccine Derivative, Strain PDK-53. *Virology*, *230*(230), 300–308.
- Klema, V. J., Ye, M., Hindupur, A., Teramoto, T., Gottipati, K., Padmanabhan, R., & Choi, K. H. (2016). Dengue Virus Nonstructural Protein 5 (NS5) Assembles into a Dimer with a Unique Methyltransferase and Polymerase Interface. *PLoS Pathogens*, *12*(2), 1–21.  
<https://doi.org/10.1371/journal.ppat.1005451>
- Knab, V. M., Gotthardt, D., Klein, K., Grausenburger, R., Heller, G., Menzl, I., ... Sexl, V. (2021). Triple-negative breast cancer cells rely on kinase-independent functions of CDK8 to evade NK-cell-mediated tumor surveillance. *Cell Death & Disease*, *12*(11), 1–12.  
<https://doi.org/10.1038/s41419-021-04279-2>
- Knuesel, M. T., Meyer, K. D., Donner, A. J., Espinosa, J. M., & Taatjes, D. J. (2009). The Human CDK8 Subcomplex Is a Histone Kinase That Requires Med12 for Activity and Can Function Independently of Mediator. *Molecular and Cellular Biology*, *29*(3), 650–661.  
<https://doi.org/10.1128/mcb.00993-08>
- Kohro, T., Tanaka, T., Murakami, T., Wada, Y., Aburatani, H., Hamakubo, T., & Kodama, T. (2004). A comparison of differences in the gene expression profiles of phorbol 12-myristate 13-acetate differentiated THP-1 cells and human monocyte-derived macrophage. *Journal of Atherosclerosis and Thrombosis*, *11*(2), 88–97. <https://doi.org/10.5551/jat.11.88>
- Krishnan, M. N., Sukumaran, B., Pal, U., Agaisse, H., Murray, J. L., Hodge, T. W., & Fikrig, E. (2007). Rab 5 Is Required for the Cellular Entry of Dengue and West Nile Viruses. *Journal of Virology*, *81*(9), 4881–4885. <https://doi.org/10.1128/jvi.02210-06>

- Kuhn, R. J., Zhang, W., Rossmann, M. G., Pletnev, S. V., Corver, J., Lenches, E., ... Strauss, J. H. (2002). Structure of dengue virus: Implications for flavivirus organization, maturation, and fusion. *Cell*, *108*(5), 717–725. [https://doi.org/10.1016/S0092-8674\(02\)00660-8](https://doi.org/10.1016/S0092-8674(02)00660-8)
- Kwon, Y. C., Meyer, K., Peng, G., Chatterjee, S., Hoft, D. F., & Ray, R. (2019). Hepatitis C Virus E2 Envelope Glycoprotein Induces an Immunoregulatory Phenotype in Macrophages. *Hepatology*, *69*(5), 1873–1884. <https://doi.org/10.1002/hep.29843>
- Lauretì, M., Narayanan, D., Rodriguez-Andres, J., Fazakerley, J. K., & Kedzierski, L. (2018). Flavivirus Receptors: Diversity, Identity, and Cell Entry. *Frontiers in Immunology*, *9*(September), 1–11. <https://doi.org/10.3389/fimmu.2018.02180>
- Lawrence, T., & Natoli, G. (2011). Transcriptional regulation of macrophage polarization: Enabling diversity with identity. *Nature Reviews Immunology*, *11*(11), 750–761. <https://doi.org/10.1038/nri3088>
- Lazear, H. M., & Diamond, M. S. (2016). Zika Virus: New Clinical Syndromes and Its Emergence in the Western Hemisphere. *Journal of Virology*, *90*(10), 4864–4875. <https://doi.org/10.1128/jvi.00252-16>
- Lee, A. J., & Ashkar, A. A. (2018). The dual nature of type I and type II interferons. *Frontiers in Immunology*, *9*(SEP), 1–10. <https://doi.org/10.3389/fimmu.2018.02061>
- Lee, D. H., & Ghiasi, H. (2017). Roles of M1 and M2 Macrophages in Herpes Simplex Virus 1 Infectivity. *Journal of Virology*, *91*(15). <https://doi.org/10.1128/jvi.00578-17>
- Lee, M.-S., Tseng, Y.-H., Chen, Y.-C., Kuo, C.-H., Wang, S.-L., Lin, M.-H., ... Hung, C. H. (2018). M2 macrophage subset decrement is an indicator of bleeding tendency in pediatric dengue disease. *Journal of Microbiology, Immunology and Infection*, *(51)*, 829–838.

- Lee, M. S., Tseng, Y. H., Chen, Y. C., Kuo, C. H., Wang, S. L., Lin, M. H., ... Hung, C. H. (2018). M2 macrophage subset decrement is an indicator of bleeding tendency in pediatric dengue disease. *Journal of Microbiology, Immunology and Infection*, 51(6), 829–838. <https://doi.org/10.1016/j.jmii.2018.08.006>
- Lee, W. S., Wheatley, A. K., Kent, S. J., & Dekosky, B. J. (2020). Antibody-dependent enhancement and SARS-CoV-2 vaccines and therapies. *Nature Microbiology*, 5(10), 1181–1191.
- Li, H., Clum, S., You, S., Ebner, K. E., & Padmanabhan, R. (1999). The Serine Protease and RNA-Stimulated Nucleoside Triphosphatase and RNA Helicase Functional Domains of Dengue Virus Type 2 NS3 Converge within a Region of 20 Amino Acids. *Journal of Virology*, 73(4), 3108–3116. <https://doi.org/10.1128/jvi.73.4.3108-3116.1999>
- Li, L., Lok, S.-M., Yu, I.-M., Zhang, Y., Kuhn, R. J., Chen, J., & Rossman, M. G. (2008). The Flavivirus Precursor Membrane-Envelope Protein Complex: Structure and Maturation. *Science (New York, N.Y.)*, 319(March), 1830–1834. <https://doi.org/10.1017/cbo9781139167291.033>
- Liang, Z., Wu, S., Li, Y., He, L., Wu, M., Jiang, L., ... Huang, X. (2011). Activation of toll-like receptor 3 impairs the dengue virus serotype 2 replication through induction of IFN- $\beta$  in cultured hepatoma cells. *PLoS ONE*, 6(8), 2–9. <https://doi.org/10.1371/journal.pone.0023346>
- Lin, R.-J., Yu, H.-P., Chang, B.-L., Tang, W.-C., Liao, C.-L., & Lin, Y.-L. (2009). Distinct Antiviral Roles for Human 2',5'-Oligoadenylate Synthetase Family Members against Dengue Virus Infection. *The Journal of Immunology*, 183(12), 8035–8043. <https://doi.org/10.4049/jimmunol.0902728>

- Lin, Z., Liu, F., Shi, P., Song, A., Huang, Z., Zou, D., ... Gao, X. (2018). Fatty acid oxidation promotes reprogramming by enhancing oxidative phosphorylation and inhibiting protein kinase C. *Stem Cell Research and Therapy*, 9(1), 1–14. <https://doi.org/10.1186/s13287-018-0792-6>
- Liu, L., Dong, H., Chen, H., Zhang, J., Ling, H., Li, Z., ... Li, H. (2010). Flavivirus RNA cap methyltransferase: Structure, function, and inhibition. *Frontiers of Biology in China*, 5(4), 286–303. <https://doi.org/10.1007/s11515-010-0660-y>
- Liu, P., Ridilla, M., Patel, P., Betts, L., Gallichotte, E., Shahidi, L., ... Jacobson, K. (2017). Beyond attachment: Roles of DC-SIGN in dengue virus infection. *Traffic*, 18(4), 218–231. <https://doi.org/10.1111/tra.12469>
- Lugo-Villarino, G., Troegeler, A., Balboa, L., Lastrucci, C., Duval, C., Mercier, I., ... Neyrolles, O. (2018). The C-type lectin receptor DC-SIGN has an anti-inflammatory role in Human M(IL-4) macrophages in response to Mycobacterium tuberculosis. *Frontiers in Immunology*, 9(JUN), 1–15. <https://doi.org/10.3389/fimmu.2018.01123>
- Luo, H., Winkelmann, E. R., Fernandez-Salas, I., Li, L., Mayer, S. V., Danis-Lozano, R., ... Wang, T. (2018). Zika, dengue and yellow fever viruses induce differential anti-viral immune responses in human monocytic and first trimester trophoblast cells. *Antiviral Research*, 151(October 2017), 55–62. <https://doi.org/10.1016/j.antiviral.2018.01.003>
- Maeß, M. B., Sendelbach, S., & Lorkowski, S. (2010). Selection of reliable reference genes during THP-1 monocyte differentiation into macrophages. *BMC Molecular Biology*, 11, 1–8. <https://doi.org/10.1186/1471-2199-11-90>

- Maeß, M. B., Wittig, B., Cignarella, A., & Lorkowski, S. (2014). Reduced PMA enhances the responsiveness of transfected THP-1 macrophages to polarizing stimuli. *Journal of Immunological Methods*, 402(1–2), 76–81. <https://doi.org/10.1016/j.jim.2013.11.006>
- Malandrino, M. I., Fucho, R., Weber, M., Calderon-Dominguez, M., Mir, J. F., Valcarcel, L., ... Herrero, L. (2015). Enhanced fatty acid oxidation in adipocytes and macrophages reduces lipid-induced triglyceride accumulation and inflammation. *American Journal of Physiology - Endocrinology and Metabolism*, 308(9), E756–E769. <https://doi.org/10.1152/ajpendo.00362.2014>
- Malavige, G. N., & Ogg, G. S. (2017). Pathogenesis of vascular leak in dengue virus infection. *Immunology*. <https://doi.org/10.1111/imm.12748>
- Mantovani, A., Sica, A., Sozzani, S., Allavena, P., Vecchi, A., & Locati, M. (2004). The chemokine system in diverse forms of macrophage activation and polarization. *Trends in Immunology*. <https://doi.org/10.1016/j.it.2004.09.015>
- Martinez-Fabregas, J., Wang, L., Pohler, E., Cozzani, A., Wilmes, S., Kazemian, M., ... Moraga, I. (2020). CDK8 Fine-Tunes IL-6 Transcriptional Activities by Limiting STAT3 Resident Time at the Gene Loci. *Cell Reports*, 33(12), 108545. <https://doi.org/10.1016/j.celrep.2020.108545>
- Martínez-Reyes, I., & Chandel, N. S. (2020). Mitochondrial TCA cycle metabolites control physiology and disease. *Nature Communications*, 11(1), 1–11. <https://doi.org/10.1038/s41467-019-13668-3>

- Matusan, A. E., Kelley, P. G., Pryor, M. J., Whisstock, J. C., Davidson, A. D., & Wright, P. J. (2001). Mutagenesis of the dengue virus type 2 NS3 proteinase and the production of growth-restricted virus. *Journal of General Virology*, *82*(7), 1647–1656.  
<https://doi.org/10.1099/0022-1317-82-7-1647>
- McDermott, M. S. J., Chumanevich, A. A., Lim, C. U., Liang, J., Chen, M., Altilia, S., ... Broude, E. V. (2017). Inhibition of CDK8 mediator kinase suppresses estrogen dependent transcription and the growth of estrogen receptor positive breast cancer. *Oncotarget*, *8*(8), 12558–12575. <https://doi.org/10.18632/oncotarget.14894>
- McNab, F., Mayer-Barber, K., Sher, A., Wack, A., & O’Garra, A. (2015). Type I interferons in infectious disease. *Nature Reviews Immunology*, *15*(2), 87–103.  
<https://doi.org/10.1038/nri3787>
- McWhorter, F. Y., Wang, T., Nguyen, P., Chung, T., & Liu, W. F. (2013). Modulation of macrophage phenotype by cell shape. *Proceedings of the National Academy of Sciences of the United States of America*, *110*(43), 17253–17258.  
<https://doi.org/10.1073/pnas.1308887110>
- Medin, C. L., Fitzgerald, K. A., & Rothman, A. L. (2005). Dengue Virus Nonstructural Protein NS5 Induces Interleukin-8 Transcription and Secretion. *Journal of Virology*, *79*(17), 11053–11061. <https://doi.org/10.1128/jvi.79.17.11053-11061.2005>
- Michelucci, A., Cordes, T., Ghelfi, J., Pailot, A., Reiling, N., Goldmann, O., ... Hiller, K. (2013). Immune-responsive gene 1 protein links metabolism to immunity by catalyzing itaconic acid production. *Proceedings of the National Academy of Sciences of the United States of America*, *110*(19), 7820–7825. <https://doi.org/10.1073/pnas.1218599110>

- Michlmayr, D., Andrade, P., Gonzalez, K., Balmaseda, A., & Harris, E. (2017). CD14+CD16+ monocytes are the main target of Zika virus infection in peripheral blood mononuclear cells in a paediatric study in Nicaragua. *Nature Microbiology*, 2(11), 1462–1470. <https://doi.org/10.1038/s41564-017-0035-0>
- Miller, J. L., DeWet, B. J. M., Martinez-Pomares, L., Radcliffe, C. M., Dwek, R. A., Rudd, P. M., & Gordon, S. (2008). The mannose receptor mediates dengue virus infection of macrophages. *PLoS Pathogens*, 4(2). <https://doi.org/10.1371/journal.ppat.0040017>
- Miller, S., Kastner, S., Krijnse-Locker, J., Bühler, S., & Bartenschlager, R. (2007). The non-structural protein 4A of dengue virus is an integral membrane protein inducing membrane alterations in a 2K-regulated manner. *Journal of Biological Chemistry*, 282(12), 8873–8882. <https://doi.org/10.1074/jbc.M609919200>
- Miller, S., & Krijnse-Locker, J. (2008). Modification of intracellular membrane structures for virus replication. *Nature Reviews Microbiology*, 6(5), 363–374. <https://doi.org/10.1038/nrmicro1890>
- Miller, S., Sparacio, S., & Bartenschlager, R. (2006). Subcellular localization and membrane topology of the dengue virus type 2 non-structural protein 4B. *Journal of Biological Chemistry*, 281(13), 8854–8863. <https://doi.org/10.1074/jbc.M512697200>
- Mills, E. L., Kelly, B., Logan, A., Costa, A. S. H., Varma, M., Bryant, C. E., ... O'Neill, L. A. (2016). Succinate Dehydrogenase Supports Metabolic Repurposing of Mitochondria to Drive Inflammatory Macrophages. *Cell*, 167(2), 457-470.e13. <https://doi.org/10.1016/j.cell.2016.08.064>

- Modhiran, N., Kalayanarooj, S., & Ubol, S. (2010). Subversion of innate defenses by the interplay between DENV and pre-existing enhancing antibodies: TLRs signaling collapse. *PLoS Neglected Tropical Diseases*, *4*(12), 1–12.  
<https://doi.org/10.1371/journal.pntd.0000924>
- Modhiran, N., Watterson, D., Muller, D. A., Panetta, A. K., Sester, D. P., Liu, L., ... Young, P. R. (2015). Dengue virus NS1 protein activates cells via Toll-like receptor 4 and disrupts endothelial cell monolayer integrity. *Science Translational Medicine*, *7*(304), 1–11.  
<https://doi.org/10.1126/scitranslmed.aaa3863>
- Modis, Y., Ogata, S., Clements, D., & Harrison, S. C. (2004). Structure of the dengue virus envelope protein after membrane fusion. *Nature*, *427*(6972), 313–319.  
<https://doi.org/10.1038/nature02165>
- Mookerjee, S. A., Nicholls, D. G., & Brand, M. D. (2016). Determining maximum glycolytic capacity using extracellular flux measurements. *PLoS ONE*, *11*(3), 1–20.  
<https://doi.org/10.1371/journal.pone.0152016>
- Moon, J. S., Hisata, S., Park, M. A., DeNicola, G. M., Ryter, S. W., Nakahira, K., & Choi, A. M. K. (2015). mTORC1-Induced HK1-Dependent Glycolysis Regulates NLRP3 Inflammasome Activation. *Cell Reports*, *12*(1), 102–115.  
<https://doi.org/10.1016/j.celrep.2015.05.046>
- Morrison, J., Aguirre, S., & Fernandez-Sesma, A. (2012). Innate immunity evasion by dengue virus. *Viruses*, *4*(3), 397–413. <https://doi.org/10.3390/v4030397>
- Mosser, D. M., & Edwards, J. P. (2008). Exploring the full spectrum of macrophage activation. *Nat Rev Immunology*, *8*(12), 958–969. <https://doi.org/10.1038/nri2448>. Exploring

- Muñoz-Jordán, J. L., Laurent-Rolle, M., Ashour, J., Martínez-Sobrido, L., Ashok, M., Lipkin, W. I., & García-Sastre, A. (2005). Inhibition of Alpha/Beta Interferon Signaling by the NS4B Protein of Flaviviruses. *Journal of Virology*, 79(13), 8004–8013.  
<https://doi.org/10.1128/jvi.79.13.8004-8013.2005>
- Murray, P. J. (2006). Understanding and exploiting the endogenous interleukin-10/STAT3-mediated anti-inflammatory response. *Current Opinion in Pharmacology*, 6(4), 379–386.  
<https://doi.org/10.1016/j.coph.2006.01.010>
- Murray, P. J. (2017). Macrophage Polarization. *Annual Review of Physiology*, 79, 541–566.  
<https://doi.org/10.1146/annurev-physiol-022516-034339>
- Nagy, C., & Haschemi, A. (2015). Time and demand are two critical dimensions of immunometabolism: The process of macrophage activation and the pentose phosphate pathway. *Frontiers in Immunology*, 6(APR), 1–8.  
<https://doi.org/10.3389/fimmu.2015.00164>
- Nanaware, N., Banerjee, A., Mullick Bagchi, S., Bagchi, P., & Mukherjee, A. (2021). Dengue Virus Infection : A Tale of Viral Exploitations and Host Responses. *Viruses*, 13(1967).
- Nanayakkara, G. K., Wang, H., & Yang, X. (2020). Proton leak regulates mitochondrial reactive oxygen species generation in endothelial cell activation and inflammation - A Novel Concept. *Arch Biochem Biophys*, (662), 68–74.  
<https://doi.org/10.1016/j.abb.2018.12.002>
- Narayan, R., & Tripathi, S. (2020). Intrinsic ADE: The Dark Side of Antibody Dependent Enhancement During Dengue Infection. *Frontiers in Cellular and Infection Microbiology*, 10(October), 1–6. <https://doi.org/10.3389/fcimb.2020.580096>

- Naveca, F. G., Pontes, G. S., Chang, A. Y. H., da Silva, G. A. V., do Nascimento, V. A., Monteiro, D. C. da S., ... Ramasawmy, R. (2018). Analysis of the immunological biomarker profile during acute zika virus infection reveals the overexpression of CXCL10, a chemokine linked to neuronal damage. *Memorias Do Instituto Oswaldo Cruz*, *113*(6), 1–13. <https://doi.org/10.1590/0074-02760170542>
- Nikitina, E., Larionova, I., Choinzonov, E., & Kzhyshkowska, J. (2018). Monocytes and macrophages as viral targets and reservoirs. *International Journal of Molecular Sciences*, *19*(9). <https://doi.org/10.3390/ijms19092821>
- Nikonova, A., Khaitov, M., Jackson, D. J., Traub, S., Trujillo-Torralbo, M. B., Kudlay, D. A., ... Johnston, S. L. (2020). M1-like macrophages are potent producers of anti-viral interferons and M1-associated marker-positive lung macrophages are decreased during rhinovirus-induced asthma exacerbations. *EBioMedicine*, *54*. <https://doi.org/10.1016/j.ebiom.2020.102734>
- O'Neill, L. A. J. (2015). A Broken Krebs Cycle in Macrophages. *Immunity*, *42*(3), 393–394. <https://doi.org/10.1016/j.immuni.2015.02.017>
- O'Neill, L. A. J., Kishton, R. J., & Rathmell, J. (2016). A guide to immunometabolism for immunologists. *Nature Reviews Immunology*. <https://doi.org/10.1038/nri.2016.70>
- O'Neill, L. A. J., & Pearce, E. J. (2016). Immunometabolism governs dendritic cell and macrophage function. *Journal of Experimental Medicine*, *213*(1), 15–23. <https://doi.org/10.1084/jem.20151570>
- Odkhuu, E., Komatsu, T., Koide, N., Naiki, Y., Takeuchi, K., Tanaka, Y., ... Yokochi, T. (2018). Sendai virus C protein limits NO production in infected RAW264.7 macrophages. *Innate Immunity*, *24*(7), 430–438. <https://doi.org/10.1177/1753425918796619>

- Oliveira, E. R. A., Mohana-Borges, R., de Alencastro, R. B., & Horta, B. A. C. (2017). The flavivirus capsid protein: Structure, function and perspectives towards drug design. *Virus Research*, 227, 115–123. <https://doi.org/10.1016/j.virusres.2016.10.005>
- Opal, S. M., & DePalo, V. A. (2000). Anti-inflammatory cytokines. *Chest*, 117(4), 1162–1172. <https://doi.org/10.1378/chest.117.4.1162>
- Ortega-Gómez, A., Perretti, M., & Soehnlein, O. (2013). Resolution of inflammation: An integrated view. *EMBO Molecular Medicine*, 5(5), 661–674. <https://doi.org/10.1002/emmm.201202382>
- Palmieri, E. M., Gonzalez-Cotto, M., Baseler, W. A., Davies, L. C., Ghesquière, B., Maio, N., ... McVicar, D. W. (2020). Nitric oxide orchestrates metabolic rewiring in M1 macrophages by targeting aconitase 2 and pyruvate dehydrogenase. *Nature Communications*, 11(1). <https://doi.org/10.1038/s41467-020-14433-7>
- Pang, T., Mak, T. K., & Gubler, D. J. (2017). Prevention and control of dengue—the light at the end of the tunnel. *The Lancet Infectious Diseases*, 17(3), e79–e87. [https://doi.org/10.1016/S1473-3099\(16\)30471-6](https://doi.org/10.1016/S1473-3099(16)30471-6)
- Park, E. K., Jung, H. S., Yang, H. I., Yoo, M. C., Kim, C., & Kim, K. S. (2007). Optimized THP-1 differentiation is required for the detection of responses to weak stimuli. *Inflammation Research*, 56(1), 45–50. <https://doi.org/10.1007/s00011-007-6115-5>
- Pé Rez, A. B., García, G., Sierra, B., Alvarez, M., Vázquez, S., Cabrera, M. V., ... Guzmán, M. G. (2004). IL-10 Levels in Dengue Patients: Some Findings From the Exceptional Epidemiological Conditions in Cuba. *Journal of Medical Virology*, 73, 230–234. <https://doi.org/10.1002/jmv.20080>

- Peck, K. M., & Lauring, A. S. (2018). Complexities of Viral Mutation Rates. *Journal of Virology*, 92(14). <https://doi.org/10.1128/jvi.01031-17>
- Perera, R., Riley, C., Isaac, G., Hopf-Jannasch, A. S., Moore, R. J., Weitz, K. W., ... Kuhn, R. J. (2012). Dengue virus infection perturbs lipid homeostasis in infected mosquito cells. *PLoS Pathogens*, 8(3). <https://doi.org/10.1371/journal.ppat.1002584>
- Perrin-Cocon, L., Aublin-Gex, A., Diaz, O., Ramière, C., Peri, F., André, P., & Lotteau, V. (2018). Toll-like Receptor 4–Induced Glycolytic Burst in Human Monocyte-Derived Dendritic Cells Results from p38-Dependent Stabilization of HIF-1 $\alpha$  and Increased Hexokinase II Expression. *The Journal of Immunology*, 201(5), 1510–1521. <https://doi.org/10.4049/jimmunol.1701522>
- Petit, M. J., Kenaston, M. W., Pham, O. H., Nagainis, A. A., Fishburn, A. T., & Shah, P. S. (2021). Nuclear dengue virus NS5 antagonizes expression of PAF1-dependent immune response genes. *PLoS Pathogens*, 17(11), 1–23. <https://doi.org/10.1371/journal.ppat.1010100>
- Pierson, T. C., & Diamond, M. S. (2012). Degrees of maturity: The complex structure and biology of flaviviruses. *Current Opinion in Virology*, 2(2), 168–175. <https://doi.org/10.1016/j.coviro.2012.02.011>
- Pierson, T. C., & Diamond, M. S. (2018). The emergence of Zika virus and its new clinical syndromes. *Nature*, 560(7720), 573–581. <https://doi.org/10.1038/s41586-018-0446-y>
- Pierson, T. C., & Kielian, M. (2013). Flaviviruses: Braking the entering. *Current Opinion in Virology*, 3(1), 3–12. <https://doi.org/10.1016/j.coviro.2012.12.001>

- Płaszczycza, A., Id, P. S., John, C., Id, N., Id, M. C., Cerikan, B., ... Id, R. B. (2019). *A novel interaction between dengue virus nonstructural protein 1 and the NS4A-2K-4B precursor is required for viral RNA replication but not for formation of the membranous replication organelle. PLOS Pathogens.*
- Platanias, L. C. (2005). Mechanisms of type-I- and type-II-interferon-mediated signalling. *Nature Reviews Immunology*, 5(5), 375–386. <https://doi.org/10.1038/nri1604>
- Pokidysheva, E., Zhang, Y., Battisti, A. J., Bator-Kelly, C. M., Chipman, P. R., Xiao, C., ... Rossmann, M. G. (2006). Cryo-EM reconstruction of dengue virus in complex with the carbohydrate recognition domain of DC-SIGN. *Cell*, 124(3), 485–493. <https://doi.org/10.1016/j.cell.2005.11.042>
- Porter, D. C., Farmaki, E., Altilia, S., Schools, G. P., West, D. K., Chen, M., ... Roninson, I. B. (2012). Cyclin-dependent kinase 8 mediates chemotherapy-induced tumor-promoting paracrine activities. *Proceedings of the National Academy of Sciences of the United States of America*, 109(34), 13799–13804. <https://doi.org/10.1073/pnas.1206906109>
- Puerta-Guardo, H., Glasner, D. R., & Harris, E. (2016). Dengue Virus NS1 Disrupts the Endothelial Glycocalyx, Leading to Hyperpermeability. *PLoS Pathogens*, 12(7), 1–29. <https://doi.org/10.1371/journal.ppat.1005738>
- Putz, E. M., Gotthardt, D., Hoermann, G., Csiszar, A., Wirth, S., Berger, A., ... Sexl, V. (2013). CDK8-mediated STAT1-S727 phosphorylation restrains NK cell cytotoxicity and tumor surveillance. *Cell Reports*, 4(3), 437–444. <https://doi.org/10.1016/j.celrep.2013.07.012>

- Qi, X. F., Kim, D. H., Yoon, Y. S., Jin, D., Huang, X. Z., Li, J. H., ... Lee, K. J. (2009). Essential involvement of cross-talk between IFN- $\gamma$  and TNF- $\alpha$  in CXCL10 production in human THP-1 monocytes. *Journal of Cellular Physiology*, 220(3), 690–697. <https://doi.org/10.1002/jcp.21815>
- Quackenbush, S. L., Linton, A., Brewster, C. D., & Rovnak, J. (2009). Walleye dermal sarcoma virus rv-cyclin inhibits NF- $\kappa$ B-dependent transcription. *Virology*, 386(1), 55–60. <https://doi.org/10.1016/j.virol.2008.12.026>
- Quartier, P., Potter, P. K., Ehrenstein, M. R., Walport, M. J., & Botto, M. (2005). Predominant role of IgM-dependent activation of the classical pathway in the clearance of dying cells by murine bone marrow-derived macrophages in vitro. *European Journal of Immunology*, 35(1), 252–260. <https://doi.org/10.1002/eji.200425497>
- Quicke, K. M., Bowen, J. R., Johnson, E. L., McDonald, C. E., Ma, H., O’Neal, J. T., ... Suthar, M. S. (2016). Zika Virus Infects Human Placental Macrophages. *Cell Host and Microbe*, 20(1), 83–90. <https://doi.org/10.1016/j.chom.2016.05.015>
- Rathore, A. P. S., & St John, A. L. (2018). Immune responses to dengue virus in the skin. *Open Biology*, 8(8), 1–9. <https://doi.org/10.1098/rsob.180087>
- Rawlinson, S. M., Pryor, M. J., Wright, P. J., & Jans, D. A. (2009). CRM1-mediated nuclear export of dengue virus RNA polymerase NS5 modulates interleukin-8 induction and virus production. *Journal of Biological Chemistry*, 284(23), 15589–15597. <https://doi.org/10.1074/jbc.M808271200>

- Reid, D. W., Campos, R. K., Child, J. R., Zheng, T., Chan, K. W. K., Bradrick, S. S., ... Nicchitta, C. V. (2018). Dengue Virus Selectively Annexes Endoplasmic Reticulum-Associated Translation Machinery as a Strategy for Co-opting Host Cell Protein Synthesis. *Journal of Virology*, 92(7). <https://doi.org/10.1128/jvi.01766-17>
- Reyes-del Valle, J., Chávez-Salinas, S., Medina, F., & del Angel, R. M. (2005). Heat Shock Protein 90 and Heat Shock Protein 70 Are Components of Dengue Virus Receptor Complex in Human Cells. *Journal of Virology*, 79(8), 4557–4567. <https://doi.org/10.1128/jvi.79.8.4557-4567.2005>
- Rhein, B. A., Powers, L. S., Rogers, K., Anantpadma, M., Singh, B. K., Sakurai, Y., ... Maury, W. (2015). Interferon- $\gamma$  Inhibits Ebola Virus Infection. *PLoS Pathogens*, 11(11), 1–28. <https://doi.org/10.1371/journal.ppat.1005263>
- Richardson, J., Molina-Cruz, A., Salazar, M. I., & Black IV, W. (2006). Quantitative analysis of dengue-2 virus RNA during the extrinsic incubation period in individual *Aedes aegypti*. *American Journal of Tropical Medicine and Hygiene*, 74(1), 132–141. <https://doi.org/10.4269/ajtmh.2006.74.132>
- Rogers, K. J., Brunton, B., Mallinger, L., Bohan, D., Sevcik, K. M., Chen, J., ... Maury, W. (2019). IL-4/IL-13 polarization of macrophages enhances Ebola virus glycoprotein-dependent infection. *PLoS Neglected Tropical Diseases*, 13(12), e0007819. <https://doi.org/10.1371/journal.pntd.0007819>
- Rosales, C. (2018). Neutrophil: A cell with many roles in inflammation or several cell types? *Frontiers in Physiology*, 9(FEB), 1–17. <https://doi.org/10.3389/fphys.2018.00113>

- Rovnak, J., Brewster, C. D., & Quackenbush, S. L. (2012). Retroviral Cyclin Enhances Cyclin-Dependent Kinase-8 Activity. *Journal of Virology*, 86(10), 5742–5751.  
<https://doi.org/10.1128/jvi.07006-11>
- Rovnak, Joel, & Quackenbush, S. L. (2010). Walleye dermal sarcoma virus: Molecular biology and oncogenesis. *Viruses*, 2(9), 1984–1999. <https://doi.org/10.3390/v2091984>
- Rovnak, Joel, & Quackenbush, S. L. (2022). Exploitation of the Mediator complex by viruses. *PLoS Pathogens*, 18(4 April), 1–9. <https://doi.org/10.1371/journal.ppat.1010422>
- Roy, D. G., Kaymak, I., Williams, K. S., Ma, E. H., & Jones, R. G. (2020). Immunometabolism in the Tumor Microenvironment. *Annual Review of Cancer Biology*, 5, 137–159.  
<https://doi.org/10.1146/annurev-cancerbio-030518-055817>
- Roy, S. K., & Bhattacharjee, S. (2021). Dengue virus: Epidemiology, biology, and disease aetiology. *Canadian Journal of Microbiology*, 67(10), 687–702.  
<https://doi.org/10.1139/cjm-2020-0572>
- Salinas, S., Schiavo, G., & Kremer, E. J. (2010). A hitchhiker’s guide to the nervous system: The complex journey of viruses and toxins. *Nature Reviews Microbiology*, 8(9), 645–655.  
<https://doi.org/10.1038/nrmicro2395>
- Sanchez, E. L., & Lagunoff, M. (2015). Viral activation of cellular metabolism. *Virology*, 479–480, 609–618. <https://doi.org/10.1016/j.virol.2015.02.038>
- Sang, Y., Miller, L. C., & Blecha, F. (2015). Macrophage Polarization in Virus-Host Interactions. *Journal of Clinical and Cellular Immunology*, 06(02).  
<https://doi.org/10.4172/2155-9899.1000311>
- Saraiva, M., & O’Garra, A. (2010). The regulation of IL-10 production by immune cells. *Nature Reviews Immunology*, 10(3), 170–181. <https://doi.org/10.1038/nri2711>

- Sariol, C. A., Martínez, M. I., Rivera, F., van Rodríguez, I., Pantoja, P., Abel, K., ... Kraiselburd, E. N. (2011). Decreased dengue replication and an increased anti-viral humoral response with the use of combined toll-like receptor 3 and 7/8 agonists in macaques. *PLoS ONE*, 6(4). <https://doi.org/10.1371/journal.pone.0019323>
- Schaeffer, E., Flacher, V., Papageorgiou, V., Decossas, M., Fauny, J. D., Krämer, M., & Mueller, C. G. (2015). Dermal CD14 + dendritic cell and macrophage infection by dengue virus is stimulated by interleukin-4. *Journal of Investigative Dermatology*, 135(7), 1743–1751. <https://doi.org/10.1038/jid.2014.525>
- Schmid, M. A., & Harris, E. (2014). Monocyte Recruitment to the Dermis and Differentiation to Dendritic Cells Increases the Targets for Dengue Virus Replication. *PLoS Pathogens*, 10(12). <https://doi.org/10.1371/journal.ppat.1004541>
- Schroder, K., Hertzog, P. J., Ravasi, T., & Hume, D. A. (2004). Interferon-: an overview of signals, mechanisms and functions. *J. Leukoc. Biol*, 75, 163–189. <https://doi.org/10.1189/jlb.0603252>
- Schuler-Faccini, L., Ribeiro, E. M., Feitosa, I. M. L., Horovitz, D. D. G., Cavalcanti, D. P., Pessoa, A., ... Sanseverino, M. T. V. (2016). Possible Association Between Zika Virus Infection and Microcephaly — Brazil, 2015. *MMWR. Morbidity and Mortality Weekly Report*, 65(3), 59–62. <https://doi.org/10.15585/mmwr.mm6503e2>
- Sedeek, M., Nasrallah, R., Touyz, R. M., & Hébert, R. L. (2013). NADPH oxidases, reactive oxygen species, and the kidney: Friend and foe. *Journal of the American Society of Nephrology*, 24(10), 1512–1518. <https://doi.org/10.1681/ASN.2012111112>

- Seif, F., Khoshmirsafa, M., Aazami, H., Mohsenzadegan, M., Sedighi, G., & Bahar, M. (2017). The role of JAK-STAT signaling pathway and its regulators in the fate of T helper cells. *Cell Communication and Signaling*, *15*(1), 1–13. <https://doi.org/10.1186/s12964-017-0177-y>
- Semba, H., Takeda, N., Isagawa, T., Sugiura, Y., Honda, K., Wake, M., ... Komuro, I. (2016). HIF-1 $\alpha$ -PDK1 axis-induced active glycolysis plays an essential role in macrophage migratory capacity. *Nature Communications*, *7*(May), 1–10. <https://doi.org/10.1038/ncomms11635>
- Shapouri-Moghaddam, A., Mohammadian, S., Vazini, H., Taghadosi, M., Esmaili, S. A., Mardani, F., ... Sahebkar, A. (2018). Macrophage plasticity, polarization, and function in health and disease. *Journal of Cellular Physiology*, *233*(9), 6425–6440. <https://doi.org/10.1002/jcp.26429>
- Shepard, D. S., Undurraga, E. A., Halasa, Y. A., & Stanaway, J. D. (2016). The global economic burden of dengue: a systematic analysis. *The Lancet Infectious Diseases*, *16*(8), 935–941. [https://doi.org/10.1016/S1473-3099\(16\)00146-8](https://doi.org/10.1016/S1473-3099(16)00146-8)
- Shiratori, H., Feinweber, C., Luckhardt, S., Linke, B., Resch, E., Geisslinger, G., ... Parnham, M. J. (2017). THP-1 and human peripheral blood mononuclear cell-derived macrophages differ in their capacity to polarize in vitro. *Molecular Immunology*, *88*(June), 58–68. <https://doi.org/10.1016/j.molimm.2017.05.027>
- Shirey, K. A., Pletneva, L. M., Puche, A. C., Keegan, A. D., Prince, G. A., Blanco, J. C. G., & Vogel, S. N. (2010). Control of RSV-induced lung injury by alternatively activated macrophages is IL-4R $\alpha$ -, TLR4-, and IFN- $\beta$ -dependent. *Mucosal Immunology*, *3*(3), 291–300. <https://doi.org/10.1038/mi.2010.6>

- Shyh-Chang, N., Zhu, H., Yvanka De Soysa, T., Shinoda, G., Seligson, M. T., Tsanov, K. M., ... Daley, G. Q. (2013). Lin28 enhances tissue repair by reprogramming cellular metabolism. *Cell*, 155(4), 778. <https://doi.org/10.1016/j.cell.2013.09.059>
- Sica, A., & Mantovani, A. (2012). Macrophage plasticity and polarization: in vivo veritas. *Journal of Clinical Investigation*, 122(3), 787–795. <https://doi.org/10.1172/JCI59643DS1>
- Silva, E. M., Conde, J. N., Allonso, D., Ventura, G. T., Coelho, D. R., Carneiro, P. H., ... Mohana-Borges, R. (2019). Dengue virus nonstructural 3 protein interacts directly with human glyceraldehyde-3-phosphate dehydrogenase (GAPDH) and reduces its glycolytic activity. *Scientific Reports*, 9(1), 1–19. <https://doi.org/10.1038/s41598-019-39157-7>
- Sinha, R. A., Singh, B. K., Zhou, J., Wu, Y., Farah, B. L., Ohba, K., ... Yen, P. M. (2015). Thyroid hormone induction of mitochondrial activity is coupled to mitophagy via ROS-AMPKULK1 signaling. *Autophagy*, 11(8), 1341–1357. <https://doi.org/10.1080/15548627.2015.1061849>
- Sittisombut, N., Maneekarn, N., Viputtikul, K., Supawadee, J., Kanjanahaluethai, A., & Kasinrerak, W. (1995). Lack of augmenting effect of interferon- $\gamma$  on dengue virus multiplication in human peripheral blood monocytes. *Journal of Medical Virology*, 45(1), 43–49. <https://doi.org/10.1002/jmv.1890450109>
- Smieja, J., Jamaluddin, M., Brasier, A. R., & Kimmel, M. (2008). Model-based analysis of interferon- $\beta$  induced signaling pathway. *Bioinformatics*, 24(20), 2363–2369. <https://doi.org/10.1093/bioinformatics/btn400>
- Smit, J. M., Moesker, B., Rodenhuis-Zybert, I., & Wilschut, J. (2011). Flavivirus cell entry and membrane fusion. *Viruses*, 3(2), 160–171. <https://doi.org/10.3390/v3020160>

- Songprakhon, P., Thaingtamtanha, T., Limjindaporn, T., Puttikhunt, C., Srisawat, C., Luangaram, P., ... Noisakran, S. (2020). Peptides targeting dengue viral nonstructural protein 1 inhibit dengue virus production. *Scientific Reports*, *10*(1), 1–16.  
<https://doi.org/10.1038/s41598-020-69515-9>
- Soo, K.-M., Khalid, B., Ching, S.-M., Tham, C. L., Basir, R., & Chee, H.-Y. (2017). Meta-analysis of biomarkers for severe dengue infections. *Peer J*, 1–25.  
<https://doi.org/10.7717/peerj.3589>
- Soo, K. M., Tham, C. L., Khalid, B., Basir, R., & Chee, H. Y. (2019). Il-8 as a potential in-vitro severity biomarker for dengue disease. *Tropical Biomedicine*, *36*(4), 1027–1037.
- Soutourina, J. (2018). Transcription regulation by the Mediator complex. *Nature Reviews Molecular Cell Biology*, *19*(4), 262–274. <https://doi.org/10.1038/nrm.2017.115>
- St Clair, L. A., Mills, S. A., Lian, E., Soma, P. S., Nag, A., Montgomery, C., ... Perera, R. (2022). Acyl-Coa Thioesterases: A Rheostat That Controls Activated Fatty Acids Modulates Dengue Virus Serotype 2 Replication. *Viruses*, *14*(240).  
<https://doi.org/10.3390/v14020240>
- Starr, T., Bauler, T. J., Malik-Kale, P., & Steele-Mortimer, O. (2018). The phorbol 12-myristate-13-acetate differentiation protocol is critical to the interaction of THP-1 macrophages with *Salmonella Typhimurium*. *PLoS ONE*, *13*(3), 1–13.  
<https://doi.org/10.1371/journal.pone.0193601>
- Steinparzer, I., Sedlyarov, V., Rubin, J. D., Eislmayr, K., Galbraith, M. D., Levandowski, C. B., ... Kovarik, P. (2019a). Transcriptional Responses to IFN- $\gamma$  Require Mediator Kinase-Dependent Pause Release and Mechanistically Distinct CDK8 and CDK19 Functions. *Molecular Cell*, *76*(3), 485-499.e8. <https://doi.org/10.1016/j.molcel.2019.07.034>

Steinparzer, I., Sedlyarov, V., Rubin, J. D., Eislmayr, K., Galbraith, M. D., Levandowski, C. B.,

... Kovarik, P. (2019b). Transcriptional Responses to IFN- $\gamma$  Require Mediator Kinase-Dependent Pause Release and Mechanistically Distinct CDK8 and CDK19 Functions.

*Molecular Cell*, 76, 1–15. <https://doi.org/10.1016/j.molcel.2019.07.034>

Stern, O., Hung, Y.-F., Valdau, O., Yaffe, Y., Harris, E., Hoffmann, S., ... Sklan, E. H. (2013).

An N-Terminal Amphipathic Helix in Dengue Virus Nonstructural Protein 4A Mediates Oligomerization and Is Essential for Replication. *Journal of Virology*, 87(7), 4080–4085.

<https://doi.org/10.1128/jvi.01900-12>

Sugimoto, M. A., Sousa, L. P., Pinho, V., Perretti, M., & Teixeira, M. M. (2016). Resolution of

inflammation: What controls its onset? *Frontiers in Immunology*, 7(APR).

<https://doi.org/10.3389/fimmu.2016.00160>

Surdziel, E., Clay, I., Nigsch, F., Thiemeyer, A., Allard, C., Hoffman, G., ... Fodor, B. D.

(2017). Multidimensional pooled shRNA screens in human THP-1 cells identify candidate modulators of macrophage polarization. *PLoS ONE*, 12(8), 1–20.

<https://doi.org/10.1371/journal.pone.0183679>

Suzuki, T., Tahara, H., Narula, S., Moore, K. W., Robbins, P. D., & Lotze, M. T. (1995). Viral

interleukin 10 (id10), the human herpes virus 4 cellular i10 homologue, induces local anergy to allogeneic and syngeneic tumors. *Journal of Experimental Medicine*, 182(2), 477–

486. <https://doi.org/10.1084/jem.182.2.477>

Swarbrick, C. M. D., Basavannacharya, C., Chan, K. W. K., Chan, S. A., Singh, D., Wei, N., ...

Vasudevan, S. G. (2017). NS3 helicase from dengue virus specifically recognizes viral RNA sequence to ensure optimal replication. *Nucleic Acids Research*, 45(22), 12904–

12920. <https://doi.org/10.1093/nar/gkx1127>

- Syed, G. H., Amako, Y., & Siddiqui, A. (2010). Hepatitis C virus hijacks host lipid metabolism. *Trends in Endocrinology and Metabolism*, *21*(1), 33–40.  
<https://doi.org/10.1016/j.tem.2009.07.005>
- Tabata, T., Petitt, M., Puerta-Guardo, H., Michlmayr, D., Wang, C., Fang-Hoover, J., ... Pereira, L. (2016). Zika Virus Targets Different Primary Human Placental Cells, Suggesting Two Routes for Vertical Transmission. *Cell Host and Microbe*, *20*(2), 155–166.  
<https://doi.org/10.1016/j.chom.2016.07.002>
- Tannahill, G. M., Curtis, A. M., Adamik, J., Palsson-Mcdermott, E. M., McGettrick, A. F., Goel, G., ... O'Neill, L. A. J. (2013). Succinate is an inflammatory signal that induces IL-1 $\beta$  through HIF-1 $\alpha$ . *Nature*, *496*(7444), 238–242. <https://doi.org/10.1038/nature11986>
- Tassaneetrithep, B., Burgess, T. H., Granelli-Piperno, A., Trumpfheller, C., Finke, J., Sun, W., ... Marovich, M. A. (2003). DC-SIGN (CD209) mediates dengue virus infection of human dendritic cells. *Journal of Experimental Medicine*, *197*(7), 823–829.  
<https://doi.org/10.1084/jem.20021840>
- Tavakoli, S., Zamora, D., Ullevig, S., & Asmis, R. (2013). Bioenergetic profiles diverge during macrophage polarization: Implications for the interpretation of 18F-FDG PET imaging of atherosclerosis. *Journal of Nuclear Medicine*, *54*(9), 1661–1667.  
<https://doi.org/10.2967/jnumed.112.119099>
- Tayal, V., & Kalra, B. S. (2008). Cytokines and anti-cytokines as therapeutics - An update. *European Journal of Pharmacology*, *579*(1–3), 1–12.  
<https://doi.org/10.1016/j.ejphar.2007.10.049>

- Tedesco, S., De Majo, F., Kim, J., Trenti, A., Trevisi, L., Fadini, G. P., ... Vitiello, L. (2018). Convenience versus biological significance: Are PMA-differentiated THP-1 cells a reliable substitute for blood-derived macrophages when studying in vitro polarization? *Frontiers in Pharmacology*, 9(FEB), 1–13. <https://doi.org/10.3389/fphar.2018.00071>
- Teles, R. M. B., Krutzik, S. R., Ochoa, M. T., Oliveira, R. B., Sarno, E. N., & Modlin, R. L. (2010). Interleukin-4 regulates the expression of CD209 and subsequent uptake of *Mycobacterium leprae* by Schwann cells in human leprosy. *Infection and Immunity*, 78(11), 4634–4643. <https://doi.org/10.1128/IAI.00454-10>
- Teo, C. S. H., & Chu, J. J. H. (2014). Cellular Vimentin Regulates Construction of Dengue Virus Replication Complexes through Interaction with NS4A Protein. *Journal of Virology*, 88(4), 1897–1913. <https://doi.org/10.1128/jvi.01249-13>
- Thaker, S. K., Ch'ng, J., & Christofk, H. R. (2019). Viral hijacking of cellular metabolism. *BMC Biology*, 17(1), 59. <https://doi.org/10.1186/s12915-019-0678-9>
- Tongluan, N., Ramphan, S., Wintachai, P., Jaresitthikunchai, J., Khongwichit, S., Wikan, N., ... Smith, D. R. (2017). Involvement of fatty acid synthase in dengue virus infection. *Virology Journal*, 14(1), 1–18. <https://doi.org/10.1186/s12985-017-0685-9>
- Traba, J., Sack, M. N., Waldmann, T. A., & Anton, O. M. (2021). Immunometabolism at the Nexus of Cancer Therapeutic Efficacy and Resistance. *Frontiers in Immunology*, 12(May), 1–16. <https://doi.org/10.3389/fimmu.2021.657293>
- Tremblay, N., Freppel, W., Sow, A. A., & Chatel-Chaix, L. (2019). The interplay between dengue virus and the human innate immune system: A game of hide and seek. *Vaccines*, 7(4). <https://doi.org/10.3390/vaccines7040145>

- Tricia, H., Walker, J., & Kenneth, C. (2015). Macrophage Polarization in AIDS: Dynamic Interface between Anti-Viral and Anti-Inflammatory Macrophages during Acute and Chronic Infection. *Journal of Clinical & Cellular Immunology*, 06(03).  
<https://doi.org/10.4172/2155-9899.1000333>
- Tsai, T. T., Chuang, Y. J., Lin, Y. S., Chang, C. P., Wan, S. W., Lin, S. H., ... Lin, C. F. (2014). Antibody-Dependent Enhancement Infection Facilitates Dengue Virus-Regulated Signaling of IL-10 Production in Monocytes. *PLoS Neglected Tropical Diseases*, 8(11).  
<https://doi.org/10.1371/journal.pntd.0003320>
- Tsai, T. T., Chuang, Y. J., Lin, Y. S., Wan, S. W., Chen, C. L., & Lin, C. F. (2013). An emerging role for the anti-inflammatory cytokine interleukin-10 in dengue virus infection. *Journal of Biomedical Science*, 20(1), 1–9. <https://doi.org/10.1186/1423-0127-20-40>
- Umareddy, I., Chao, A., Sampath, A., Gu, F., & Vasudevan, S. G. (2006). Dengue virus NS4B interacts with NS3 and dissociates it from single-stranded RNA. *Journal of General Virology*, 87(9), 2605–2614. <https://doi.org/10.1099/vir.0.81844-0>
- Urcuqui-Inchima, S., Cabrera, J., & Haenni, A. L. (2017). Interplay between dengue virus and Toll-like receptors, RIG-I/MDA5 and microRNAs: Implications for pathogenesis. *Antiviral Research*, 147(June), 47–57. <https://doi.org/10.1016/j.antiviral.2017.09.017>
- Van den Bossche, J., Baardman, J., & de Winther, M. P. J. (2015). Metabolic characterization of polarized M1 and M2 bone marrow-derived macrophages using real-time extracellular flux analysis. *Journal of Visualized Experiments*, 2015(105), 1–7. <https://doi.org/10.3791/53424>
- Van den Bossche, J., O'Neill, L. A., & Menon, D. (2017). Macrophage Immunometabolism: Where Are We (Going)? *Trends in Immunology*, 38(6), 395–406.  
<https://doi.org/10.1016/j.it.2017.03.001>

- van der Windt, G. J. W., Everts, B., Chang, C. H., Curtis, J. D., Freitas, T. C., Amiel, E., ... Pearce, E. L. (2012). Mitochondrial Respiratory Capacity Is a Critical Regulator of CD8 + T Cell Memory Development. *Immunity*, *36*(1), 68–78.  
<https://doi.org/10.1016/j.immuni.2011.12.007>
- Viola, A., Munari, F., Sánchez-Rodríguez, R., Scolaro, T., & Castegna, A. (2019). The metabolic signature of macrophage responses. *Frontiers in Immunology*.  
<https://doi.org/10.3389/fimmu.2019.01462>
- Vivier, E., Tomasello, E., Baratin, M., Walzer, T., & Ugolini, S. (2008). Functions of natural killer cells. *Nature Immunology*, *9*(5), 503–510. <https://doi.org/10.1038/ni1582>
- Weber-Nordtt, R. M., Riley, J. K., Greenlund, A. C., Moore, K. W., Darnell, J. E., & Schreiber, R. D. (1996). Stat3 recruitment by two distinct ligand-induced, tyrosine- phosphorylated docking sites in the interleukin-10 receptor intracellular domain. *Journal of Biological Chemistry*, *271*(44), 27954–27961. <https://doi.org/10.1074/jbc.271.44.27954>
- West, A. P., Houry-Hanold, W., Staron, M., Tal, M. C., Pineda, C. M., Lang, S. M., ... Shadel, G. S. (2015). Mitochondrial DNA stress primes the antiviral innate immune response. *Nature*, *520*(7548), 553–557. <https://doi.org/10.1038/nature14156>
- Westerling, T., Kuuluvainen, E., & Mäkelä, T. P. (2007). Cdk8 Is Essential for Preimplantation Mouse Development. *Molecular and Cellular Biology*, *27*(17), 6177–6182.  
<https://doi.org/10.1128/mcb.01302-06>
- Witalisz-Siepracka, A., Gotthardt, D., Prchal-Murphy, M., Didara, Z., Menzl, I., Prinz, D., ... Sexl, V. (2018). NK cell-specific CDK8 deletion enhances antitumor responses. *Cancer Immunology Research*, *6*(4), 458–466. <https://doi.org/10.1158/2326-6066.CIR-17-0183>

- Wolf, A., Agnihotri, S., Micallef, J., Mukherjee, J., Sabha, N., Cairns, R., ... Guha, A. (2011). Hexokinase 2 is a key mediator of aerobic glycolysis and promotes tumor growth in human glioblastoma multiforme. *Journal of Experimental Medicine*, 208(2), 313–326.  
<https://doi.org/10.1084/jem.20101470>
- Wu, D., Sanin, D. E., Everts, B., Chen, Q., Qiu, J., Buck, M. D., ... Pearce, E. J. (2016). Type 1 Interferons Induce Changes in Core Metabolism that Are Critical for Immune Function. *Immunity*, 44(6), 1325–1336. <https://doi.org/10.1016/j.immuni.2016.06.006>
- Wu, S. J. L., Grouard-Vogel, G., Sun, W., Mascola, J. R., Brachtel, E., Putvatana, R., ... Frankel, S. S. (2000). Human skin Langerhans cells are targets of dengue virus infection. *Nature Medicine*, 6(7), 816–820. <https://doi.org/10.1038/77553>
- Xie, X., Gayen, S., Kang, C., Yuan, Z., & Shi, P.-Y. (2013). Membrane Topology and Function of Dengue Virus NS2A Protein. *Journal of Virology*, 87(8), 4609–4622.  
<https://doi.org/10.1128/jvi.02424-12>
- Xie, X., Zou, J., Zhang, X., Zhou, Y., Routh, A. L., Kang, C., ... Shi, P. Y. (2019). Dengue NS2A Protein Orchestrates Virus Assembly. *Cell Host and Microbe*, 26(5), 606-622.e8.  
<https://doi.org/10.1016/j.chom.2019.09.015>
- Yang, W., Wu, Y. H., Liu, S. Q., Sheng, Z. Y., Zhen, Z. Da, Gao, R. Q., ... An, J. (2020). *SI00A4+ macrophages facilitate zika virus invasion and persistence in the seminiferous tubules via interferon-gamma mediation. PLoS Pathogens* (Vol. 16).  
<https://doi.org/10.1371/journal.ppat.1009019>
- Yao, Y., Xu, X. H., & Jin, L. (2019). Macrophage polarization in physiological and pathological pregnancy. *Frontiers in Immunology*, 10(MAR), 1–13.  
<https://doi.org/10.3389/fimmu.2019.00792>

- Yarilina, A., Park-Min, K. H., Antoniv, T., Hu, X., & Ivashkiv, L. B. (2008). TNF activates an IRF1-dependent autocrine loop leading to sustained expression of chemokines and STAT1-dependent type I interferon-response genes. *Nature Immunology*, *9*(4), 378–387. <https://doi.org/10.1038/ni1576>
- Yu, C. Y., Liang, J. J., Li, J. K., Lee, Y. L., Chang, B. L., Su, C. I., ... Lin, Y. L. (2015). Dengue Virus Impairs Mitochondrial Fusion by Cleaving Mitofusins. *PLoS Pathogens*, *11*(12), 1–24. <https://doi.org/10.1371/journal.ppat.1005350>
- Yu, I.-M., Holdaway, H. A., Chipman, P. R., Kuhn, R. J., Rossmann, M. G., & Chen, J. (2009). Association of the pr Peptides with Dengue Virus at Acidic pH Blocks Membrane Fusion. *Journal of Virology*, *83*(23), 12101–12107. <https://doi.org/10.1128/jvi.01637-09>
- Yu, I., Zhang, W., Holdaway, H. A., Li, L., Kostyuchenko, V. A., Chipman, P. R., ... Chen, J. (2008). Structure of the Immature Dengue Virus at Low pH Primes Proteolytic Maturation. *Science (New York, N.Y.)*, *13*(March), 1834–1838.
- Yu, S., Ge, H., Li, S., & Qiu, H.-J. (2022). Modulation of Macrophage Polarization by Viruses: Turning Off/On Host Antiviral Responses. *Frontiers in Microbiology*, *13*(February). <https://doi.org/10.3389/fmicb.2022.839585>
- Yu, T., Gan, S., Zhu, Q., Dai, D., Li, N., Wang, H., ... Xiao, Y. (2019). Modulation of M2 macrophage polarization by the crosstalk between Stat6 and Trim24. *Nature Communications*, *10*(1). <https://doi.org/10.1038/s41467-019-12384-2>
- Zhang, F., Wang, H., Wang, X., Jiang, G., Liu, H., Zhang, G., ... Du, J. (2015). TGF- $\beta$  induces M2-like macrophage polarization via SNAIL-mediated suppression of a pro-inflammatory phenotype. *Oncotarget*, *7*(32), 52294–52306.

- Zhang, Jing, & Zhang, Q. (2019). Using Seahorse Machine to Measure OCR and ECAR in Cancer Cells. In *Cancer Metabolism Methods and Protocols Methods in Molecular Biology* (pp. 353–363). Retrieved from <http://www.springer.com/series/7651>
- Zhang, Jingshu, Lan, Y., Li, M. Y., Lamers, M. M., Fusade-Boyer, M., Klemm, E., ... Sanyal, S. (2018). Flaviviruses Exploit the Lipid Droplet Protein AUP1 to Trigger Lipophagy and Drive Virus Production. *Cell Host and Microbe*, 23(6), 819-831.e5. <https://doi.org/10.1016/j.chom.2018.05.005>
- Zhao, L., Huang, X., Hong, W., Qiu, S., Wang, J., Yu, L., ... Zhang, F. (2016). Slow resolution of inflammation in severe adult dengue patients. *BMC Infectious Diseases*, 16(1), 1–9. <https://doi.org/10.1186/s12879-016-1596-x>
- Zhao, X., Feng, D., Wang, Q., Abdulla, A., Xie, X. J., Zhou, J., ... Yang, F. (2012). Regulation of lipogenesis by cyclin-dependent kinase 8 - Mediated control of SREBP-1. *Journal of Clinical Investigation*, 122(7), 2417–2427. <https://doi.org/10.1172/JCI61462>
- Zhu, F., Zhou, Y., Jiang, C., & Zhang, X. (2015). Role of JAK-STAT signaling in maturation of phagosomes containing Staphylococcus aureus. *Scientific Reports*, 5, 1–11. <https://doi.org/10.1038/srep14854>
- Zou, J., Xie, X., Wang, Q.-Y., Dong, H., Lee, M. Y., Kang, C., ... Shi, P.-Y. (2015). Characterization of Dengue Virus NS4A and NS4B Protein Interaction. *Journal of Virology*, 89(7), 3455–3470. <https://doi.org/10.1128/jvi.03453-14>
- Zulu, M. Z., Martinez, F. O., Gordon, S., & Gray, C. M. (2019). The Elusive Role of Placental Macrophages: The Hofbauer Cell. *Journal of Innate Immunity*, 447–456. <https://doi.org/10.1159/000497416>